The Role of MARCKS in Mast Cell Regulated Exocytosis

Brookelyn J. Haddock

A thesis submitted to the faculty of the University of North Carolina at Chapel Hill in partial fulfillment of the requirements for the degree of Masters of Science in the Department of Cell and Molecular Physiology.

Chapel Hill

2010

Approved by

Advisor: Dr. C. William Davis

Reader: Dr. Carol Otey

Reader: Dr. Richard Cheney

ABSTRACT

Brookelyn J. Haddock

The Role of MARCKS in Mast Cell Regulated Exocytosis

Under the Supervision of C. William Davis

MARCKS is implicated as a critical regulator of regulated exocytosis. We studied the role of MARCKS in mast cell regulated exocytosis by comparing the secretion of embryonic hepatic-derived WT and MARCKS-deficient mast cells. Mast cells in suspension showed no secretory differences, however, adherent MARCKS-deficient cells demonstrated enhanced secretion and accelerated release of secretory cargo compared to WT. Surprisingly, application of purported MARCKS inhibitory peptides showed no MARCKS-specific inhibition. Thus, while MARCKS is not essential for mast cell regulated exocytosis, it does negatively modulate secretion.

In a separate study, conserved regions of MARCKS were tested for their necessity in the subcellular targeting of MARCKS from the PM to the cytosol, believed to be crucial for its multiple functions. We confirmed this movement using live cell imaging of HEK293 cells transfected with full-length MARCKS constructs. Notably, phosphorylated MARCKS associated with cytosolic membranes, and only myristoylation and PKC phosphorylation affected the translocation process.

Table of Contents

List of Figures

List of Abbreviations

AKAP	A Kinase Anchoring Protein
Apo	Apochromatic
Arp 2/3	Actin-Related Proteins 2/3
ATP	Adenosine trisphosphate
BMMCs	Bone Marrow-Derived Mast Cells
BSA	Bovine Serum Albumin
Ca2+	Calcium ion
CaCl2	Calcium Chloride
CCL1	CC Chemokine Ligand 1
CF	Cystic Fibrosis
CO2	Carbon Dioxide
COPD	Chronic Obstructive Pulmonary Disorder
DAG	Diacylglycerol
DMEM	Dulbecco's Modified Essential Medium
ΔMH2	MH2-Deletion MARCKS
DNA	Deoxyribonucleic Acid
DNP	2, 4-Dinitrophenol
EGF	Epidermal Growth Factor
eHMCs	Embryonic-Derived Hepatic Mast Cells
eYFP	enhanced Yellow Fluorescent Protein
F-actin	Filamentous Actin

FBS	Fetal Bovine Serum
FcεRI	High-Affinity IgE Tyrosine Kinase Receptor
FcγR	IgG-binding tyrosine kinase receptor
FITC	Fluorescein isothiocyanate
Fluor	Fluorochromatic
FRAP	Fluorescent Recovery After Bleaching
G2A	Non-myristolatable MARCKS
GBM	Glioblastoma Multiforme
GPCR	G-Protein Coupled Receptor
HEK293	Human Embryonic Kidney Cells
IgE	Immunoglobulin E
IgG	Immunoglobulin G
IL-3	Interleukin-3
IP3	Inositoltrisphosphate
KCl	Potassium Chloride
LPS	Lipopolysaccharide
MANS	MARCKS N-terminal Sequence
MARCKS	Myristoylated Alanine-Rich C Kinase Substrate
MgCl2	Magnesium Chloride
MH2	MARCKS-Homology 2
mL	Milliliters
MPSD	MARCKS PSD Peptide
mRNA	Message RNA

MRP	MARCKS-Related Protein
NA	Numerical Aperture
NaCl	Sodium Chloride
ng	Nanograms
nM	Nanomolar
NONG	Non-myristoylated MANS Peptide
PARs	Proteinase-Activated Receptor
PBS	Phosphate Buffered Saline
PCD	Primary Ciliary Dyskinesia
PCR	Polymerase Chain Reaction
PFA	Paraformaldehyde
Phe	Phenylalanine
PIP2	Phosphatidylinositol 4,5-bisphosphate
PIPES	1,4-Piperazinediethanesulfonic Acid
PKC	Protein Kinase C
PLC	Phospholipase C
PLD	Phospholipase D
PM	Plasma Membrane
PMA	Phorbol 12-myristate 13-acetate
PMN	Polymorphonuclear cell
PSD	Phosphorylation Site Domain
PsPi	Pseudo-Phosphorylated MARCKS
RA	Rheumatoid Arthritis

RNS	Random NH2-terminal Sequence
RPMI 1640	Roswell Park Memorial Institute 1640 Media
S1P	Sphingosine-1 Phosphate
SCF	Stem Cell Factor
SE	Standard Error
SG	Secretory Granule
SG Buffer	Siraganian Buffer
SM	Scrambled MARCKS
SNARE	Soluble NSF(N-ethylaleimide-sensitive) fusion protein adaptor protein receptor
Syk	Spleen tyrosine kinase
TNF-α	Tumour Necrosis Factor alpha
t-SNARES	PM-associated SNARES
v-SNARES	Vesicle-associated SNARES
WASP	Wiskott-Aldrich Syndrome Protein
WT	MARCKS-sufficient
μM	Micromolar
μm	Micrometers

Chapter 1

The Role of MARCKS in Regulating Regulated Exocytosis

Significance of Regulated Exocytosis

Exocytosis, one of the cellular events separating eukaryotes from prokaryotes, is used to insert proteins into the plasma membrane (PM) and to release materials, including signaling molecules, to the extracellular environment. Exocytic secretion is commonly divided into constitutive and regulated pathways, the former being responsible for protein insertion and tonic secretion, while the latter generally relates to neurotransmission, and exocrine, endocrine, paracrine and autocrine secretion. Constitutive exocytosis does not require receptor activation and its rate of release is limited only by the rate of cargo synthesis. In contrast, regulated exocytosis requires receptor activation, and cargo, packaged into secretory vesicles or granules (SGs), and is held in a reserve pool until an extracellular ligand activates the pathway. This regulated exocytic pathway is generally found in specialized secretory cells and it regulates many aspects of physiology, host defense (Sanchez-Mejorada & Rosales, 1998; Watanabe, *et al.,* 1999; Baumann, *et al.,* 2001; Burley, *et al.,* 2007; Davis & Dickey, 2008) and synaptic neurotransmission (Li, *et al.,* 2005; Jacques & Abdel-Samad, 2007).

Regulated exocytosis of mucins from goblet cells in a healthy respiratory system is a crucial part of mucociliary clearance, a host defense mechanism enabling the airways to clear

Fig. 1.1: The regulated exocytic pathway of secretory cells

Based on the actin barrier hypothesis, resting cells have a meshwork of actin filaments serving as a barrier and negatively regulating secretion by inhibiting SG access to docking sites on the PM. After stimulation, a signal transduction pathway activates numerous second messengers resulting in destabilization of the actin barrier and release of intracellular calcium stores. Following disruption of the actin barrier, by unknown mechanism, SGs dock with exocytic fusion sites on the PM and are primed for membrane fusion and cargo exocytosis via SNARE-mediated mechanisms. A localized calcium signal is required for the final exocytic event.

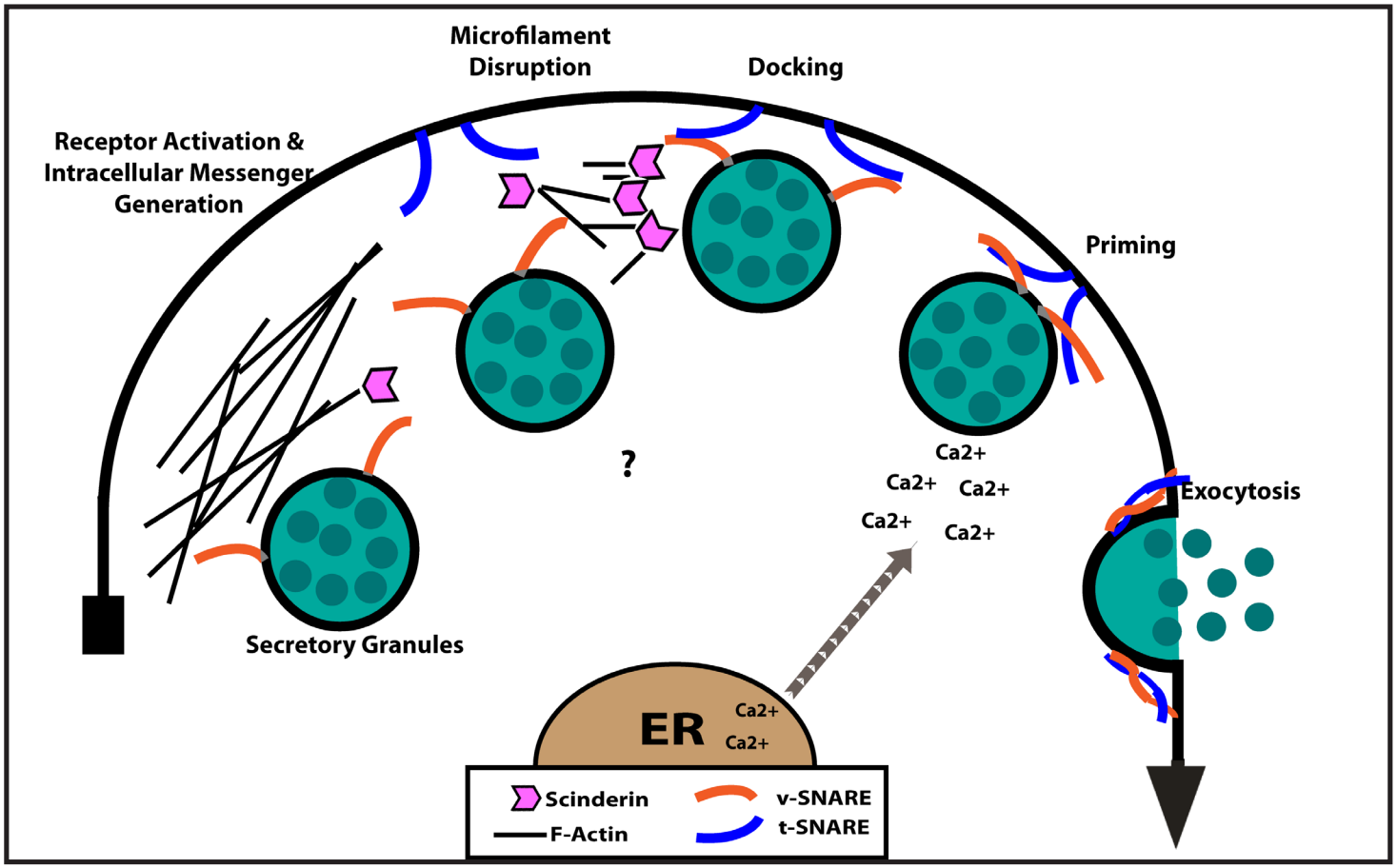
Microfilament
Disruption
Docking
Receptor Activation &
Intracellular Messenger
Generation
Priming
?
Ca2+
Ca2+
Ca2+
Ca2+
Ca2+
Exocytosis
Secretory Granules
ER
Ca2+
Ca2+
Scinderin
F-Actin
v-SNARE
t-SNARE

away inhaled contaminants and bacteria and preventing infection. Mucins maturate to form mucus, which is transported along the luminal surface of the airway epithelium by rhythmically beating cilia on ciliated cells to clear particulates and pathogens from the lungs. Multiple respiratory disorders, such as cystic fibrosis (CF) and primary ciliary dyskinesia (PCD), despite having different pathologies, suffer from excessive mucin secretion in the upper airways and lungs through involvement of the inflammation response (Davis & Dickey, 2008). This aberrant secretion, combined with inability to remove pathogens from the lungs, leads to clogged airways, accumulated immune cells, and dry, viscous mucus, eventually resulting in asphyxiation. If mucin secretion could be inhibited in lung pathologies, patient morbidity could be significantly reduced.

However, excessive mucin secretion is not the only regulated exocytic pathway contributing to respiratory diseases. Asthma and chronic obstructive pulmonary disorder (COPD) are characterized by inflammation due to hypersensitivity of immune cells inducing bronchoconstriction. Mast cells are critical secretory immune cells recognized to be involved in this process (Bradding, *et al.*, 2006; Gonzalo, *et al.*, 2007; Kalin, *et al.*, 2008; Ryzhov, *et al.*, 2008). Significantly, mast cells initiate the inflammatory response by utilizing regulated exocytosis to release pro-inflammatory and chemotactic mediators to activate and recruit other immune cells. Levels of these released products, due to increased regulated exocytosis or an increased number of mast cells, are typically increased compared to non-pathological conditions and can initiate a more severe inflammatory reponse to the same amount of stimuli (Bradding, *et al.*, 2006; Gonzalo, *et al.*, 2007; Ryzhov, *et al.*, 2008). For example, one chemokine product released from mast cells that functions as a trigger of pulmonary inflammation response, including mucus hypersecretion, was found to be increased five-fold in asthmatics (Gonzalo,

et al., 2007). These studies demonstrate that regulated exocytosis from mast cells alone can potentiate respiratory disorders, along with other types of secretory cells involved in the respiratory system. Consequently, understanding the regulatory aspects of regulated exocytosis may provide potential therapeutic targets in numerous cell types for many disorders; in this study, we focus on the potential role of the MARCKS protein in exocytic secretion.

Mechanisms of Regulated Exocytosis

Though sharing similar components, secretory cells undergoing regulated exocytosis can be subdivided into numerous categories. One division is between neuronal and non-neuronal secretion. Neuronal secretion is stimulated by an action potential, resulting in an immediate influx of calcium. Resting neuronal cells contain a readily releasable pool of secretory vesicles partially bound to the PM, so vesicle exocytosis occurs in milliseconds (Carr & Munson, 2007). In contrast, the larger vesicles of non-neuronal cells are distant from and unbound to the PM prior to receptor activation. These SGs must not only fuse with the PM to release their cargo, like neuronal cells, but in addition they must first migrate to and dock with the PM. Due to these additional steps, regulated exocytosis in non-neuronal cells takes place in seconds to minutes, even though exocytic fusion, per se, occurs in the millisecond time frame. Regulated exocytic pathways can also be divided between excitable cells and secretory cells. Excitable cells are activated by calcium influx through V-gated channels, while secretory cells are activated by receptor-mediated processes that generally trigger a mobilization of intracellular calcium (Ca2+). Notably, some secretory cells, such as chromaffin cells, are also excitable cells. Mast cells, utilized in these studies, are non-neuronal, secretory cells, and undergo the type of regulated exocytosis depicted in Fig. 1.1.

In resting secretory cells, a meshwork of cortical actin filaments lies between the PM and intracellular SGs that functions as a barrier to prevent contact (Bader, *et al.,* 2004; Malacombe, *et al.*, 2006). Upon receptor activation, a signaling cascade is initiated, including activation of protein kinase C (PKC), which results in disruption of the barrier (Trifaro, *et al.,* 2002; Peng & Beaven, 2005; Davis & Dickey, 2008). This disruption, hypothesized to be mediated by MARCKS and/or scinderin (Vitale, *et al.,* 1991; Trifaro, *et al.,* 2002; Eitzen, 2003; Pene, *et al.*, 2005), allows SGs to dock on the PM. Like all regulated exocytic pathways, the SG binding to the PM, and membrane fusion steps that follow are mediated by SNARE [soluble NSF (N-ethylaleimide-sensitive fusion protein) adaptor protein receptor] proteins. SNAREs are localized to the cytoplasmic surface of both vesicles and the PM. Vesicle-associated SNARES (v-SNARES) include VAMPs, a large protein family, while PM-associated SNARES (t-SNARES) include the SNAP 23/25 family of proteins and Syntaxin. When v-SNARES and t-SNARES come into contact and assemble, they form a stable complex made up of a quadruple α-helix, a process termed priming. Upon a suitable, generally localized calcium signal, the SNARE complex undergoes a calcium-mediated conformational change that coils the helical structure and releases the energy necessary for fusion between the two membranes. SNARE assembly, priming, and mediation of membrane fusion is a highly regulated process controlled by multiple proteins, including members of the Munc 18 and Munc 13 families, complexins, and synaptotagmins. Once membrane fusion occurs, the SNARE complex forms a fusion pore, through which the contents of the SG are released into the extracellular environment (Rizo, *et al.,* 2006; Davis & Dickey, 2008; Melicoff, *et al.,* 2009). Additionally, a recent re-examination of evidence has suggested that actin cytoskeletal remodeling, believed crucial for initial cortical actin disruption and SG trafficking and docking, may also be a critical regu-

lator of membrane fusion and pore formation (Bader, *et al.,* 2004; Malacombe, *et al.,* 2006).

The different mechanisms and regulators involved in regulated exocytosis at each point of the pathway are understood to varying degrees. The portions of regulated exocytosis shared by non-neuronal and neuronal cells, specifically the SNARE-mediated mechanisms and regulation of docking, priming and membrane fusion, have been relatively well characterized. In comparison, much less has been elucidated about the disparate portions of regulated exocytosis: namely, the mechanisms and regulators responsible for the actin barrier disruption, SG trafficking and SG docking that occur after secretory cell activation. An important regulatory role for actin remodeling in regulated exocytosis has been ascribed to MARCKS (Trifaro, *et al.*, 2000; Trifaro, *et al.,* 2002; Eitzen, 2003). We have focused on this hypothesis, taking advantage of an available gene-interrupted mouse model (Stumpo, *et al.,* 1995; Swierczynski, *et al.,* 1996).

Myristoylated Alanine Rich C Kinase Substrate (MARCKS) Gene Family

MARCKS is a ubiquitously expressed PKC substrate previously demonstrated to regulate actin cytoskeleton dynamics in numerous cell processes (Myat, *et al.,* 1997; Disatnik, *et al.,* 2004; Finlayson & Freeman, 2009; Eckert, *et al.*, 2010). MARCKS and its only other family member, MARCKS-related protein (MRP), have three conserved domains: an N-terminal consensus sequence site for myristoyl modification, a MARCKS homology domain 2 (MH2) of unknown function, and a phosphorylation site domain (PSD) containing the serine residues phosphorylated by PKC (Stumpo, *et al.,* 1989; Aderem, 1992) (Fig. 1.2). The PSD is also a highly basic region implicated in actin (Yarmola, *et al.,* 2001), calmodulin (Aderem, 1992; Aderem, 1995; Qin & Cafiso, 1996) and phosphatidylinositol 4,5-bisphosphate (PIP2) (Wang,

Fig. 1.2: Conserved Regions of MARCKS Sequence. The two-member MARCKS gene family has three regions of highly conserved sequence. The first is a co-translational myristoyl consensus sequence site. The second is the MH2 domain of unknown function. The third region is the PSD domain where the serines phosphorylated by PKC are located. Additionally, an N-terminal sequence is shown, which has been implicated in MARCKS targeting, though not formally identified as a domain.

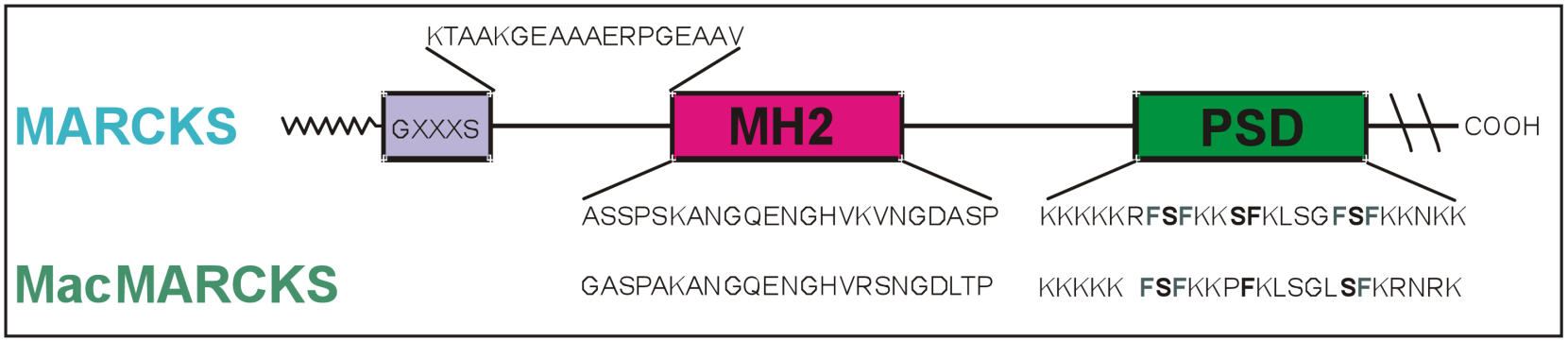
KTAAKGEAAAERPGEAAV
MARCKS
GXXXS
MH2
PSD
COOH
ASSPSKANGQENGHVKVNGDASP
KKKKKRFSFKKSFKLSGFSFKKNKK
MacMARCKS
GASPAKANGQENGHVRSNGDLTP
KKKKK FSFKKPFKLSGLSFKRNRK

et al., 2001; Wang, *et al.,* 2002) binding to membranes. Structurally, MARCKS is a natively unfolded protein that binds to the cytosolic leaflet of the PM in resting cells (Qin & Cafiso, 1996; Tzlil, *et al.,* 2008). PKC phosphorylation electrostatically neutralizes the PSD of both MARCKS and MRP, and causes translocation from the plasma membrane (PM) to the cytosol, a movement hypothesized to be crucial to the function of these two cytoskeletal-associated proteins (Ohmori, *et al.,* 2000; Disatnik, *et al.,* 2004; van den Bout, *et al.,* 2007; Tzlil, *et al.,* 2008).

Other than a clear understanding of MARCKS/MRP activation and translocation, however, the exact function and mechanism of the MARCKS family proteins has not yet been fully elucidated. Functions in cell attachment, cell spreading, (Myat, *et al.,* 1997; Disatnik, *et al.,* 2004; Eckert, *et al.*, 2010) integrin-associated signaling, (Vuori & Ruoslahti, 1993) phagocytosis, (Zhu, *et al.,* 1995; Carballo, *et al.,* 2009) and regulated exocytosis (Elzagallaai, *et al.,* 2000; Rose, *et al.,* 2001; Jerdeva, *et al.,* 2005; Li, *et al.,* 2005; Eliyahu, *et al.,* 2005; Eliyahu, *et al.,* 2006; Park, *et al.,* 2006; Andreas, *et al.*, 2009) have all been suggested for the MARCKS gene family.

MARCKS and Immune Challenge

MARCKS and MRP are regulated spatially, developmentally, and in response to immune challenge (Rose, *et al.,* 1996; Yokoyama, *et al.*, 1998; Chun, *et al.,* 2009). Neutrophils primed for inflammatory responses by pretreatment with inflammatory mediators, tumour necrosis factor alpha (TNF-α) or lipopolysacchharide (LPS), demonstrated increased protein synthesis of MARCKS (Thelen, *et al.,* 1990). In a macrophage cell line activated by LPS, MRP transcription levels were also increased (Chang, *et al.,* 1999). A recent study suggests

this upregulation of MRP and MARCKS is related to chemotactic transmigration of these activated macrophages (Chun, *et al.,* 2009), while others suggest it is involved with macrophage phagocytosis and cell spreading (Zhu, Bao, Li, 1995; Underhill, *et al.,* 1998; Zhou & Li, 2000). In another cell type, murine microglia, when activated by LPS to transform them to phagocytic macrophage-like immune cells, significantly increased protein levels of MARCKS and MRP (Rose, *et al.,* 1996). Pretreatment of isolated human neutrophils with the MARCKS-NH^2 terminus (MANS) peptide was correlated to decreased F-actin amounts and inhibition of both their migration upon immune activation and β2 integrin-mediated adhesion (Eckert, *et al.*, 2010). Conclusions about which function MARCKS and MRP serve when they are up-regulated in response to inflammatory challenge remain disparate due to the fact that studies of cells derived from MRP or MARCKS-deficient mouse models do not always agree with overexpression, peptide, and knockdown studies. In the absence of a complete knockdown of the MARCKS family members, there is always the possibility of non-physiological effects due to abnormally high levels of MARCKS transfection/infection copy number and/or interference due to the presence of endogenous MARCKS. Unfortunately, practical utility of MRP and MARCKS-deficient mice has been severely hindered by the perinatal lethality of the mice due to neurological problems (Stumpo, *et al.*, 1995; Swierczynski, *et al.*, 1996).

MARCKS Family and Disease

Since MARCKS and MRP have been implicated as critical regulators of important cellular processes like regulated exocytosis, cell attachment, and cell mobility, it is not surprising that these proteins are being investigated for possible links to disease. The diseases studied in relation to the MARCKS family range from neurological pathologies to cancer and inflamma-

tion disorders. What all of these investigations have in common is that they apply previously purported MARCKS functions to their ramifications for pathological conditions.

The perinatal lethality of MARCKS-deficiency in mice, due to failure of the neural tube to close, implicates an important role for MARCKS in normal neurological development. Three types of neuropathies are currently linked to MARCKS. First, when a peptide corresponding to the PSD sequence of MARCKS (MPSD) was acutely infused into the hippocampus of rats, it resulted in significant *in vivo* impairment of working (changing) memory, along with a smaller impairment of long-term reference memory, as assessed by performance in a 16-arm radial arm maze (Timofeeva, *et al.,* 2009). A possible mechanism of action, though, for this effect is extracellular inhibition of nicotinic acetylcholine receptors preventing activation of neurotransmitter release (Gay, *et al.*, 2008, Timofeeva, *et al.*, 2009). This research suggests that MARCKS could be a target for cognitive impairment diseases, such as Alzheimers. Second, MARCKS overexpression has been linked to the most malignant type of adult brain tumor, glioblastoma multiforme (GBM). Both operative specimens and xenograft explant tumors significantly overexpressed MARCKS protein. In glioma cell lines transfomed to simulate the conditions found in 50% of all GBMs, overexpression of epidermal growth factor (EGF) receptors, MARCKS was subsequently upregulated. To validate these overexpression results, researchers showed that siRNA knockdown of MARCKS in these same glioma cells significantly decreased cell attachment and invasion compared to control (Micallef, *et al.,* 2009). Thus, according to these two studies, MARCKS may be involved in neuronal plasticity and could function as a promoter of tumor invasiveness. Finally, a recent, though tentative connection has been suggested between MARCKS and psychiatric diseases. Alterations in PKC's activation state result from therapeutic treatments for diseases like bipolar disorder, mania, depression

and schizophrenia (Szando, *et al.*, 2009; Kim, *et al.,* 2009). In mania, manic episodes are associated with increased PKC activity marked by increased levels of phosphoMARCKS protein in the prefrontal cortex membrane. Lithium, an anti-mania treatment, significantly decreased these levels of phosphoMARCKS (Szando, *et al.,* 2009). Another therapy for treating mood disorders, electroconvulsive treatment, when modeled in rats resulted in a temporal increase in phosphorylation of three major brain PKC substrates, one of which was MARCKS (Kim, *et al.,* 2009). Since this finding is recent, the specific connection to any MARCKS function has not yet been investigated. Only further studies will reveal whether or not MARCKS could be a future therapeutic target for mood disorders.

A function for MARCKS family members has also been implicated in numerous cancer studies for playing a role in cell invasion, an important component of cancer metastasis. Invasive bladder cancer cells, treated with phorbol ester to keep MARCKS perpetually phosphorylated, resulted in reduced cell motility and invasiveness (Yokoyama, *et al.*, 1998). Another group, in contrast, showed that treatment of cells with microRNA targeting MARCKS led to increased invasion of prostate cancer cells, suggesting MARCKS as a possible tumor suppressor in prostate cancer (Li, *et al.*, 2009). It seems that increased levels of phosphorylated MARCKS could act as a metastatic tumor suppressor, while decreased levels of total MARCKS protein could promote tumor invasiveness. The answer could be as simple as the fact that MARCKS function in suppressing tumor invasiveness correlates to its activation via phosphorylation: if less MARCKS is available for phosphorylation, less MARCKS-mediated inhibition of invasiveness occurs. Unfortunately, a clear mechanistic model of MARCKS function as a tumor suppressor has not yet been elucidated.

Knockdown of MRP, the other MARCKS family member, in a transformed murine

Fig. 1.3: MARCKS-Mediated Actin Barrier Hypothesis. At rest, the actin barrier negatively regulates secretion, but after receptor activation actin filament disruption results in SGs docking to the PM where exocytosis eventually occurs. The mechanism of actin destabilization, while it remains unknown, is believed to involve PKC phosphorylation of MARCKS, which induces MARCKS' translocation from the PM to the cytosol. However, the causal relationship between MARCKS' translocation and the actin barrier destabilization has not been rigorously studied. PhosphoMARCKS has also been suggested to associate with SGs after translocation and could be involved in SG trafficking to the PM.

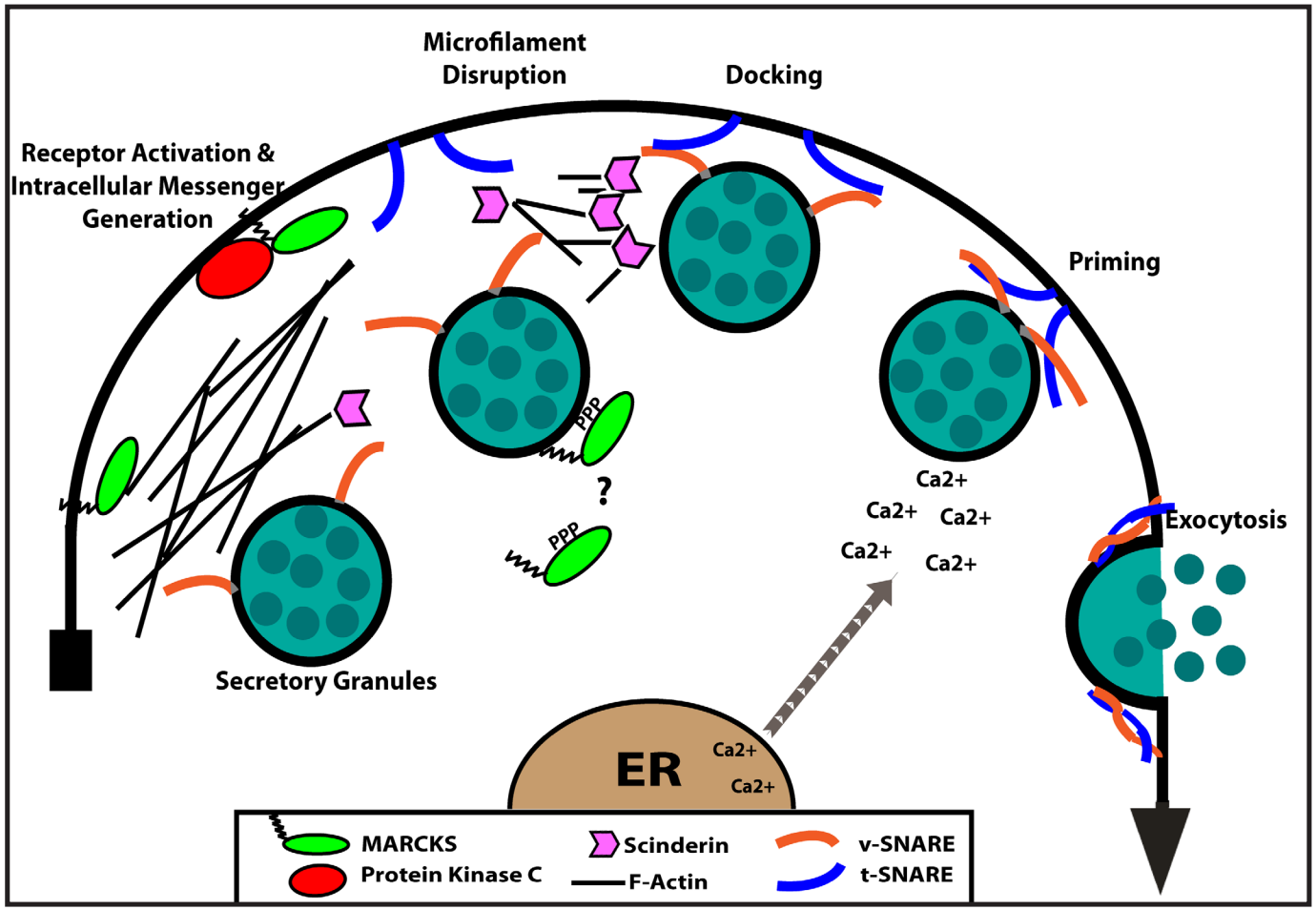
Microfilament
Disruption
Docking
Receptor Activation &
Intracellular Messenger
Generation
Priming
PPP
?
PPP
Ca2+
Ca2+
Ca2+
Ca2+
Ca2+
Exocytosis
Secretory Granules
ER
Ca2+
Ca2+
MARCKS
Protein Kinase C
Scinderin
F-Actin
v-SNARE
t-SNARE

mammary cell line and in a prostate cancer cell line decreased tumor cell migration and invasion, opposite to findings with MARCKS. These results suggested that MRP might act as a promoter of tumor invasiveness. Confusingly, though, the same study demonstrated that the inhibition of MRP expression correlated to decreased tumor numbers and size in oncogenic mice. Conclusions drawn by the researchers were that MRP is involved in adherens junction formation, and that it promotes invasiveness in the early stages of metastasis, while inhibiting the signaling required for the later stages of tumorigenesis (Finlayson & Freeman, 2009). All results, therefore, only indicate that both MARCKS family members are involved in tumor cell attachment and invasion, with contradiction between MARCKS and MRP studies suggesting they may either be tumor suppressors or promoters.

In another pathology area, arthritis, MARCKS gene expression was found to be up-regulated in normal human chondrocytes when they were exposed to the pro-inflammatory cytokine-loaded supernatant of rheumatoid arthritis (RA) synovial fibroblasts. The upregulation of MARCKS was also correlated with increased joint structure damage due to increased chondrocyte secretion of matrix degrading proteins (Andreas, *et al.,* 2009). However, researchers did not indicate whether human chondrocytes from RA patients pathologically express higher levels of MARCKS compared to non-RA patients. The evidence linking MARCKS to joint structure degradation remains correlative, rather than causative, but the initial correlation is well demonstrated.

MARCKS and Regulated Exocytosis

The role of MARCKS in regulated exocytosis has been investigated for almost a decade. Since MARCKS-deficient mice die perinatally (Stumpo, *et al.,* 1995; Swierczynski, *et*

al., 1996), alternative experimental approaches have been used; most commonly applying synthetic peptides representing the conserved MARCKS domains to study the resulting effects on secretion. In chromaffin cells, a PKC-dependent, MARCKS-dependent role is postulated based on the evidence that permeabilized cells treated with the MARCKS PSD (MPSD) peptide, which inhibits MARCKS phosphorylation, have a decreased rate of catecholamine release (Doreian, *et al.,* 2009). Significantly, a control peptide, in which the PKC-phosphorylated serines were mutated to alanines, showed no inhibition of MARCKS phosphorylation. This model is supported by the further observation that MARCKS knockdown with siRNA reduced cortical F-actin disassembly and catecholamine secretion, measured as a decrease in vesicle fusion events (Rose, *et al.,* 2001; Jerdeva, *et al.,* 2005; Park, *et al.,* 2006). Taken together, these results suggest that for regulated exocytosis of neurotransmitters, phosphorylated MARCKS serves a positive regulatory role in cortical F-actin disassembly and chromaffin cell secretion. In platelets, when the MPSD peptide inhibited the regulated exocytosis of serotonin, the same critical positive regulatory role was suggested (Elzagallaai, *et al.,* 2000). Thus, in aggregate, these studies suggest that MARCKS is an important regulator of regulated exocytosis.

A major criticism, however, of studies utilizing the MPSD is that the peptide may affect secretion by inhibiting extracellular receptor activation (Gay, *et al.*, 2008) or by competing with all PKC substrates, not just by its MARCKS-specific effects, . The possibility of non-specific effects being attributed to MARCKS-specific functions is an important issue, particularly in cells also expressing MRP and other polybasic domain proteins with PSD homology (GAP43, CAP23, Adducins, A kinase anchoring protein 12 and 79) (Aderem, 1995; Matsuoka, Li, & Bennett, 2000; Streb & Miano, 2005). The answer to how the MPSD functions mechanistically would give insight into answering these issues of specificity.

PSD peptide studies, though, are not the only investigations linking MARCKS to regulated exocytosis. Studies in a human intestinal endocrine cell line (BON) demonstrated that MARCKS overexpression increased neurotensin secretion, whereas MARCKS siRNA knockdown inhibited secretion. Additionally, the ability of MARCKS overexpression to enhance regulated exocytosis was neutralized in full-length MARCKS mutants lacking PKC phosphorylation or myristoylation (Li, *et al.,* 2005). In oocyte cortical granules, exocytosis has been shown to require phosphorylatable MARCKS, not just actin depolymerization and PKC activation (Eliyahu, *et al.,* 2005; Eliyahu, *et al.,* 2006). In aggregate, these studies suggest that MARCKS membrane binding, phosphorylation and subsequent translocation is critical for MARCKS positive regulatory role in regulated exocytosis.

Another study demonstrated an upregulation of MARCKS expression in human chondrocytes, while also observing an increase in secretion. In this study, when the cytokine-rich supernatant from synovial fibroblasts of rheumatoid arthritis patients was placed in culture with human chondrocytes, MARCKS' gene expression was upregulated. The secretion from these human chondrocytes was also potentiated (Andreas, *et al.,* 2009). This study, however, does not provide any causal link between the change in MARCKS expression and the increased chondrocyte secretion. It is possible that the increased levels of pro-inflammatory cytokines could alone enhance secretion, while the presence of an activated immune situation upregulates MARCKS for an unrelated purpose.

MARCKS Translocation

Much of the evidence for MARCKS' role in regulated exocytosis is centered on the ability of MARCKS to be phosphorylated by PKC and translocate from the PM to the cyto-

sol. A mechanism proposed by Stuart McLaughlin for this cycling on and off the membrane is the myristoyl-electrostatic switch model. Briefly, insertion of the myristoyl moiety of unphosphorylated MARCKS into the PM provides a weak interaction that stabilizes the protein on the PM. Positively charged residues on the basic PSD electrostatically interact with acidic phospholipids while its five Phe residues insert into the hydrophobic region of the lipid bilayer. These multiple weak interactions synergistically create a tight membrane association. Phosphorylation by PKC of three serine residues within the PSD neutralizes its positive charges, destabilizing association between MARCKS and the PM, inducing translocation to the cytosol (Tzlil, *et al.,* 2008; Seykora, *et al.,* 1996). However, the functional significance of this translocation is not yet understood in detail, but an early suggestion was that the PSD bound the cortical actin filaments of the actin barrier in secretory cells. In this model, MARCKS in resting cells anchors actin filaments to the PM, stabilizing the actin barrier, and MARCKS translocation destabilizes the actin filaments, resulting in actin barrier disruption (Trifaro, *et al.,* 2002; Jerdeva, *et al.,* 2005; Park, *et al.,* 2006).

The importance of MARCKS' translocation for normal cell spreading on the extracellular matrix proteins, particularly fibronectin, a ligand for the α5β1 integrin-mediated receptor signaling pathway has also been demonstrated (Disatnik, *et al.,* 2004; Myat, *et al.,* 1997). Two independent studies demonstrated parallel results in fibroblasts and myoblasts, respectively, by utilizing overexpression of MARCKS mutants. In fibroblasts, overexpression of a MARCKS mutant, in which the reversible membrane binding of a single myristoyl group was mutated to the more permanent binding of two palmitoyl groups, prevented translocation to the cytosol following PKC phosphorylation. Inhibition of MARCKS translocation resulted in attenuation of cell spreading into lamellae and impaired cell spreading on the fibronectin substratum

Fig. 1.4: Two possible mechanisms for MARCKS-mediated actin barrier disruption

(A) The Actin Tethering Model proposes that actin filaments are tethered to the PM by binding to two unphosphorylated MARCKS. When MARCKS is phosphorylated and translocates, these actin filaments are destabilized.

(B) The PIP2 Sequestration model proposes that MARCKS sequesters PIP2, an important signaling molecule, and upon translocation releases PIP2 for its various functions, including actin destabilization.

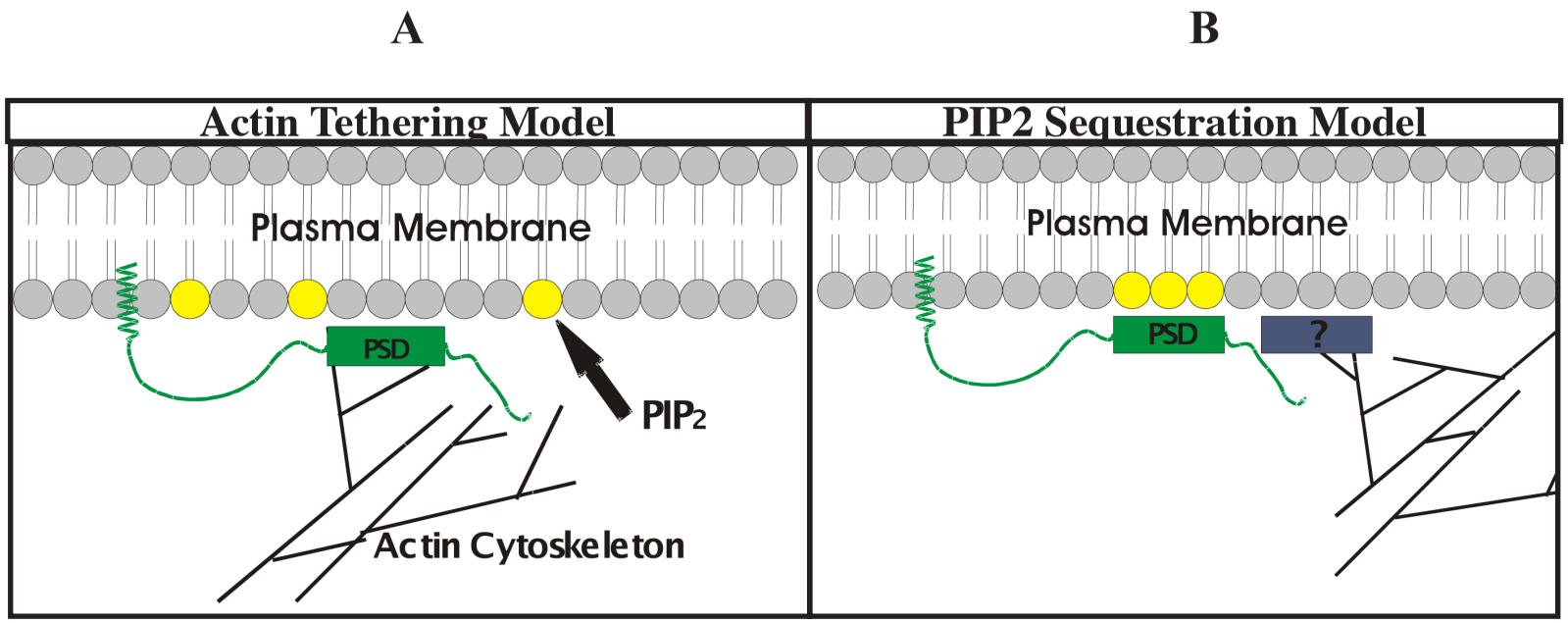
A
B
Actin Tethering Model
PIP2 Sequestration Model
Plasma Membrane
Plasma Membrane
PSD
PSD
?
PIP2
Actin Cytoskeleton

(Myat, *et al.,* 1997). In myoblasts, full-length MARCKS mutants insensitive to PKC phosphorylation also inhibited cell spreading and corresponded to decreased actin polymerization and focal adhesion formation. Significantly, these researchers elucidated another critical component of the MARCKS translocation process. When phosphatase inhibitors were added, the prolonged presence of full-length phosphoMARCKS, localized to the cytosol, also inhibited cell spreading (Disatnik, *et al.,* 2004). Consequently, the role of MARCKS in cell spreading seems to require the ability of MARCKS to bidirectionally translocate from the PM to the cytosol and back. In fact, a study of a transformed astrocytoma cell line in which MARCKS was knocked down with two different siRNAs, demonstrated impaired cell attachment, spreading, and motility (Micallef, *et al.,* 2009). Most notably, the cells had a "rounded morphology" just as Disatnik, *et al.*, 2004, described. The conclusion is that lack of reversible translocation, due to decreased amounts of MARCKS or due to inability to detach from the PM, all result in a similar rounded cell morphology, impaired cell spreading, and possibly impaired motility.

Proposed Mechanisms for MARCKS-mediated Regulated Exocytosis

This process of reversible, bidirectional movement of MARCKS between the PM and the cytosol has become the model subcellular behavior included in any proposed mechanism for MARCKS function (Fig. 1.3). Interestingly, timing of actin barrier disruption correlates with PKC phosphorylation of MARCKS and its translocation to the cytosol (Arbuzova, *et al.,* 2002; Ehre, *et al.,* 2005). Down-regulation of MARCKS using a MARCKS N-terminal sequence (MANS) peptide has been shown to diminish mucin secretion, but the peptide's specificity to MARCKS and its unknown mechanism of action raise important questions (Singer, *et al.,* 2004; Li, *et al.,* 2001). Consequently, MARCKS'translocation remains indirectly linked to

destabilization of the actin barrier and exocytic secretion.

Existing evidence supports the relationship between MARCKS activation and secretion; however, the three major models for the mechanistic function of MARCKS propose three distinct mechanisms of action.

1. *MARCKS operates as a tether between actin filaments of the barrier and the PM when secretory cells are at rest.* This model (Fig. 1.4 A) is derived from studies demonstrating that a peptide corresponding to the non-phosphorylated MARCKS PSD is capable of *in vitro* binding and cross-linking of filamentous actin (F-actin). This activity corresponds well with the hypothesis that unphosphorylated MARCKS effectively binds F-actin, tethering the cortical actin barrier to the PM. Correlatively, phosphorylated PSD peptides were observed to have reduced binding affinity for F-actin, along with decreased cross-linking activity, suggesting that phosphorylation of MARCKS PSD by PKC induces a conformational change that diminishes accessibility to the actin binding sites (Yarmola, *et al.,* 2001; Tapp, *et al.,* 2005). Consequently, this mechanism proposes that prior to PKC phosphorylation, MARCKS tethers actin filaments to the PM, but after PKC phosphorylation, MARCKS translocation destabilizes the barrier (Trifaro, *et al.,* 2002; Jerdeva, *et al.,* 2005; Park, *et al.,* 2006).

It is known, however, that full-length MARCKS does not exhibit as marked an ability to bind or cross-link actin as the PSD peptide alone, and studies directly testing MARCKS' interactions with actin in living cells have not been performed to date (Yarmola, et al., 2001; Tapp, *et al.,* 2005). According to this model, MARCKS-deficiency results in loss of actin tethering and disruption of the actin barrier, even under resting conditions. Hence, we should observe increased regulated secretion, possibly even under baseline conditions in MARCKS-deficient cells.

2. *MARCKS sequesters phosphatidylinositol 4,5-bisphosphate (PIP2) in the PM.* Stoichiometrically, one MARCKS PSD can electrostatically sequester three to four PIP2 molecules (Fig. 1.4 B). In aggregate, the MARCKS PSD is believed to be capable of sequestering a significant fraction of PIP2 in membranes in vitro (Wang, *et al.,* 2001; Wang, *et al.,* 2002; Tzlil, *et al.*, 2008). PIP2 is the substrate for the second messengers DAG and IP3, as well as an activator of many cytoskeletal regulatory proteins involved in polymerization and treadmilling (Sundaram, *et al.*, 2004). These cytoskeletal regulators may include phospholipase D (PLD), an activator which induces downstream release of phosphatidic acid, and WASP proteins, which promote formation of Arp 2/3 complexes (Caroni, 2001; Sundaram, *et al.,* 2004). Free PIP2 in the PM can inhibit actin-severing molecules like scinderin, promoting actin nucleation and polymerization at the PM (Trifaro, *et al.,* 2000). Sequestration of PIP2 in MARCKS-enriched microdomains would reduce these PIP2 activities within the PM. Upon receptor activation and MARCKS translocation, local PIP2 pools become available for lateral diffusion in the PM where it will be available to PLC for conversion into DAG and IP3 (Wang, *et al.,* 2001); additionally, it will activate PLD and cytoskeletal remodeling proteins necessary for SG delivery and fusion to the PM (Wang, *et al.,* 2001; Trifaro, *et al.,* 2002; Wang, *et al.,* 2002). With this model, unphosphorylated MARCKS sequesters PIP2, creating a local PIP2 reservoir which MARCKS translocation would release, allowing generation of DAG and IP3. These second messengers would in turn activate calcium signaling to release scinderin to sever the actin barrier filaments and initiate the necessary SG trafficking. Accordingly, MARCKS-deficient cells would have increased PIP2-mediated stabilization of the cortical actin barrier, resulting in decreased regulated secretion, contrary to the increased secretion predicted by Figure 1.4A.

3. MARCKS tethers actin filaments to secretory granule membranes for transit to the PM. Recent advances have demonstrated that actin filaments do not simply play an inhibitory role in regulated exocytosis via the actin barrier, but that de novo actin polymerization around the SGs may also be important for SG delivery to the PM (Caroni, 2001; Eitzen, 2003; Park, *et al.,* 2006). As described in model #1, MARCKS can bind to and cross-link F-actin (Yarmola, *et al.*, 2001; Tapp, *et al.*, 2005). Recent data also suggest that MARCKS associates with SG membranes, tethering actin filaments to the SG membrane for trafficking to the PM (Singer, *et al.,* 2004). Evidence of MARCKS associating with lysosomal membranes has been previously demonstrated, and intracellular membrane association implicated based on FRAP (fluorescent recovery after photobleaching) experiments showing that MARCKS is relatively immobile once it translocates to the cytoplasm (Ohmori, *et al.,* 2000 ; Allen & Aderem, 1995). However, it is not clear whether MARCKS must associate with SG membranes to carry out its function in regulated exocytosis (Singer, *et al.,* 2004). According to this model, MARCKS-deficiency would be expected to reduce exocytic release by impairing SG trafficking. This mechanism proposes a regulatory role for MARCKS independent of the negative or positive regulatory roles in actin barrier disruption, as predicted by the two previous hypotheses.

MARCKS' role in regulated exocytosis remains incompletely understood. If unphosphorylated MARCKS is involved as a tether, which connects the actin barrier to the PM, increased mobility permitted by absence of MARCKS would result in increased regulated exocytosis, per the actin-tethering model. However, the same increased regulated exocytosis would not be expected if MARCKS is instead involved in PIP2 sequestration. If MARCKS is involved in other stages of cytoskeletal remodeling, a decrease in regulated exocytosis would

be expected due to interference with actin dynamics necessary for SG delivery to the PM. If MARCKS is involved in both actin barrier disruption and SG trafficking, the observed effects on regulated exocytosis would be much more convoluted. As a first step in unraveling the complexities of MARCKS function in regulated secretion, we tested whether or not MARCKS is essential for the process, using embryonic mast cells from MARCKS-deficient mice (Kitamura, *et al.*, 1979; Xia, *et al.,* 1997).

Physiological Significance of Mast Cells

Mast cells are key players in inflammatory reactions of all kinds, including acute and chronic allergic reactions, as well as innate immune responses to pathogens (Watanabe, *et al.,* 1999; Bischoff & Kramer, 2007; Metz & Maurer, 2007, Metcalfe, 2008). These cells can be found in two states: immature, bone marrow-derived progenitors and mature, mast cells adherent to tissue (Jamur, *et al.*, 2005; Metcalfe, 2008). Various receptor pathways can activate mast cells resulting in initiation of the inflammatory response, infiltration and differentiation of numerous immune cells and resulting pathological complications. In humans, a disease termed mastocytosis, characterized by the aberrant proliferation of mast cells, has expanded into a group of seven pathological variants, ranging in severity and prognostic life expectancy (Metcalfe, 2008). In cardiac tissue, resident mast cells have been implicated in ischemia reperfusion injury, graft rejection after cardiac transplant and beginning and end-stage cardiac hypertrophy leading to cardiac failure (Shiota, *et al.,* 2003; Balakumar *et al.,* 2007).

In the respiratory system, mast cell activation can lead to a hypersensitivity response resulting in excessive mucus secretion in the upper airways and lungs, as well as lung edema and bronchospasms associated with asthma (Prussin & Metcalfe, 2003; Metz & Maurer, 2007

Fig. 1.5: Mast cell regulated exocytic pathways

Mast cell regulated exocytosis can be activated through various receptors. FcεRI, is a tyrosine kinase receptor commonly utilized in mast cell secretion studies. G-protein coupled receptors present in the membrane vary by tissue, but often include complement receptors and proteinase-activated receptors (PARs). Activation of PLC by either receptor pathway results in generation of the second messengers DAG and IP3. DAG activates PKC, which would in turn phosphorylate MARCKS and induce MARCKS translocation to the cytosol. Both IP3 and Sphingosine-1 phosphate (S1P) are signaling molecules that can be activated to mobilize calcium for secretion.

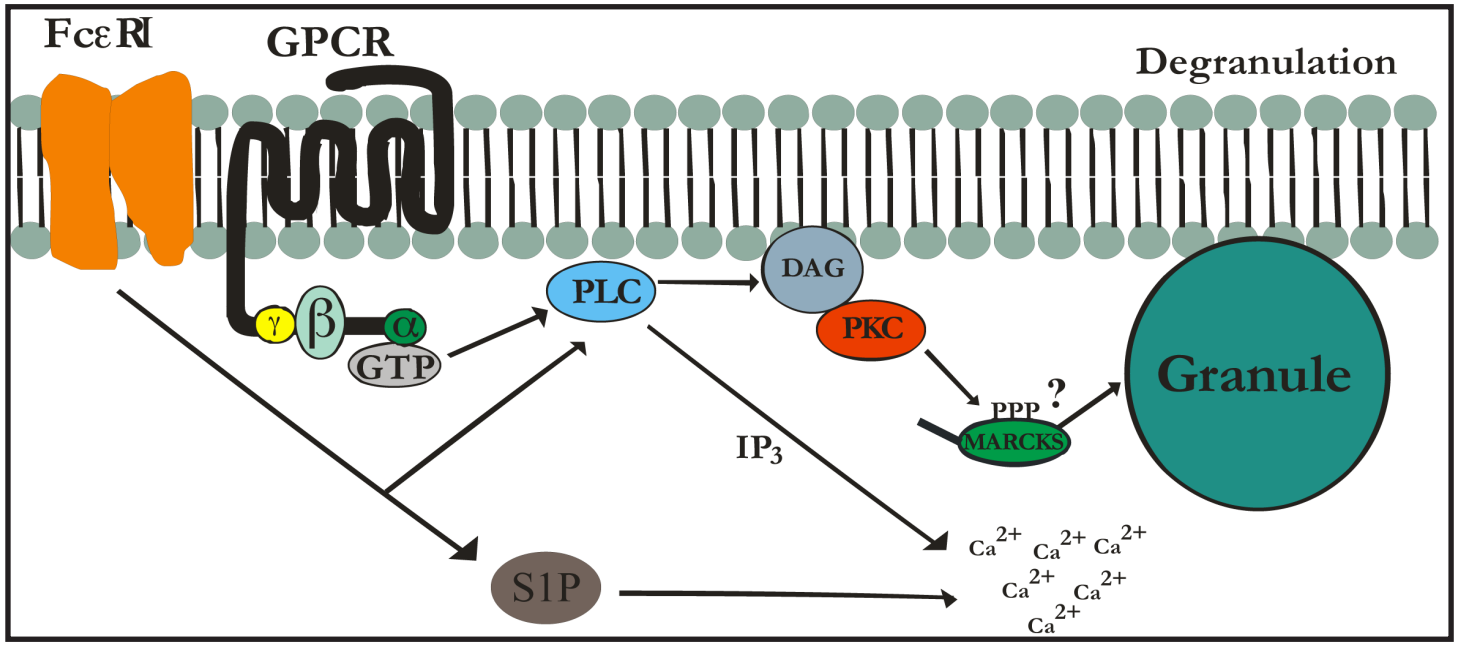
FcεRI
GPCR
Degranulation
γ
β
α
GTP
PLC
DAG
PKC
PPP
?
MARCKS
Granule
IP3
S1P
Ca2+ Ca2+ Ca2+
Ca2+ Ca2+
Ca2+

Gonzalo, *et al.,* 2007). Polymorphonuclear cell (PMN) infiltration is part of a typical inflammatory response and in pathological situations can result in significant tissue damage. Under conditions of allergic sensitization, lung alveoli of mast cell-deficient mice were found to have significantly attenuated PMN infiltration compared to mast cell-sufficient controls. This mast cell-deficiency did not affect initial alveolar inflammation, probably initiated by resident macrophages, rather only affecting the resulting PMN chemotaxis (Baumann *et al.,* 2001). Another study showed that increased mast cell accumulation sensitized mice so that an enhanced inflammatory response was observed for both antigen-mediated and chemically-induced activation (Kalin, *et al.*, 2008). Additionally, multiple regulated exocytic products of mast cells have been linked to the airway hypertensive response associated with asthma and bronchoconstriction (Bradding, *et al.*, 2006; Gonzalo, *et al.*, 2007; Ryzhov, *et al.*, 2008). Exocytic release of the CC chemokine ligand 1 (CCL1) has been identified as a mast cell-dependent product that triggers the pulmonary inflammation response, including mucus hypersecretion. The study included the observation that asthmatics had a five-fold increase in the level of CCL1, indicating that mast cell regulated exocytosis significantly contributes to the airway hyperresponsiveness and inflammation associated with asthma (Gonzalo, *et al.*, 2007).

In the systemic circulation, mast cells contribute to multiple kinds of hypersensitivity including acute inflammatory responses and autoimmune vasculitis (necrotizing inflammation of vessel walls). Mast cell-deficient mice showed significantly attenuated PMN infiltration when cutaneous vasculitis was induced in vivo. These observations are donor variable and have been attributed to FcγRs and complement receptors found on mast cells (Baumann *et al.,* 2001; Watanabe *et al.,* 1999). Additionally, the ability to induce skin vasculitis in FcR-deficient mice was returned with transfer of wild type bone marrow-derived mast cells, but not macro-

phages (Sanchez-Mejorada and Rosales, 1998; Baumann *et al.,* 2001; Watanabe *et al.,* 1999). All of these roles for mast cells result from their ability to release numerous pro-inflammatory mediators, such as TNF-α, interleukins, lipid mediators, tryptase, chymase, serotonin and histamine into the resident tissue through regulated exocytosis upon receptor activation (Metz and Maurer, 2007; Prussin and Metcalfe, 2003).

Mechanism of Mast Cell Degranulation

The mechanism by which mast cell degranulation induces these multiple immune functions has long been studied. Mast cell degranulation (Fig. 1.5) is a form of regulated exocytosis and can be mediated through the receptor tyrosine kinase FcεRI, a high affinity immunoglobulin E (IgE) receptor (Stinchcombe *et al.,* 2004). FcεRI belongs to a family of membrane receptors found on hematopoietic cell types recognizing different immunoglobulins. Specifically, IgE-mediated degranulation has been linked to cutaneous and systemic anaphylaxis (Sanchez-Mejorada and Rosales, 1998; Watanabe *et al.,* 1999; Baumann *et al.,* 2001).

In the process of degranulation, IgE is involved in a positive feedback loop. Presence of IgE increases the surface expression of FcεRI, which in turn enhances mediator release upon antigen activation (Yamaguchi, *et al.,* 1999). This corresponds well with the idea of type I hypersensitivity after passive sensitization. First, IgE binds to the FcεRI. Antigen binding to this immune complex crosslinks and activates the receptor, inducing tyrosine kinase phosphorylation. Tyrosine phosphorylation activates Spleen tyrosine kinase (Syk), which initiates numerous pathways for mediator formation, degranulation and calcium mobilization. Calcium mobilization is an obligate event for degranulation and is mediated through the secondary messenger sphingosine-1-phosphate (S1P) and inositol trisphosphate (IP3) for tyrosine

kinase receptors (Lee *et al.,* 2005). Notably, Syk activates PLC inducing the formation of diacylglycerol (DAG), which activates PKC to act on its substrates (Sanchez-Mejorada and Rosales, 1998). Other membrane receptors of the FcR family, the FcγRs, bind immunoglobulin G (IgG) and operate via much the same mechanism. These have been shown through gene disruption studies to be the key players in type III systemic anaphylactic responses and PMN infiltration-derived tissue damage.

The other class of receptors involved in mast cell degranulation is G protein-coupled receptors (GPCRs). Numerous GPCRs can be found on mast cells including protease-activated receptors (PARs), peptide receptors, and purinergic receptors (Suto, *et al.*, 1996; van der Kleij *et al.,* 2003; Bulanova, *et al.,* 2005). The pathway each receptor initiates is diverse and dependent on different G proteins. Since MARCKS is regulated by PKC phosphorylation and present in WT eHMCs (Fig. 2.1), regulated exocytic pathways involving PKC activation can be used to determine the specific effects of MARCKS on secretion utilizing null MARCKS embryonic hepatic-derived mast cells (eHMCs) (Kitamura, *et al.*, 1979; Xia, *et al.,* 1997).

Chapter 2

MARCKS acts as a negative modulator of FcepsilonR-mediated mast cell regulated exocytosis

ABSTRACT

A variety of data on Myristoylated alanine-rich C kinase substrate (MARCKS) suggest a possible correlation between its plasma membrane (PM) to cytosol translocation in activated secretory cells and regulated exocytosis. Unfortunately, the MARCKS null mouse, with its perinatally lethal phenotype caused by defects in the development of the neural tube, has thwarted efforts to use this mouse model as a tool in determining if the relationship is causal. Embryonic mast cells, though, are one type of secretory cell which can be isolated and cultured from the MARCKS null mouse. We studied the role of MARCKS in mast cell regulated exocytosis by comparing the secretion of embryonic hepatic-derived MARCKS-sufficient (WT) and MARCKS-deficient mast cells stimulated through the high affinity IgE receptor, FcεRI. When mast cells were stimulated with antigen while in suspension, conditions frequently used for mast cell secretion assays, no difference was detected. However, MARCKS-deficient cells did demonstrate potentiated secretion compared to WT cells when adherent cells were stimulated, a condition mimicking the microenvironment of mature mast cells in all major organs. Kinetically, MARCKS null cells exhibited enhanced early release of secretory cargo versus WT-derived cells, suggesting a role for MARCKS as a negative regulator of secretion. As an independent approach, we applied peptides with N-terminal sequences that are purported to

exercise a MARCKS-specific inhibition to the mast cells and found no MARCKS-specific inhibition: both WT and MARCKS-deficient cells were inhibited equally. Thus, MARCKS appears not to be essential in regulated exocytosis in mast cells. It appears, instead, to modulate secretion in a negative fashion, by mechanisms that remain to be elucidated.

INTRODUCTION

MARCKS and the homologous MRP comprise a two-member gene family. Both were discovered as PKC substrates regulated developmentally and spatially (Blackshear, 1993; Yokoyama, *et al.*, 1998) and purportedly serve many diverse functions in cell adhesion, motility and secretion. Typically, both are intimated to effect these functions through regulation of the actin cytoskeleton (Umekage & Kato, 1991; Blackshear, *et al.*, 1992; Lobach, *et al.*, 1993; Yokoyama, *et al.*, 1998; Chu, *et al.*, 2002; Arbuzova, *et al.*, 2002; Disatnik, *et al.*, 2004; Eckert, *et al.*, 2010). MARCKS, specifically, has been implicated as a regulator of regulated exocytosis in a wide variety of immune, endocrine, and exocrine secretory cell types (Rose, *et al.*, 2001; Li, *et al.*, 2001; Singer, *et al.*, 2004; Li, *et al.*, 2005; Eliyahu, *et al.*, 2005; Eliyahu, *et al.*, 2006; Park, *et al.*, 2006). Cargo for regulated exocytosis is stored in secretory granules (SGs) or vesicles, which, following cell activation and initiation of second messenger signaling, negotiate through a network of cortical actin filaments lying between them and the PM. Rapid disruption and remodeling of the actin allows SGs to migrate to exocytic docking sites on the PM, enabling SNARE-mediated fusion and cargo exocytosis (Bader, *et al.,* 2004; Malacombe, *et al.,* 2006; Rizo, *et al.,* 2006).

Notably, the regulatory components involved in the remodeling of cortical actin remain significantly less well understood than other portions of the regulated exocytic pathway (Bader, *et al.,* 2004; Malacombe, *et al.,* 2006). Some studies have linked MARCKS to regulated exocytosis without implicating any particular mechanism of action (Elzagallaai, *et al.*, 2000; Li, *et al.*, 2005; Doreian, *et al*., 2009), while others have specifically investigated the relationship between MARCKS and actin dynamics (Rose, *et al.*, 2001; Jerdeva, *et al.*, 2005; Park, *et al.*, 2006). A hypothesis for the initial disruption of cortical actin postulates that the proteins

MARCKS and scinderin regulate this event (Vitale, *et al.*, 1991; Rose, *et al.*, 2001; Trifaro, *et al.*, 2002; Arbuzova, *et al.*, 2002; Pene, *et al.*, 2005). In resting cells, MARCKS is found localized to the PM along with the cortical actin filaments (Ehre, *et al.,* 2005; Malacombe, *et al.,* 2006). Previous experiments have demonstrated that following extracellular activation, multiple PKC isoforms are activated and MARCKS, a major PKC substrate, is among the proteins phosphorylated (Lobach, *et al.,* 1993; Aderem, 1995; Trifaro, *et al.*, 2002). PKC phosphorylation induces MARCKS to translocate from the PM to the cytosol, which according to the hypothesis, results in actin destabilization by removal of its tether to the PM. Ca2+-activated scinderin-mediated filament severing may also contribute to this process (Ohmori, *et al.,* 2000; Trifaro, *et al.*, 2000; Trifaro, *et al.*, 2002). With actin filament destabilization, the SGs access exocytic docking sites, fuse with the PM, and release their cargo (Bader, *et al.,* 2004; Malacombe, *et al.,* 2006; Rizo, *et al.,* 2006; Davis & Dickey, 2008).

Chromaffin cell secretion studies have led to the proposal of a significant role for MARCKS in regulated exocytosis, based on experiments where treatment of cells with MARCKS PSD peptides and siRNA decreased regulated secretion (Rose, *et al.*, 2001; Park, *et al.*, 2006; Doreian, *et al.*, 2009). Taken together, these results suggest that MARCKS is a positive, possibly essential, regulator of regulated exocytosis. Similar results were shown for regulated exocytosis in platelets (Elzagallaai, *et al.*, 2000;), oocytes (Eliyahu, *et al.*,2005; Eliyahu, *et al.*, 2006), normal human bronchial epithelial cells (Li, *et al.*, 2001; Singer, *et al.*, 2004), and endocrine cells (Liu, *et al.*, 1994; Rose, *et al.*, 2001; Li, *et al.*, 2005; Jerdeva, *et al.*, 2005; Park, *et al.*, 2006; Doreian, *et al.*, 2009). We sought to test whether the complete absence of MARCKS affected regulated exocytosis in a similar manner, by making use of the MARCKS-deficient mouse. Since this mouse has a perinatally lethal phenotype due to defects

in neural tube closure (Umekage & Kato, 1991; Blackshear, *et al.*, 1992; Lobach, *et al.*, 1993), we adapted culture systems for growing embryonic hepatic-derived mast cells to address this question (Xia, *et al.*, 1997).

MATERIALS & METHODS

Mast Cell Culture and Isolation

Bone marrow-derived mast cells (BMMCs) were isolated from the femurs of 6–10 week old C57/BL6J. Once isolated, cells were cultured in complete medium consisting of RPMI 1640 media supplemented with L-glutamine, 10% fetal bovine serum (FBS), 1M Hepes Buffer, non-essential amino acids, sodium pyruvate, β-mercaptoethanol, penicillin/ streptomycin, 20 ng/mL IL-3 (Peprotech), and 20 ng/mL murine stem cell factor (Peprotech) and incubated at 37ºC in a 5% CO2 atmosphere. Cultures were resuspended into fresh media every 3–4 days ,and after 4–5 weeks mast cells were assayed for the presence of the FcεRI on the cell surface, a marker of mature mast cells (Jamur, *et al.*, 2005).

Embryonic hepatic-derived mast cells (eHMCs) resulting from the mating of either MARCKS or MRP heterozygotes were isolated from homogenized livers of E14-E18 embryos on a C57Bl/6J genetic background (Barker, 1968; Xia, *et al.*, 1997). Cells were cultured in suspension with complete medium and incubated at 37ºC in a 5% CO2 atmosphere for 4–5 weeks. Mast cells in suspension were resuspended into fresh media every 3-4 days. The maturity of the mast cell cultures was assessed for 5 week old mast cells using the same methods described in the following section.

Immunohistochemical Analyses of Mast Cell Purity and Maturation

Five week old mast cells were allowed to adhere overnight to fibronectin-coated glass coverslips contained in 6-well plates. Media was then removed from the cells and the cells were gently rinsed three times with Siraganian Buffer (SG buffer). Prior to labeling, cells were blocked for one hour at room temperature with the mouse CD32/CD16 antibody (1:50)

to reduce non-specific labeling of lower affinity IgE FcR family members. Cells were then incubated for one hour with the primary mouse anti-DNP IgE antibody (1:25) (BD Biosciences). After three rinses with SG buffer, cells were incubated with a rat anti-mouse FITC-anti IgE antibody (BD Biosciences) for one hour at room temperature, then fixed with 4% paraformaldehyde (PFA) in PBS for 7 minutes.The coverslips were mounted onto glass slides using the Prolong Gold Antifade (Invitrogen) mounting media. Slides were stored in the dark at 4ºC until the imaging experiments. Approximately 100 cells were analyzed using a widefield Leica DMIRB inverted microscope with a 40X oil PlanFluor objective (1.25 NA) and FITC dichroic filter settings (Excitation: 480/40; Emission: 535/50). Three independent experiments confirmed a >99% pure and mature mast cell population (Suppl. Fig. S1). All microscopy work was performed in the Michael Hooker Microscopy Facility at UNC-Chapel Hill. As a second staining technique, cells from the same cultures were adhered to coverslips, blocked with the CD32/CD16 antibody, as above, and incubated with the mouse FITC-anti FcεRI alpha subunit antibody (1:25) for one hour at room temperature (eBioscience) before fixation. Coverslips were mounted onto glass slides and once more >99% pure culture of mature mast cells were detected.

***In vitro* β-hexosaminidase secretion assays**

Cells (1 X 10^6/ mL) were sensitized overnight at 37ºC with DNP-IgE (250 ng/mL; clone SPE-7; Sigma). After sensitization, cells were removed from the presence of IgE. For suspension assays, cells were centrifuged down and resuspended in fresh media for 24 hours prior to activation. For adherent assays, cells were centrifuged down, resuspended in fresh

media, and incubated in fibronectin-coated wells (20 ug/mL) of a 96-well plate overnight. Complete medium was then replaced with 100 uL of SG Buffer [119 mM NaCl, 5 mM KCl, 25 mM PIPES disodium salt, 5.6 mM glucose, 1 mM CaCl2, 0.4 mM MgCl2, and 0.1% BSA]. Cells were challenged with varying doses of bovine DNP-albumin conjugate (DNP) (1-100 ng/mL; Calbiochem) or Buffer as control at 37ºC for the time period specified. All dose response studies utilized a thirty minute incubation. The amount of secretion was measured as the % of total cellular β-hexosaminidase secreted into the supernatant, calculated as (hexosaminidase released) / (total hexosaminidase in the supernatant and lysate). Each measurement was taken in triplicate and the mean value was calculated from seven or more independent experiments.

MANS Peptides Studies

The MANS (MA-GAQFSKTAAKGEAAAERPGEAAVA) and RNS (MA-GTAPAAE-GAGAEVKRASAEAKQAF) peptides were kindly provided by Dr. Kenneth Adler at North Carolina State University. The non-myristoylated MANS (NONG) peptide was synthesized by Tufts University Core Facility with the sequence of the MANS peptide but lacking the Glycine residue to which the myristoyl moiety is normally attached. Adherent eHMCs were incubated overnight with DNP-IgE (250 ng/mL; clone SPE-7; Sigma) at 37ºC, prior to an overnight incubation with fibronectin-coated wells of a 96-well plate. Fifteen minutes prior to activation with 3 ng/mL of DNP-BSA, cells were pretreated with SG Buffer containing either 50 or 100 uM concentrations of one of the MANS peptides: MANS, RNS, or NONG. Cells were then activated with 3 ng/mL of DNP-BSA and incubated at 37ºC for thirty minutes. The remaining steps of the secretion assay were performed as described in the above *in vitro* β-hexosaminidase secretion assays section.

3-D Cell Reconstruction

Adherent eHMCs were sensitized overnight at 37ºC with DNP-IgE (250 ng/mL; clone SPE-7; Sigma), then incubated for specified time periods on fibronectin-coated (20 ug/mL) temperature-controlled glass bottom dishes (Bioptechs). Cells were incubated in a SG buffer bath containing the lipophilic membrane dye, FM 4-64 FX fixable analog (Invitrogen). Ten minutes after addition of FM 4-64, cells were imaged using Leica SP2 laser scanning confocal microscope with a 561 HeNe laser line and a 63X 1.4 NA PlanApo oil objective. Images were captured using detector window settings for Texas Red (Excitation: 561 HeNe laser line, Emission: 580-680). The image series of x-y plane sections were captured at designated steps along the z-axis and imported into Volocity (v4.4 Perkin Elmer), a 3-D rendering program. From the renderings, cell height and cross-sectional area measurements were quantitated. All microscopy work was performed in the Michael Hooker Microscopy Facility at UNC-Chapel Hill.

Cortical Actin Volume Quantitation

Adherent eHMCs were sensitized overnight at 37C with DNP-IgE (250 ng/mL; clone SPE-7; Sigma), then incubated on fibronectin-coated (20 ug/mL) glass coverslips for 24 hours. Unadherent cells were aspirated off and cells were fixed with 4% paraformaldehyde. For 15 minutes, cells were permeabilized with 0.1% Triton X-100 (Sigma), washed, then incubated with Alexa Fluor 488-phalloidin for 25 minutes. Coverslips were mounted onto slides and imaged using a Leica SP2 laser scanning confocal microscope with a 561 HeNe laser line and a 63X 1.4 NA PlanApo oil objective. The z-stack images were then imported into Volocity. Each individual cell was isolated as a region of interest and phalloidin intensity, thresholded to exclude background intensity, was used to delineate the parameters of the cell. A conflu-

ent mask was then generated by having any regions of low fluorescent intensity, which were encompassed on all sides by areas of high intensity included in the calculation. From the cell perimeter determing using the mask applied to each optical section of a cell, cell volume was calculated.

Statistical Analysis of Mean Values

Statistical differences between the means of two groups were determined by the unpaired two-tail student's t-test. *P* values below 0.05 are regarded as statistically significant and are indicated by asterisks.

Factorial Combination Analysis

The number of possible combinations for the total sixteen data sets taken six at a time were calculated using the equation ${}_nC_r = n!/(r!(n-r)!)$ and totaled 8,008. Each possible combination and its corresponding p-value was generated by MatLab (The MathWorks, Inc., MA) software using an algorithm kindly written by Abijhit Gurjarpadhye (Virginia Tech, VA). The percent of p-values greater than 0.05 was calculated after sorting the values in ascending order using Microsoft Excel.

Figure 2.1: WT eHMCs express both homologous MARCKS gene family members MARCKS and MRP cDNA levels are shown for both WT (+/+) and MARCKS-deficient (–/ –) eHMCs. The approximately 400 and 300 kb cDNA products were reverse transcribed from equal levels of isolated mRNA.

(A) MARCKS null eHMCs clearly lack MARCKS cDNA, while WT eHMCs demonstrate a strong level of expression.

(B) Both MARCKS WT and null eHMCs, express MRP. Significantly, MARCKS-deficient cells do not show a compensatory upregulation due to loss of MARCKS.

A

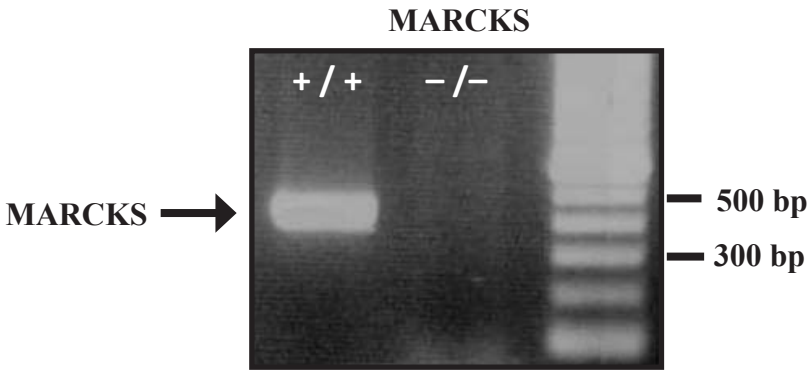

B

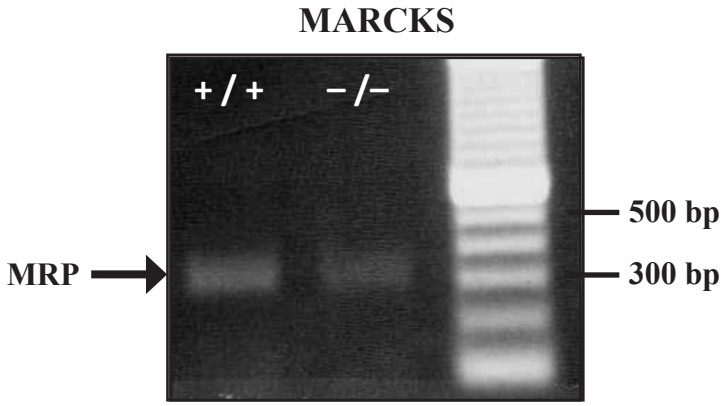

RESULTS

To study the direct effects of MARCKS-deficiency on regulated exocytosis, we first adapted a sytstem for isolating, differentiating, and studying secretory cells from mouse embryos, a critical step since gene disruption results in mouse perinatal lethality (Blackshear, *et al.*, 1992; Lobach, *et al.*, 1993). We chose to isolate mast cells, immune cells specialized for regulated exocytic secretion (Watanabe, *et al.*, 1999; Prussin & Metcalfe, 2003; Shiota, *et al.*, 2003; Balakumar, *et al.*, 2007; Bischoff & Kramer, 2007; Metz & Maurer, 2007; Metcalfe, 2008). Previous studies have demonstrated that both MARCKS and MRP are expressed in other types of immune cells, and even upregulated in response to inflammatory stimuli (Thelen, *et al.*, 1990; Rose, *et al.*, 1996; Chang, *et al.*, 1999).

The most common source for isolating mast cells for *in vitro* differentiation is from the bone marrow of 6-12 week old mice, where immature, mast cell progenitors are located (Jamur, *et al.*, 1995). Since this isolation source was a system unsuitable for our purposes, we adapted the technique to isolate mast cells from embryonic livers, a tissue source where mature mast cells would be localized (Barker, 1968; Xia, *et al.*, 1997), allowing us to obtain WT, MARCKS-deficient, and MRP-deficient embryonic hepatic-derived mast cells (eHMCs). The use of eHMCs as a mast cell secretory system was validated by comparing the responsivity of WT BMMCs, derived from adult mice, to eHMC cultures activated with ionomycin, (Suppl. Fig. S2), phorbol ester-mediated enhancement of ionomycin response (Suppl. Fig. S3), and antigen stimulation of the high-affinity IgE tyrosine kinase receptor, FcεRI (Suppl. Fig. S5). Phorbol ester-mediated enhancement of ionomycin activation in mast cells did exhibit one variation between WT BMMCs and eHMCs. While pretreatment with almost all PMA doses increased BMMC responsivity to activation with 0.5 uM ionomycin, eHMCs demonstrated

no significant difference at any PMA dose when activated with 0.5 uM ionomycin (results not shown). However, when eHMCs were pretreated with PMA at varying doses and stimulated with a lower dose of ionomycin, 0.25 uM, a similar enhancement of secretion was observed in eHMCs. Thus, overall, results from both systems were comparable, and secretory responses were within the range of previously published data in every case (Sudo, *et al.*, 1996; Hua, *et al.*, 2007; Ryzhov, *et al.*, 2008; Melicoff, *et al.*, 2009).

The lack of MARCKS cDNA expression was confirmed in MARCKS-deficient eHMCs; WT and MARCKS null cells expressed similar levels of MRP cDNA (Fig. 2.1). To determine the effects of MARCKS-deficiency on the ability of mast cells to exocytose SG contents, we measured the activity of secreted β-hexosaminidase, an enzyme contained within the SGs. WT and MARCKS-deficient eHMCs under suspension conditions were compared and, surprisingly, no differences in secretory behavior were detected. Both genotypes demonstrated similar responsivity for both spontaneous release (4.25+/- 0.71 versus 2.89+/- 0.68% of total hexosaminidase content) and FcεRI-stimulated regulated exocytosis (maximal stimulated release of 17.25 +/- 2.48 versus 20.92 +/- 3.46% of total hexosaminidase content) (Suppl. Fig. S6).

Mature mast cells, unlike the hematopoietic mast cells in the bone marrow, are found localized in, and adherent to, the extracellular matrix of resident and target organ tissue (Kitamura, 1979; Columbo, *et al.*, 1995; Metcalfe, 2008). When mast cells were adhered to substratum proteins of the extracellular matrix, an increase in mast cell sensitivity to agonist stimulation was demonstrated, an effect attributed to a primed state of cell activation for adherent cells (Vuori & Ruosahlti, 1993; Columbo, *et al.*, 1995; Kruger-Krasagakes, *et al.*, 1999). Notably, MARCKS expression has also been shown to be increased in immune cells primed for immune

Figure 2.2: Adherence to fibronectin enhances regulated exocytosis in WT eHMCs

WT eHMCs were primed with anti-DNP IgE and either allowed to adhere to fibronectin (open) (n=16) or left in suspension (filled) (n=7) for 24 hours prior to stimulation with DNP-BSA for thirty minutes.

Values were measured as the amount of β-hexosaminidase activity released into the supernatant compared to the total activity from both supernatant and cell lysate. The release of cells stimulated through FcεRI was subtracted from the spontaneous release from unactivated cells. (Error bars represent S.E.; ** $p<0.01$.; ***$p<0.001$)

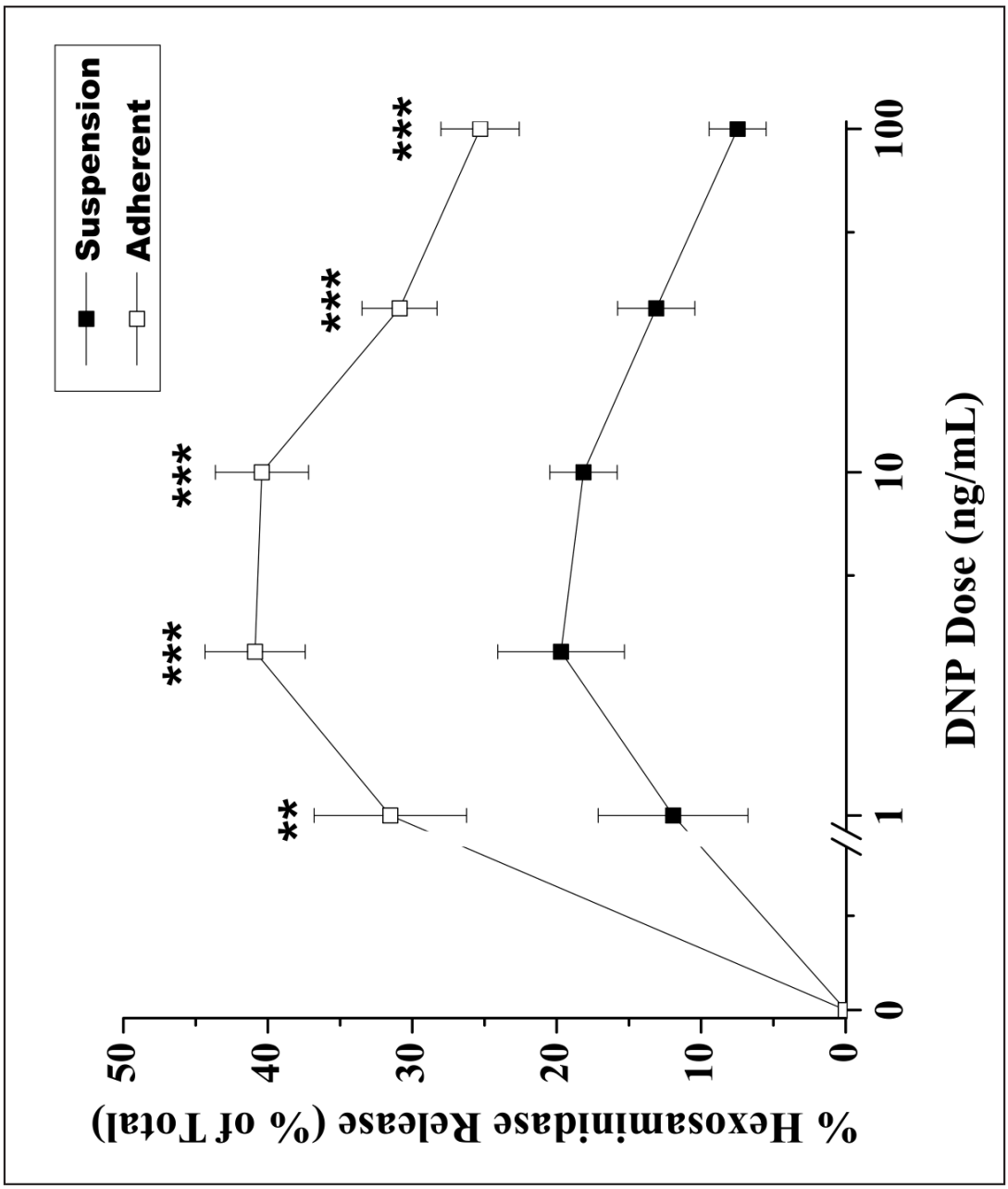
Suspension
Adherent
% Hexosaminidase Release (% of Total)
DNP Dose (ng/mL)
0
10
20
30
40
50
0
1
10
100
**
***
***
***
***

Figure 2.3: MARCKS-deficiency enhances regulated exocytosis in adherent cells

(A) WT (+/+) and MARCKS-deficient (– / –) eHMCs were adhered to fibronectin for 24 hours prior to stimulation with DNP-BSA at five different doses for thirty minutes. The amount of hexosaminidase release from the cells, after subtraction of spontaneous release (<5%), is compared between WT (n=16) and MARCKS-deficient (n=16) cells in a dose-effect study.

(B) The amount of total hexosaminidase activity, a measure of the amount of hexosaminidase content released and contained within the cell, was similar between WT (n=16) and MARCKS null cells (n=16).

(Error bars represent S.E.; * $p<0.05$; *** $p<0.001$)

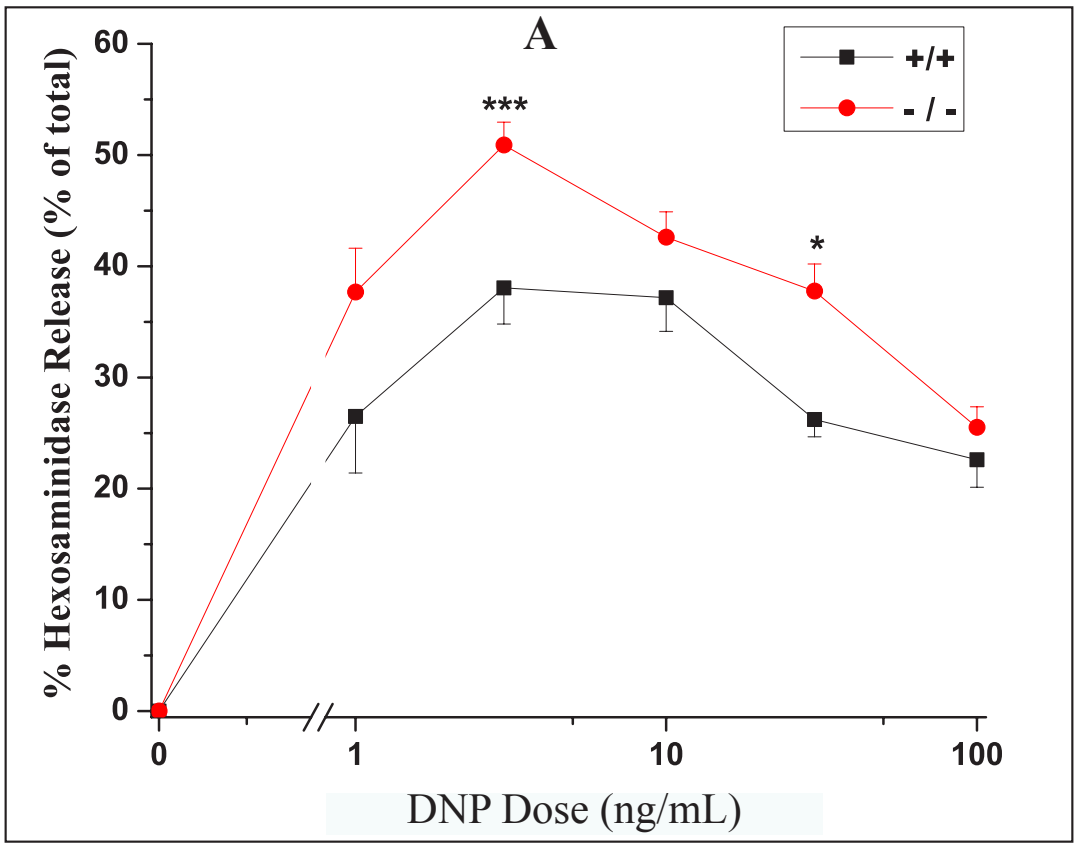
A
+/+
- / -
***
*
% Hexosaminidase Release (% of total)
60
50
40
30
20
10
0
0
1
10
100
DNP Dose (ng/mL)

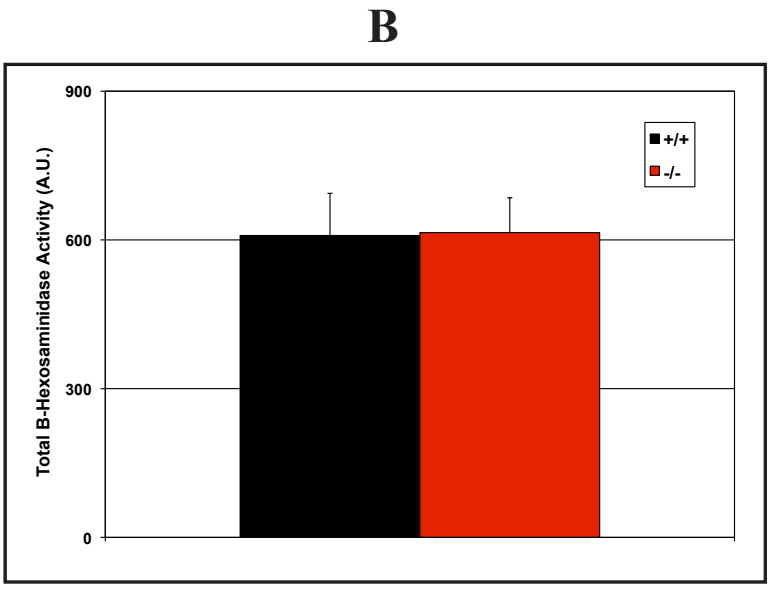
B
900
600
300
0
Total B-Hexosaminidase Activity (A.U.)
+/+
-/-

challenge (Thelen, *et al.*, 1990; Rose, *et al.*, 1996; Chang, *et al.*, 1999). Therefore, we tested the secretory responses of adherent WT and MARCKS-deficient eHMCs after adherence to fibronectin for 24 hours. WT eHMC secretion levels from cells adhered to fibronectin, prior to DNP stimulation, experimentally confirmed the observations from previous studies by demonstrating an approximately three-fold increase in the amount of secretion compared to cells stimulated under suspension conditions (Fig. 2.2). Cells under both conditions, though, had similar hexosaminidase contents (Suppl. Fig. S4).

A comparison of adherent WT and MARCKS-deficient cells in the resting state, however, did reveal a significantly different cell morphology phenotypes. As shown in Supplementary Figure S7, the frequency distributions for both average cross-sectional areas and cell heights in living MARCKS null cells stained with the membrane dye, FM 4-64, were left-shifted compared to WT cells, indicating decreased cell volumes for MARCKS null cells. These results were confirmed using phalloidin to label cortical actin filaments. Both methods suggested an approximately 30% decrease in cell volume for MARCKS-deficient cells compared to WT (Suppl. Fig. S7-S8).

Modulation of mast cell regulated exocytosis induced by MARCKS-deficiency

After adherence to fibronectin, WT and MARCKS null cells showed clearly different responses to activation by DNP: the MARCKS null cells responded more vigorously than WT cells at every DNP concentration tested (Fig. 2.3A). Although the differences were not statistically significant at three of the five DNP concentrations tested, at the peak of the response (3 ng/mL) the MARCKS null cells secreted 34 +/-5% more hexosaminidase than WT. This differential is of a magnitude which could well be significant pathologically (see Discussion). The

Figure 2.4: MRP-deficiency is similar to WT secretory behavior

Adherent WT (+/+) and MRP-deficient (– / –) mast cells were tested for their respective antigen-stimulated responsivity. No differences were detected between WT (filled) (n=4) and MRP null (open) (n=3) mast cells. The dose response curve demonstrates the β-hexosaminidase release in response to each DNP-BSA concentration through the tyrosine kinase FcεRI-mediated pathway. Once more, the peak stimulatory response for WT and MRP-deficient cells was at the antigen concentration of 3 ng/mL of DNP-BSA. The WT and MRP null mast cells derived from embryos of the same litter were isolated from mice kindly provided by Dr. Perry Blackshear at the National Institute of Environmental Health Sciences and allowed to adhere to fibronectin for 24 hours prior to DNP stimulation.

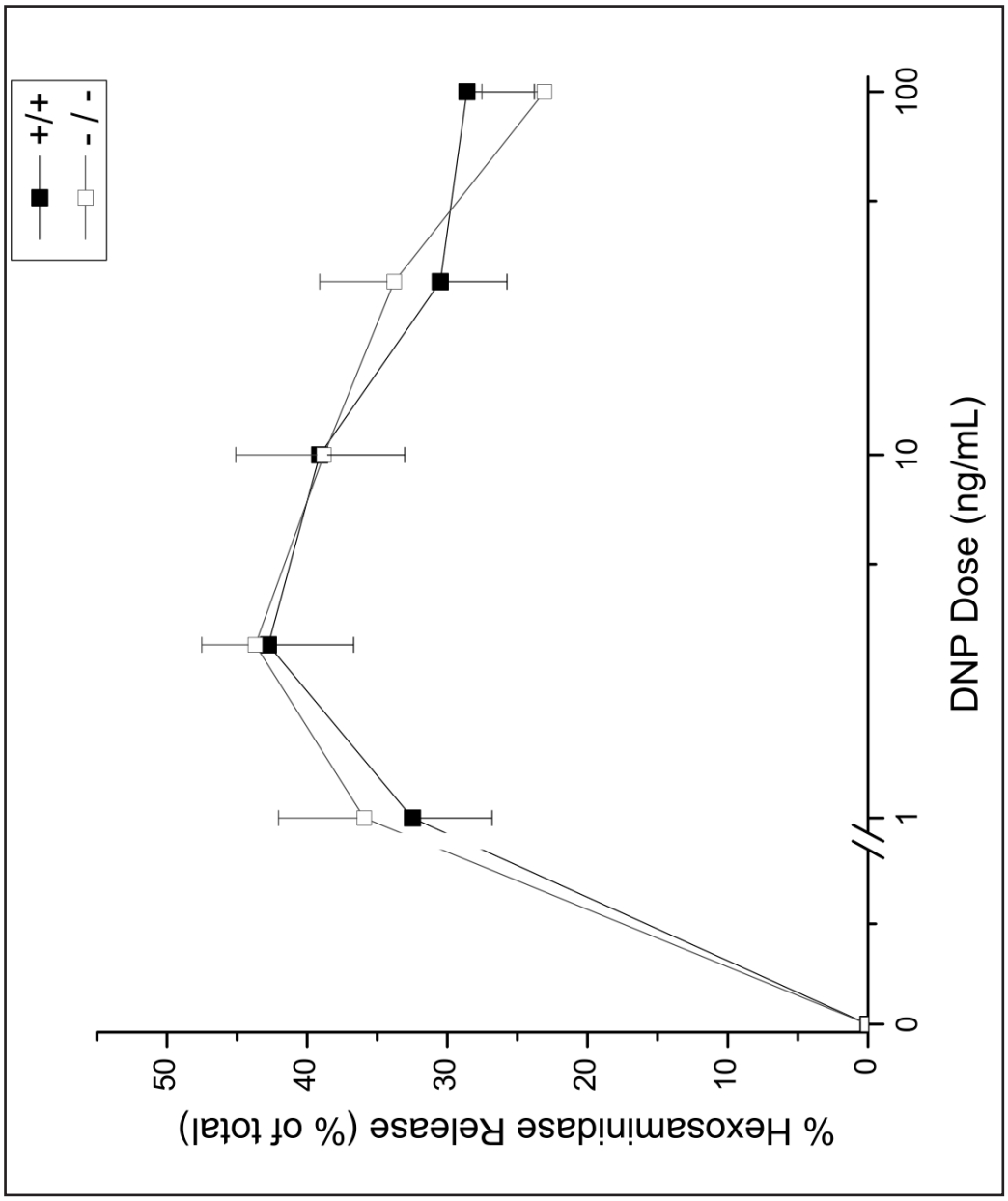
% Hexosaminidase Release (% of total)
0
10
20
30
40
50
0
1
10
100
DNP Dose (ng/mL)
+/+
- / -

Figure 2.5: MARCKS-deficiency accelerates the rate of regulated exocytic release

The time course of hexosaminidase release from WT and MARCKS-deficient eHMCs adhered to fibronectin for 24 hours before the cells were activated with 3 ng/mL DNP-BSA at various time periods prior to the full thirty minute incubation period. MARCKS-deficient eHMCs demonstrated an enhanced release of hexosaminidase within the first two minutes compared to WT release (n=6 null embryos, n=10 WT embryos). Each time point value represents the amount of hexosaminidase released at that time point normalized to the total amount of hexosaminidase released during the full thirty minute incubation period. * $p<0.05$

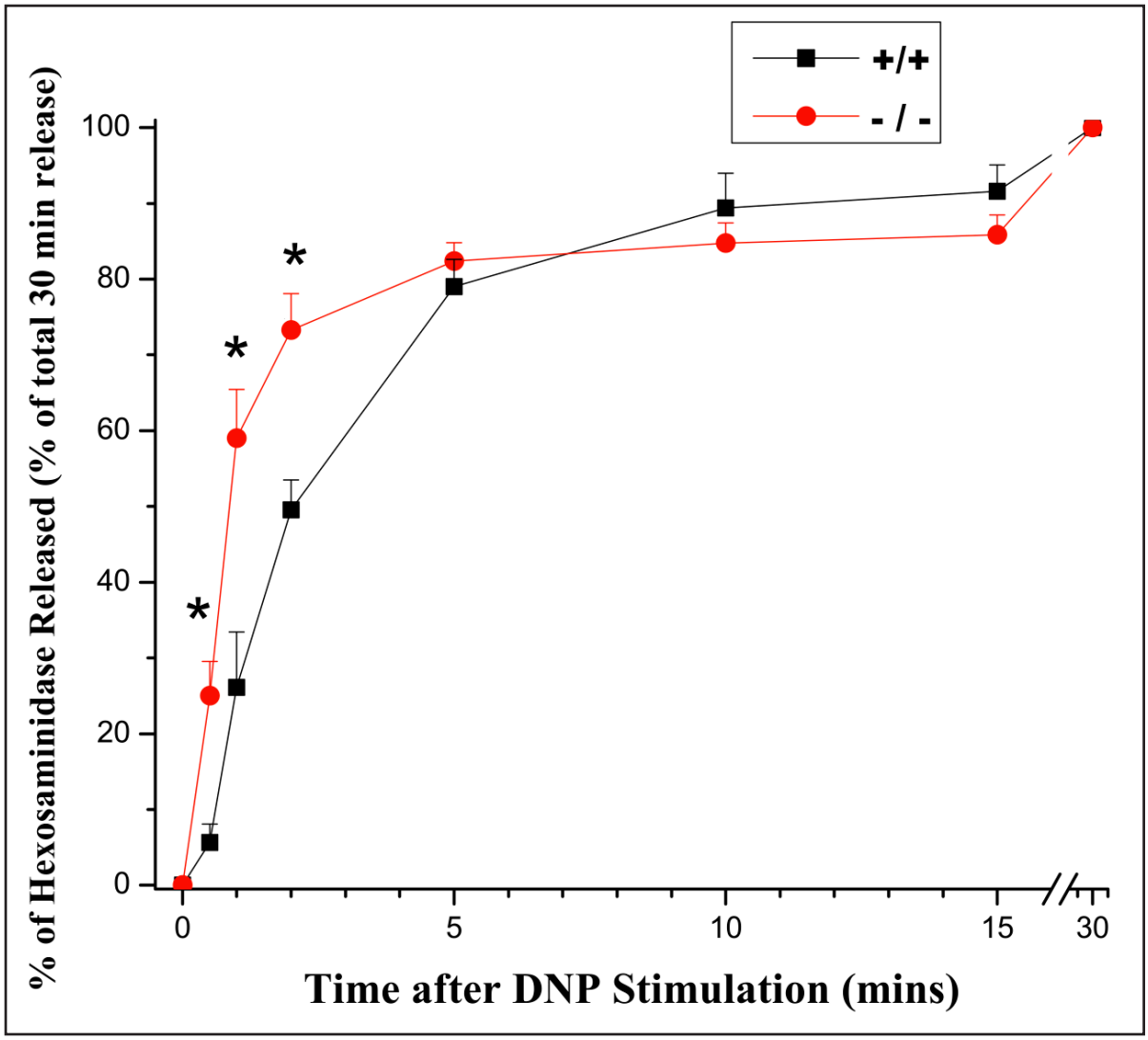
+/+
- / -
% of Hexosaminidase Released (% of total 30 min release)
100
80
60
40
20
0
*
*
*
0
5
10
15
30
Time after DNP Stimulation (mins)

enhancement of secretion seen with 24 hours of fibronectin adherence after stimulation with 3 ng/mL of DNP was also observed with cells stimulated after 96 hours of fibronectin adherence (Suppl. Fig. S9). However, the total cellular content of hexosaminidase remained similar between WT and MARCKS-deficient cells in every experiment (Fig. 2.3B), suggesting that MARCKS-deficiency is modulating the magnitude of regulated exocytic cargo released, not the amount exocytic cargo contained within the cells (Fig. 2.3A).

MRP-deficiency does not modulate mast cell regulated exocytosis

To determine if the potentiation of mast cell regulated exocytosis resulting from MARCKS-deficiency was a MARCKS-specific function, the effect of MRP-deficiency was tested. MRP null mice are also perinatally lethal due to abnormal neuronal development, therefore, MRP-deficient and WT littermate eHMCs were derived from embryos provided by Dr. Perry Blackshear, NIEHS, and their secretory responses compared. The results indicated that DNP induced essentially identical responses (Fig. 2.4); hence, the role of MARCKS in regulated exocytosis appears to be distinct.

MARCKS alters the kinetics of release for regulated exocytic SG cargo.

In the above experiments, the amount of regulated exocytosis was assayed after an incubation period with DNP-BSA for 30 minutes, a long enough time period to complete the regulated exocytic process and exhibited a significantly increased amount of regulated exocytosis in MARCKS null cells compared to WT cells. Next, we examined whether the kinetics of cargo release were affected by MARCKS-deficiency. We measured the amount of regulated exocytosis in WT and MARCKS-deficient eHMCs at different time points beginning thirty seconds after DNP

addition. At earlier time points (30 seconds–2 minutes), MARCKS-deficiency resulted in the release of more secretory cargo compared to WT eHMCs (Fig. 2.5). At five minutes, the secretory responses of WT and MARCKS null eHMCs were similar, with cells already releasing approximately 80% of the total amount released during the thirty minute incubation. Taking the thirty minute time point (WT=37.28 +/- 2.90 versus null 47.52+/- 5.12% of total hexosaminidase released) as a complete response, the $t_{1/2}$ for SG content release for WT cells was 2.35 +/- 0.26 minutes compared to the quicker $t_{1/2}$ of 0.98 +/- 0.15 minutes in MARCKS null mast cells.

It is important to note, however, that despite the difference in the kinetics of the secretory responses between WT and MARCKS-deficient eHMCs, in these studies no significant difference was found between the magnitude of the responses at thirty minutes between MARCKS null and WT cells ($0.08 > p > 0.05$). This apparent lack of difference in the amount of secretion, which is in contrast to Fig. 2.3, likely resulted from a relatively small sample size, as illustrated by analysis of the original thirty minute data set presented in the Appendix.

MARCKS peptides do not demonstrate a MARCKS-specific effect in mast cells.

An experimental perturbation to test the role of MARCKS in secretion, one used with increasing frequency, is an exposure of WT cells to a myristoylated, 24-residue N-terminal MANS peptide, or a randomized control (RNS) peptide (Li, *et al.*, 2004; Singer, *et al.*, 2004; Takashi, *et al.*, 2006). Inhibition by the MANS peptide is taken to indicate competitive interaction between the peptide and native MARCKS for intracellular binding sites (Li, *et al.*, 2004; Singer, *et al.*, 2004). To address the apparent contradiction between the results of studies using the MANS peptide, indicating significant inhibition, and our observations indicating a non-

essential role for MARCKS in mast cell secretion, we tested the effects of the MANS and RNS peptides on the secretory responses of WT and MARCKS-deficient eHMCs. Additionally, we tested a non-myristoylated MANS (NONG) peptide that lacked the N-terminal Glycine necessary for myristoylation, and, therefore, the ability to permeate the PM.

The MANS peptide, as previously reported for other cell types, significantly inhibited regulated exocytosis in eHMCS at each dose tested (Fig. 2.6). However, MARCKS null eHMCs exhibited a similar inhibition by the MANS peptide as WT eHMCs, suggesting that the mechanism of inhibition was not MARCKS-specific. Interestingly, pretreatment with the RNS peptide caused inhibition of WT and MARCKS null eHMC regulated exocytosis compared to untreated controls at the highest concentration tested but not the lower concentration (Fig. 2.6). When WT and MARCKS-deficient eHMCs were pretreated with the non-myristoylated NONG peptide, eHMC secretion was inhibited even more effectively than the inhibition with the MANS peptide. Pretreatment with the highest concentration of NONG peptide almost completely abolished the secretory response in both mast cell genotypes. These results suggest an extracellular, non-specific mechanism for MANS peptide inhibition of mast cell regulated exocytosis.

Figure 2.6: MANS peptide is not MARCKS-specific in mast cells

WT and MARCKS-deficient eHMCs were pretreated with either the MANS, RNS or NONG peptide, at the specified concentrations, fifteen minutes prior to FcεRI stimulation demonstrated similar effects between WT (filled) and MARCKS-deficient cells (open).

WT and MARCKS null cells were pretreated with the RNS peptide (circles) at various concentrations. While no difference was detected between the genotypes, both demonstrated an increased percent of inhibition at the largest peptide concentration. MANS peptide (triangles) also inhibited both WT and MARCKS-deficient cells equally. The NONG peptide (squares) revealed similar responsivity between both genotypes. However, the NONG peptide almost completely inhibited regulated exocytosis at the highest peptide concentration. The amount of inhibition was calculated as the % of hexosaminidase release in cells untreated with peptides compared to cells treated with peptides.

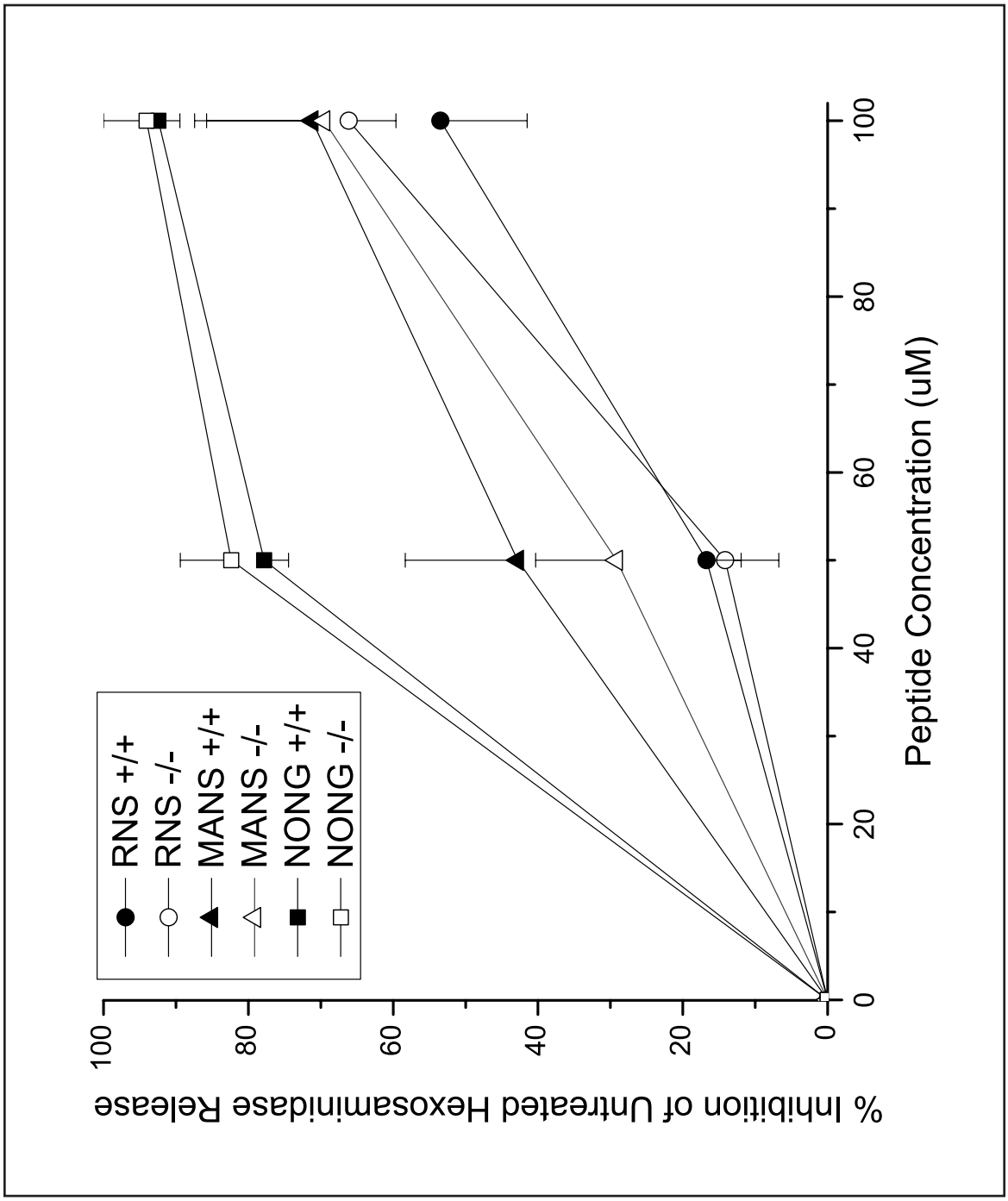
% Inhibition of Untreated Hexosaminidase Release
Peptide Concentration (uM)
0
20
40
60
80
100
RNS +/+
RNS -/-
MANS +/+
MANS -/-
NONG +/+
NONG -/-

DISCUSSION

Mast cells, key immune cells in the inflammatory response, have been linked to multiple pathologies including airway inflammation (Bradding, *et al.*, 2006; Kalin, *et al.*, 2008), skin vasculitis (Sanchez-Mejorada & Rosales, 1998; Watanabe *et al.,* 1999; Baumann *et al.,* 2001; Dugina, *et al.*, 2003; Tam, *et al.*, 2004), and cardiac hypertension and hypertrophy (Shiota, *et al.,* 2003; Balakumar, *et al.*, 2007; Gonzalo, *et al.*, 2007). All of these functions depend on the ability of mast cells to release pro-inflammatory mediators and enzymes into the extracellular environment, principally through regulated exocytosis, in response to pathogens and immune challenge (Watanabe, *et al.*, 1999; Baumann, *et al.*, 2001; Balakumar, *et al.*, 2007; Bischoff & Kramer, 2007; Metz & Maurer, 2007). Regulated secretion of pro-inflammatory mediators such as TNF-α, interleukins, lipid mediators, tryptase, chymase, serotonin and histamine from mast cells results in polymorphonuclear (PMN) chemotaxis and activation of other immune cells, leading to significant tissue damage when chronic inflammation occurs (Metcalfe, 2008). Understanding the regulated secretory pathway, a critical aspect of mast cell function, could be important for the development of future therapeutic targets in multiple diseases.

Previous peptide and siRNA studies in several types of secretory cells have indicated that the ubiquitously expressed MARCKS protein may serve a crucial, positive regulatory role in regulated exocytosis in secretory cells (Elzagallaai, *et al.*, 2000; Rose, *et al.*, 2001; Jerdeva, *et al.*, 2005; Park, *et al.*, 2006; Doreian, *et al.*, 2009). A major obstacle, however, of these approaches to cell perturbation is the possibility of non-specific effects. For peptides, it is also the possibility of competition with MRP or other polybasic domain proteins, and other PKC substrates (Aderem, 1995; Matsuoka & Bennett, 2000; Streb & Miano, 2005). Gene knockdown by siRNAs, similarly, can have unintended effects on the expression of other genes by

interfering with the cell's RNA processing machinery, and siRNA knockdown often lacks good controls against non-specific inhibition. Embryonic mast cells provide the advantage of allowing isolation of both WT and MARCKS-deficient cells on the same genetic background. Additionally, MARCKS expression is upregulated in immune cells primed by inflammatory stimuli (Rose, *et al.,* 1996; Thelen, *et al.,* 1990; Yokoyama, *et al.*, 1998; Chun, *et al.,* 2009), similar to the process of passive sensitization utilized for FcεRI-mediated mast cell activation. FcεRI, a high-affinity IgE receptor, is an essential component of allergic inflammation which activates mast cells only after they are first sensitized with IgE, a process which primes the cells by increasing cell surface expression of the receptor and crosslinks these surface receptors so that subsequent IgE challenge leads to activation of FcεRI (Thelen, *et al.,* 1990; Aderem, 1992; Rose, *et al.,* 1996; Chun, *et al.,* 2009). Once activated, the well-characterized receptor-mediated pathway initiates the release of pre-formed pro-inflammatory mediators through regulated exocytosis and induces *de novo* production of other pro-inflammatory cytokines (Hata, *et al.*, 1998; Sanchez-Mejorada & Rosales, 1998; Peng & Beaven, 2005; Rivera & Gilfillan, 2006).

BMMCs studies stimulating the cells in suspension, an assay commonly used in the field, led us to first test eHMCs in suspension by comparing the magnitude of the secretory response from WT and MARCKS-deficient eHMCs stimulated via FcεRI. WT and MARCKS null cells tested under these suspension conditions showed no significant difference in the amount of regulated exocytosis at five different DNP concentrations (Suppl. Fig. S5). The dose response curve, similar to previously published data, exhibited an increase in the secretory response of both genotypes up to approximately 10 ng/mL DNP, while the two doses higher than 10 ng/mL correlated with a dose-dependent decrease in the secretory response. These results suggested that MARCKS was not essential for regulated exocytosis in mast cells.

Earlier studies also tested mast cells under adherent conditions and showed that mature mast cells, *in vivo,* display increased sensitivity and responsiveness to immune challenge due to cell adherence to the extracellular matrix of resident tissue (Vuori & Ruosahlti, 1993; Columbo, *et al.*, 1995; Kruger-Krasagakes, *et al.*, 1999). Fibronectin, specifically, has been shown in several previous studies to potentiate secretion in mast cells (Vuori & Ruosahlti, 1993; Columbo, *et al.*, 1995; Kruger-Krasagakes, *et al.*, 1999) We confirmed this enhanced sensitivity to immune challenge *in vitro* by comparing WT eHMC secretory responses in cells adherent to fibronectin and cells in suspension: adherent WT cells demonstrated a three-fold increase in the amount of secretion, relative to cells in suspension (Fig. 2.2).

Based on these observations, the necessity of MARCKS for regulated exocytosis under adherent conditions was tested. WT and MARCKS null eHMCs activated with the same five DNP doses, after overnight adherence to fibronectin, revealed some surprising results. DNP elicited greater secretory responses from MARCKS-deficient cells at every concentration tested; these differences were statistically significant at 3 and 30 ng/mL, highly so at the peak response (3 ng/mL) (Fig. 2.3). At this maximal stimulation, the secretory response of adherent MARCKS-deficient mast cells was increased approximately one-third relative to the amount of WT release. Even when eHMCs were allowed to adhere to fibronectin for four days, MARCKS null cells still exhibited a potentiated amount of regulated secretion at the maximal dose, with an approximately one-fifth increase in the amount of secretory release compared to WT cells (n=3) (Suppl. Fig. S9).

However, this modulatory effect of MARCKS-deficiency on the magnitude of the regulated secretory response was much less potent than the effect of MARCKS-deficiency on the time course of release (Fig. 2.5). The absence of MARCKS significantly accelerated the rate

of release for secretory cargo by approximately 2.4 fold, inducing release of half of the total regulated exocytic cargo in approximately one minute, versus approximately 2.4 minutes in WT. These results suggest a role for MARCKS in the initial events of regulated exocytosis in modulating early events during activation of the pathway. Another study linked the translocation of MARCKS to the rapid and early release of adrenocorticotropin, rather than association with the slower, sustained release found in the later time period (Liu, *et al.*, 1994), an observation that correlatively suggested a role for MARCKS in the initial kinetics of cargo release. Our results causally support this modulatory role for MARCKS in the rate of release for mast cells, since cells lacking MARCKS are capable of immediately initiating exocytic release, without the activation barrier seen in WT cells.

As noted in Results, there was no significant difference in the secretory responses of WT and MARCKS-deficient eHMCs at the thirty minute incubation point in these studies (WT=37.28 +/- 2.90 versus null=47.52 +/- 5.12% of total hexosaminidase released), in contrast to the original observation of an approximately 34% increase in null cell secretory response compared to WT (Fig. 2.3). Likely, the lack of statistical significance is due to a smaller sample size (n=6 for MARCKS null for Fig. 2.5 versus n=16 in Fig. 2.3). To test this possibility we systematically computed all possible 8,008 combinations of the 16 data points, taken six at a time, for WT and MARCKS-deficient cells, examining each smaller data subset for statistical significance using the student's two-tailed t-test (Appendix A). The results indicated that 49.8% of the WT versus MARCKS null secretion data subsets failed to achieve a statistically significant level of $p<0.05$.

Next, to confirm that the regulatory function for MARCKS in mast cells is specific to MARCKS, the second family member, MRP, present in both WT and MARCKS-deficient cells

Figure 2.8: Increased SG density-mediated model for the MARCKS-deficient increase in regulated exocytosis. Cell morphology studies of adherent WT and MARCKS-deficient eHMCs revealed significantly smaller MARCKS null cells compared to WT cells. With the same amount of secretory content, these conditions would result in more densely packed SGs with a reduced amount of SG trafficking required prior to membrane fusion events. SGs would then be released more quickly compared to WT SG release due to this closer proximity of the SGs to the PM.

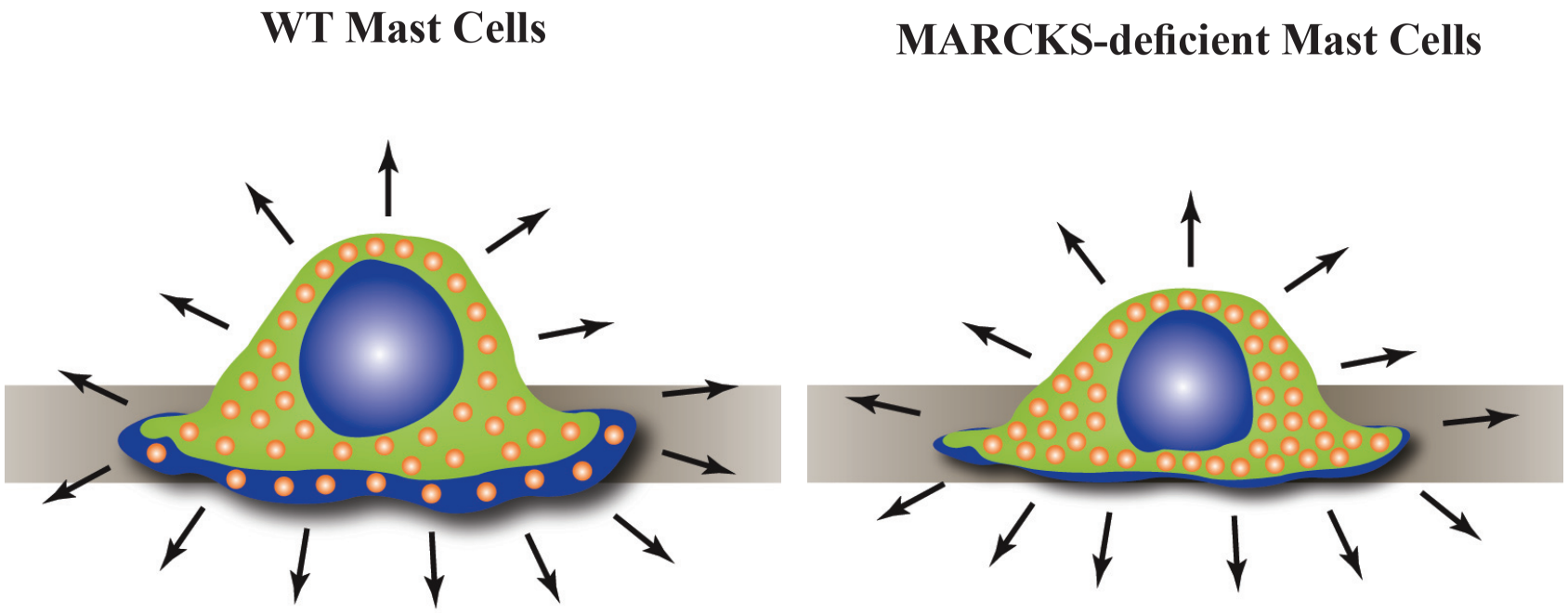
WT Mast Cells
MARCKS-deficient Mast Cells

(Fig. 2.1) was tested. MRP null cells completely mimicked WT secretory behavior (Fig. 2.4). The MARCKS and MRP double null mouse, unfortunately, is embryonically lethal, with the embryos succumbing prior to the development of mast cell progenitor cells, so eHMCs could not be obtained from the double null mice (personal communication, DJ Stumpo and PS Blackshear). Notably, the lack of the MARCKS null phenotype in adherent MRP-deficient eHMCs (Fig. 2.4) supports the idea of a MARCKS-specific regulatory function in mast cell regulated exocytosis.

Thus, these FcεRI-mediated secretion studies demonstrated two observations. First, the presence of MARCKS is not essential for mast cell regulated exocytosis. Second, in contrast to reports from previous studies, MARCKS negatively regulates mast cell secretion, likely through modulation of the rate of release, possibly a cell-specific function.

Inhibitiory Peptides

A synthetic myristoylated peptide representing the N-terminal 24-residues of the MARCKS protein has been shown to inhibit secretion in human airway goblet cells, isolated human neutrophils, and eisonophil-like, monocyte/macrophage and natural killer cell lines (Li, *et al.*, 2001; Singer, *et al.*, 2004; Takashi, *et al.*, 2006). Consistent with our finding that MARCKS is not essential for regulated mast cell secretion, we found that the inhibition effected by the MANS peptide is not dependent on the expression of MARCKS (Fig. 2.6): both WT and MARCKS null cells exhibited similar responsivity to the peptide. Additional observations supported this finding. First, the highest concentration (100 μM) tested of the RNS peptide, the randomized peptide, also had a significant inhibitory effect, suggesting inhibition is at least partially independent of peptide sequence. Second, and more significant, the NONG peptide, a

non-myristoylated peptide unable to permeate the PM, had an even greater inhibition than the MANS peptide in both WT and MARCKS null cells. This result clearly indicates that the site of inhibition is on the cell surface of mast cells. Additionally, the almost complete abolishment of mast cell secretion suggests that the NONG peptide could potentially be an even more effective therapeutic inhibitor of secretion, despite a non-specific mode of action, if it were also found to be non-toxic and lack other deleterious side effects. Overall, though, our results indicate that the implicated mechanism of the MANS peptide for inhibiting mast cell secretion is non-specific, and may be due to an electrostatic interaction that does not require entrance into the cell or MARCKS expression.

Inflammation and Pathology

Activation of mast cells in the respiratory system leads to a hypersensitivity response and PMN infiltration, causing airway obstruction and tissue damage (Prussin & Metcalfe, 2003; Metz and Maurer, 2007). Researchers have demonstrated PMN chemotaxis from the blood to be a largely mast cell-mediated process (Baumann, *et al.*, 2001; Bradding, *et al.*, 2006; Gonzalo, *et al.*, 2007; Kalin, *et al.*, 2008; Ryzhov, *et al.*, 2008). Since mast cells are critical promoters of the chemotactic process, even the small one-third increase in mediator release in MARCKS null cells could significantly enhance the amount of PMN infiltration and subsequent airway obstruction and tissue damage during an inflammatory response. Additionally, because mast cells are preferentially localized so their contents can be released near blood vessels, the effect of the accelerated amount of release in a shorter time period, as observed in MARCKS null cells, could also potentiate significantly the amount of PMN infiltration. One study found that an approximately 50% enhancement in the FcεRI-mediated degranulation of

mouse-derived BMMCs, owing to deletion of the protein, RabGEF1, correlated with increased mortality, chronic and severe skin inflammation and significantly increased serum concentrations of histamine and IgE (Tam, *et al.*, 2004). Though these results were derived from a mouse where RabGEF1 was knocked out in all cell types, the severe inflammation pathology observed clearly indicates the pronounced effects that can result from increased mast cell regulated exocytosis.

Mechanism of Action

In aggregate, our studies suggest that MARCKS is not essential for regulated secretion, at least in mast cells. Rather, if the protein participates directly in the regulation of the exocytic mechanism, it is as a negative modulator. This possibility is in accordance with a long-standing hypothesis that MARCKS stabilizes cortical actin filaments in pre-activated cells (Trifaro, *et al.*, 2000; Rose, *et al.*, 2001). This hypothesis for a MARCKS-mediated actin barrier disruption postulates that phosphorylation of MARCKS by PKC, which induces its translocation from the PM to the cytosol, directly or indirectly regulates cortical actin destabilization and subsequently allows secretory granules to be trafficked to and fuse with the PM to undergo exocytosis (Arbuzova, *et al.*, 2002; Ehre, *et al.*, 2005; Pene, *et al.*, 2005 Jerdeva, *et al.*, 2005; Park, *et al.*, 2006). The exact mechanism of how MARCKS could mediate these events has not yet been elucidated, but previous studies have demonstrated that MARCKS translocation correlated with shorter actin filaments or decreased cortical actin below the PM (Rose, *et al.*, 2001; Salli, *et al.*, 2003; Ehre, *et al.*, 2005).

Alternatively, MARCKS could be modulating regulated exocytosis indirectly by regulating cell shape and/ or size under adherent conditions. The altered features of resting

MARCKS-deficient cells, decreased cross-sectional area and cell height, and an approximately 30% cell volume decrease, support this hypothesis (Supp. Fig. S7-S8). One result of MARCKS-deficiency is a loss of cellular extensions and smaller cells, possibly giving rise to the 'rounded' morphology described by other researchers, (Micallef, *et al.*, 2009; Disatnik, *et al.*, 2004). Since the amount of total cellular hexosaminidase remained similar between the WT and MARCKS null cells, the resulting increase in granule density could cause the mast cells to release cargo within an abbreviated time course. (Fig. 2.7).

In conclusion, our results suggest a negative, modulatory role for MARCKS in the regulated secretion of mast cells. This negative regulation is expressed primarily as accelerated kinetics of secretion, possibly mediated by a change in cortical actin dynamics and/or cell size.

Supplementary Data Figures for Chapter 2

Supplemental Figure S1: Immunohistochemical verification of pure, mature mast cell cultures

Introduction: Embryonic hepatic-derived mast cells were isolated from homogenized livers of E14-E18 embryos and cultured for 5 weeks in media supplemented with SCF and IL-3. Cells were assayed for maturity by the presence of the high affinity IgE receptor on the cell surface (See Chapter 2 Materials and Methods for detailed protocol).

(**A**) As a control, eHMCs adherent to fibronectin-coated glass coverslips were blocked for one hour with the CD32/CD16 antibody (1:50) at room temperature. Cells were then stained for one hour with secondary rat FITC-anti-mouse IgE antibody (1:75) without prior incubation for one hour with the primary DNP-IgE antibody. Cells were then fixed with 4% PFA and the coverslips mounted onto glass slides. The control lacked significant cell surface staining.

(**B**) Adherent cells were first incubated with the blocking CD32/CD16 antibody for one hour at room temperature, rinsed, and incubated with the primary mouse anti-DNP IgE antibody (1:25) for one hour. After rinsing with PBS, the secondary rat anti-mouse IgE antibody (1:75) was applied for one hour before cells were fixed and mounted for imaging experiments.

(**C**) Cells were blocked with the CD32/CD16 antibody and incubated with mouse FITC-anti-FcεRI alpha antibody (1:25) (eBiosciences) for one hour at RT. Coverslips of the adherent mast cells were mounted onto glass slides and imaged for cell surface expression.

Conclusions: Both staining methods, repeated in three independent experiments, confirmed the eHMC cultures to be >99% pure.

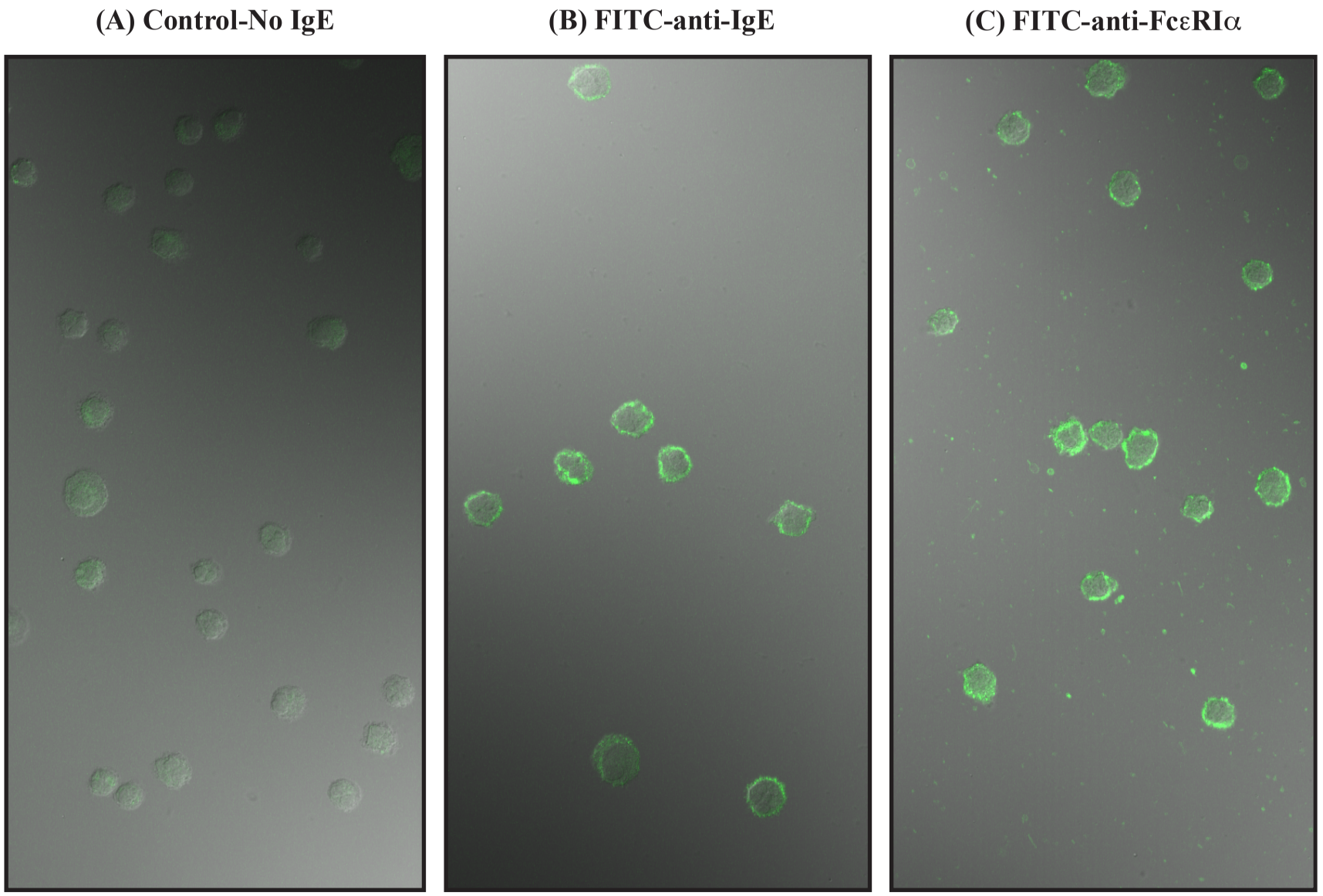
(A) Control-No IgE
(B) FITC-anti-IgE
(C) FITC-anti-FcεRIα

Supplemental Figure S2: Ionomycin activation of BMMCs and eHMCs

Introduction: Hematopoietic bone marrow-derived mast cells were derived from 6–12 week old mice and activated with the calcium ionophore, ionomycin after 5 weeks of culturing and maturation with SCF and IL-3.

(**A**) Secretory responses of WT (+/+) BMMCs stimulated with ionomycin at varying doses while in suspension. Values were quantitated as the amount of β-hexosaminidase activity released into the supernatant compared to the total amount of β-hexosaminidase activity from both supernatant and cell lysate. The background spontaneous release (<5%) was subtracted from DNP-stimulated cells, to show the DNP-specific secretory response. (Error bars represent S.E. from three independent experiments; * $p<0.05$; ** $p<0.01$.; ***$p<0.001$ compared to the amount of spontaneous release)

(**B**) Secretory responses of WT (+/+) suspension eHMCs stimulated with ionomycin. Peak responsivity of both BMMCs and eHMCs to ionomycin was 1 μM. (Error bars represent S.E. from three independent experiments; ** $p<0.01$.; ***$p<0.001$ compared to the amount of spontaneous release)

Conclusions: Both WT BMMCs and eHMCs in suspension had similar dose-dependent responses to stimulation with ionomycin, a calcium ionophore.

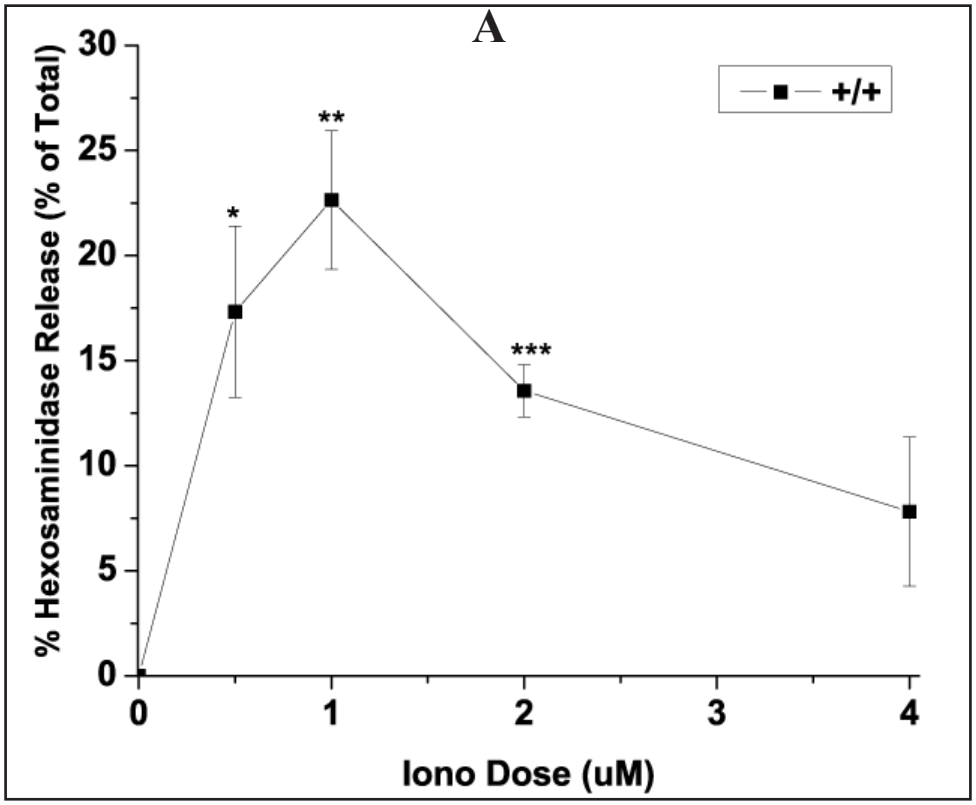
A
% Hexosaminidase Release (% of Total)
30
25
20
15
10
5
0
+/+
*
**
***
0
1
2
3
4
Iono Dose (uM)

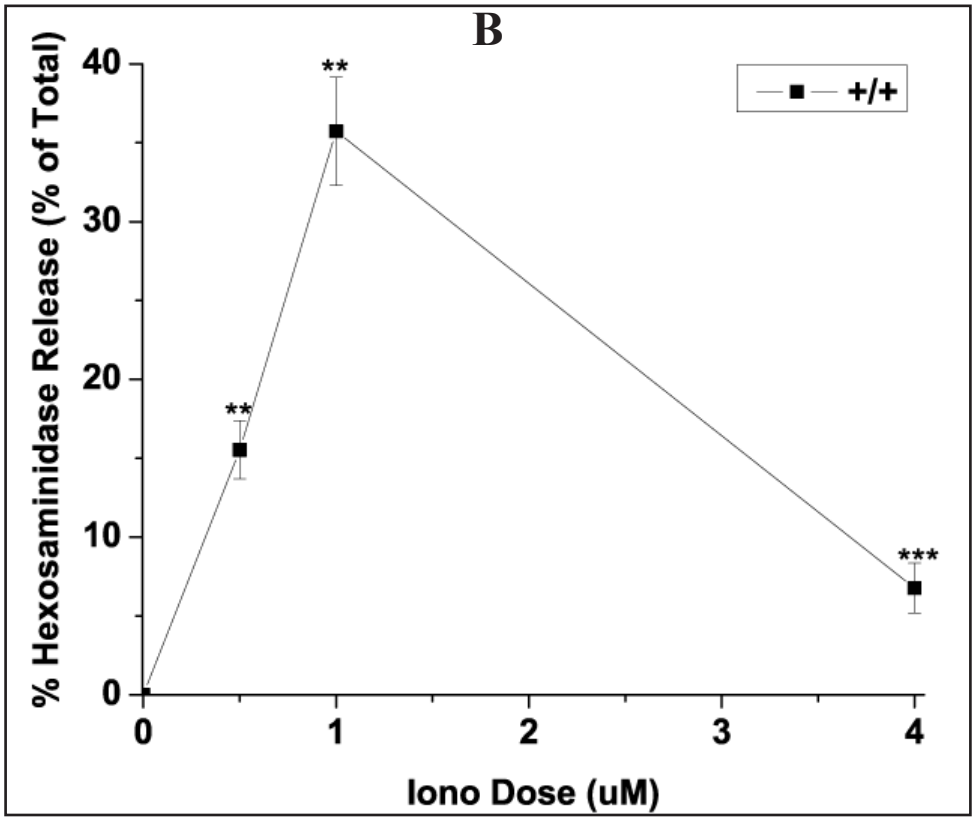
B
% Hexosaminidase Release (% of Total)
40
30
20
10
0
+/+
**
**
***
0
1
2
3
4
Iono Dose (uM)

Supplemental Figure S3: PMA enhancement of submaximal ionomycin stimulation for WT cells

Introduction: Mast cells treated with PMA, a DAG mimic, were activated with submaximal ionomycin doses after 5 weeks of culturing and maturation with SCF and IL-3.

(**A**) Secretory responses of suspension BMMCs stimulated with varying doses of PMA along with 0.5 μM ionomycin. An maximal enhancement of approximately 2.6-fold was obtained at the PMA dose of 100 nM.

(**B**) The dose response shows the secretory behavior of suspension eHMCs stimulated with varying doses of PMA and 0.25 μM ionomycin. While the maximal 1.8-fold enhancement in eHMCs was lower than the fold change observed for BMMCs, this peak increase occurred at the same PMA dose of 100 nM.

Values are shown as the fold change of PMA-enhanced treatment at each dose. Secretory responses of cells stimulated with ionomycin and PMA, at each specific dose, were normalized to the secretory response of control cells treated only with ionomycin. (Error bars represent S.E. from three independent measurements; * $p<0.05$; ** $p<0.01$; *** $p<0.001$ compared to the amount of release from ionomycin only treatment)

Conclusions: WT BMMCs and eHMCs in suspension demonstrated similar dose-dependent responses to PMA enhancement of submaximal ionomycin stimulation.

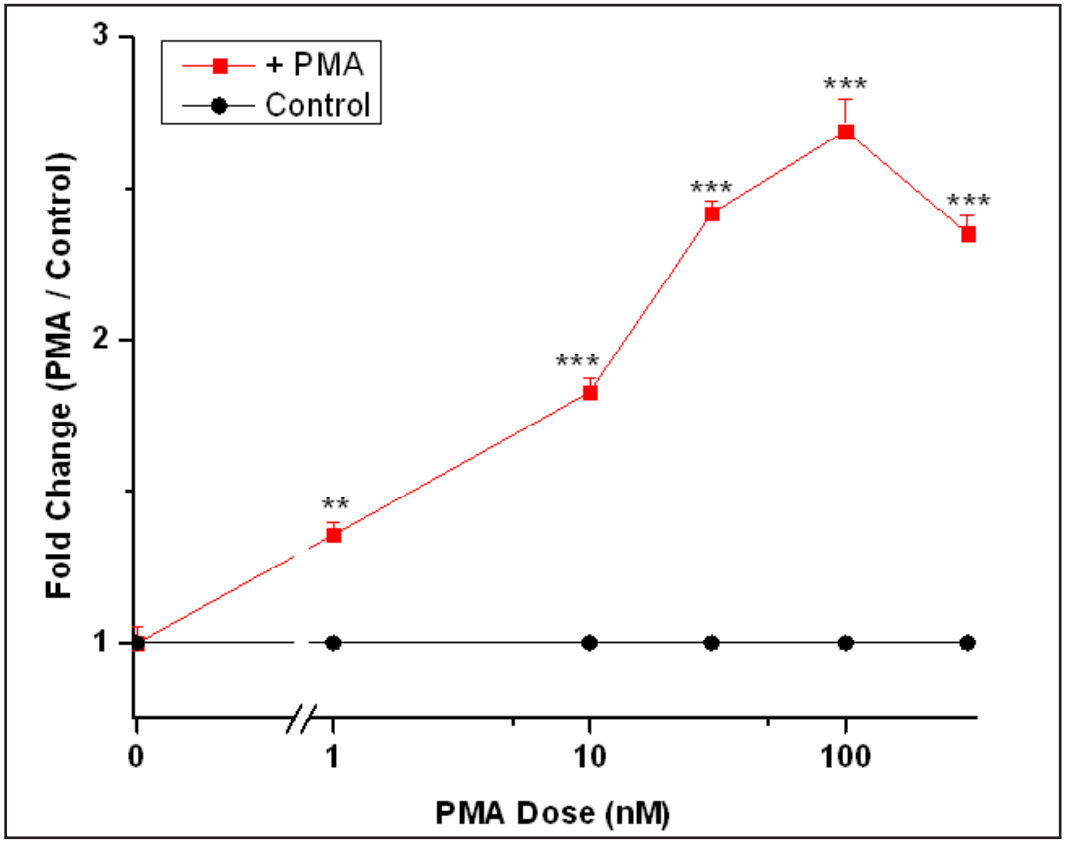
+ PMA
Control
Fold Change (PMA / Control)
PMA Dose (nM)
3
2
1
0
1
10
100
**
***
***
***
***

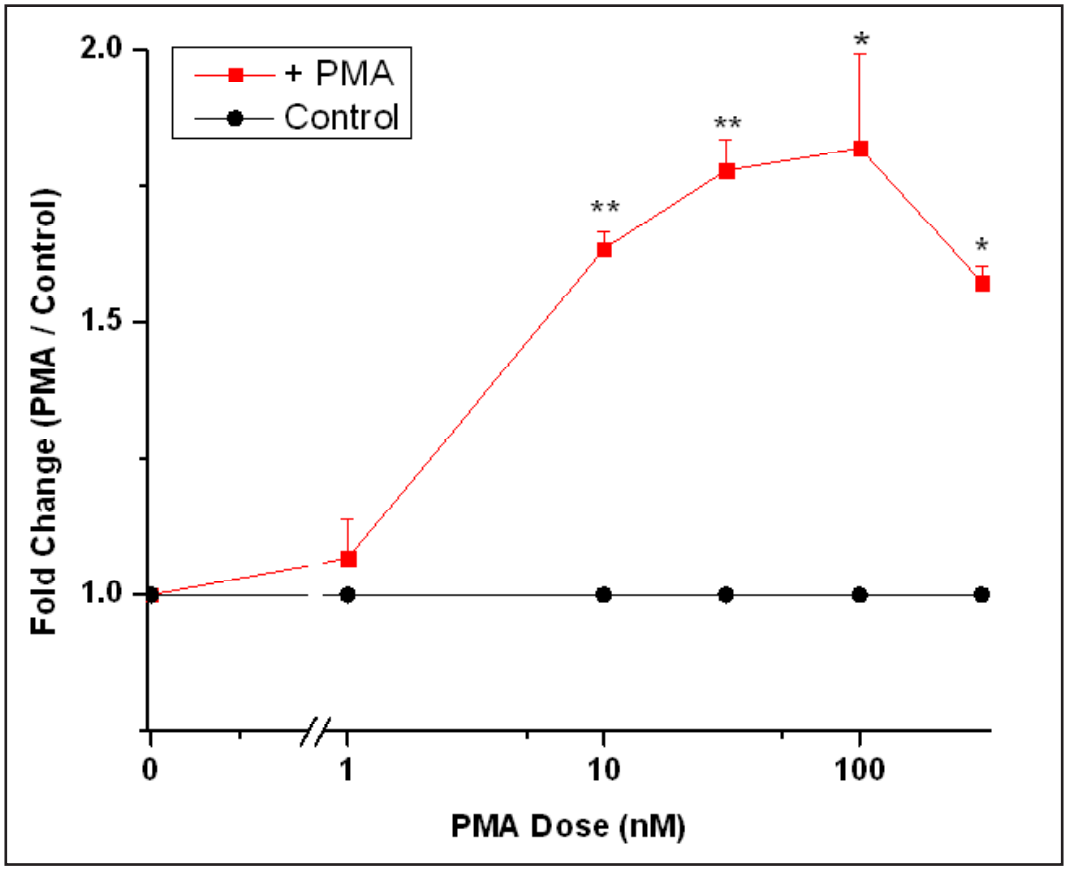
+ PMA
Control
Fold Change (PMA / Control)
PMA Dose (nM)
2.0
1.5
1.0
0
1
10
100
**
**
*
*

Supplemental Figure S4: BMMC and eHMC Total β-Hexosaminidase Content

Introduction: The total amount of cellular hexosaminidase, quantitated as absorbance units (A.U.) of cleaved hexosaminidase substrate, as a measure of the total amount of hexosaminidase in the cell lysate and supernatant combined was compared between WT BMMCs and WT eHMCs under various experimental conditions.

(A) The total cellular hexosaminidase for WT BMMCs in suspension (n=7).

(B) The total amount of cellular hexosaminidase activity for WT adherent (n=19) and suspension (n=7) eHMCs. No significant difference in the total amount of cellular hexosaminidase was detected between adherent (open) and suspension (filled) eHMCs.

Conclusions: The levels for the total amount of β-hexosaminidase content were quantitatively similar between WT BMMCs and WT eHMCs under any experimental conditions. These results support the validity of eHMCs as a mast cell model.

A

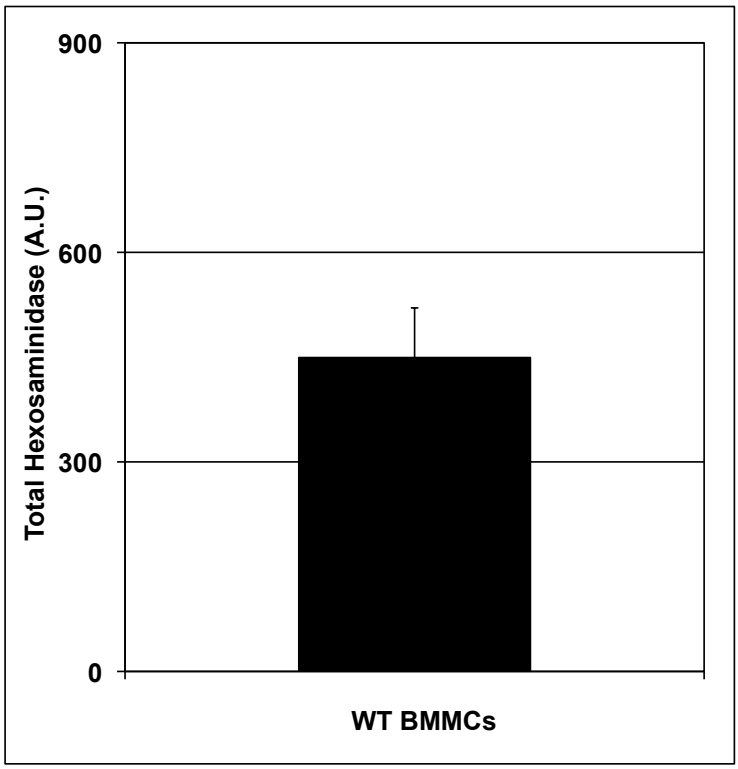
900
600
300
0
Total Hexosaminidase (A.U.)
WT BMMCs

B

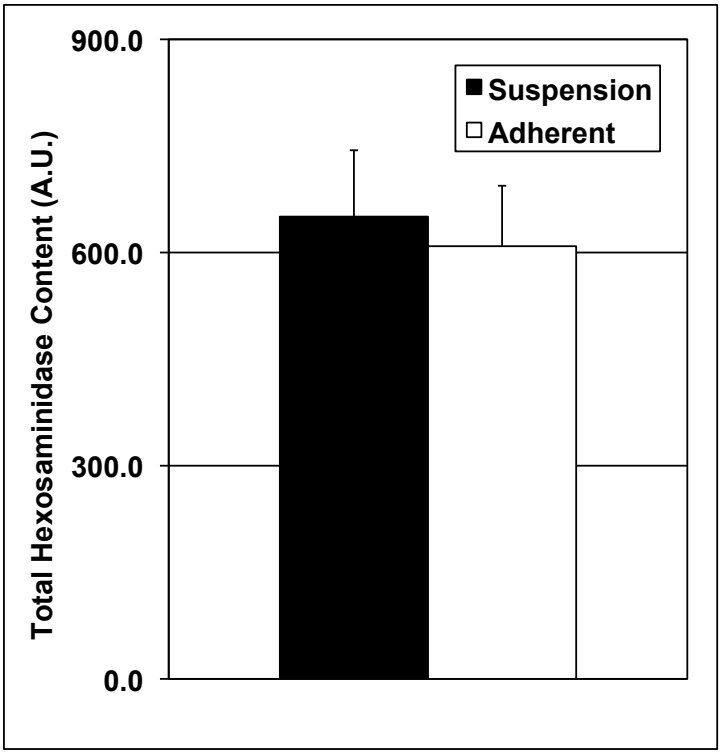
900.0
600.0
300.0
0.0
Total Hexosaminidase Content (A.U.)
Suspension
Adherent

Supplemental Figure S5: WT BMMC Responsivity to DNP Stimulation

Introduction: WT bone marrow-derived mast cells mast cells were activated by cross-linking the high-affinity IgE receptor, FcεRI, with DNP after 5 weeks of culturing and maturation (See Materials and Methods Section for Chapter 2).

Secretory responses of WT (+/+) BMMCs stimulated with varioius DNP doses while in suspension. Mean values represent at least three independent experiments (n=7).

Conclusions: The dose-dependent response of WT BMMCs to DNP was similar to the biphasic responsiveness seen in WT eHMCs (Fig. 2.2).

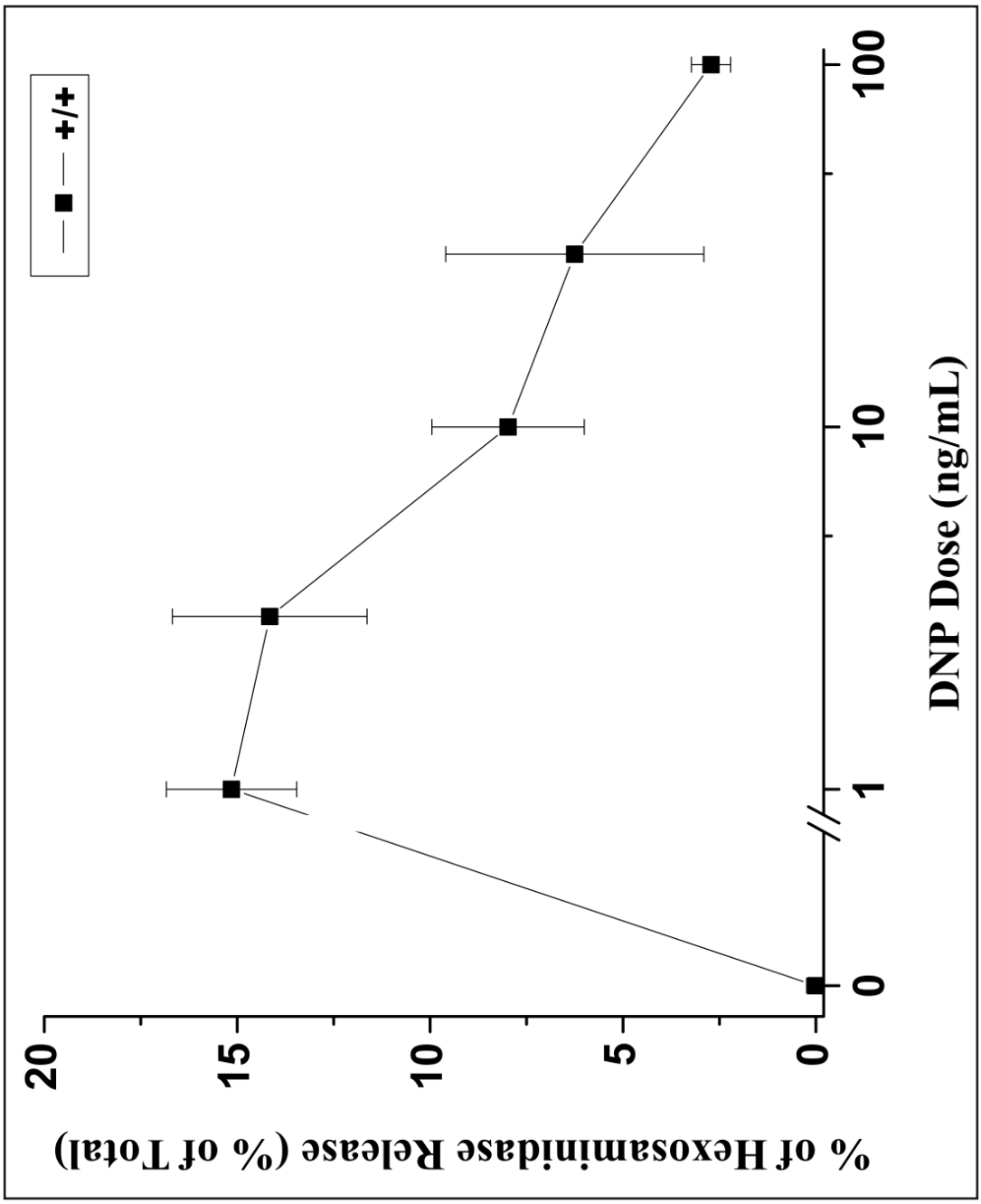
% of Hexosaminidase Release (% of Total)
0
5
10
15
20
0
1
10
100
DNP Dose (ng/mL)
+/+

Supplemental Figure S6: DNP-stimulated regulated exocytosis of suspension eHMCs

Introduction: The amount of regulated exocytosis was compared between WT (+/+) and MARCKS-deficient (– / –) eHMCS utilizing the suspension secretion assay at various DNP doses.

A comparison between the two genotypes (n=7) demonstrated no significant differences, even though the responses of the MARCKS null eHMCs were typically higher than the WT response curve at the non-inhibitory doses.

Conclusions: MARCKS-deficiency is not essential for mast cell regulated exocytosis and does not alter regulated exocytosis in eHMCs in suspension.

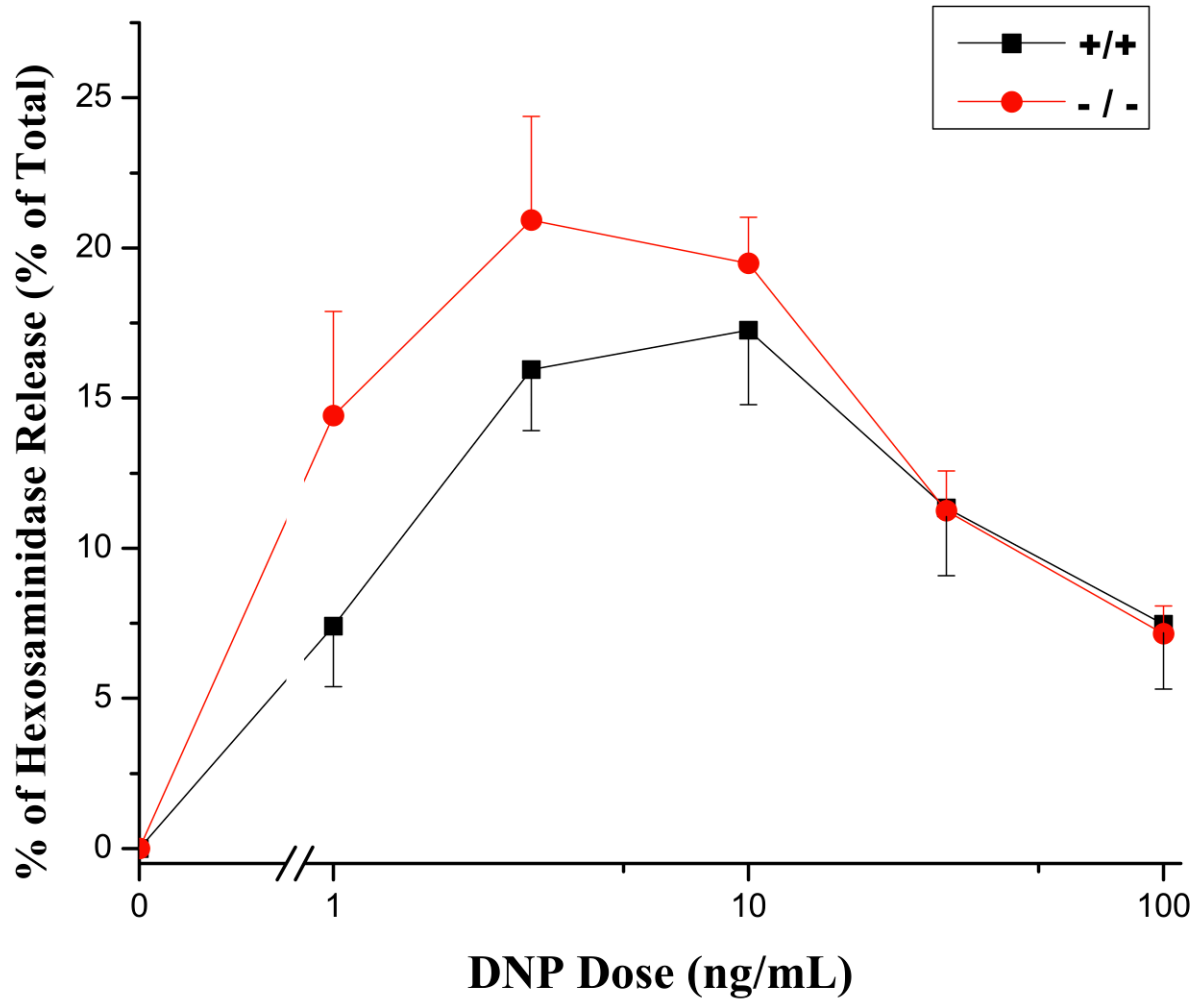
+/+
- / -
% of Hexosaminidase Release (% of Total)
0
5
10
15
20
25
0
1
10
100
DNP Dose (ng/mL)

Supplemental Figure S7: Phenotypic characterization of adherent eHMCs in the resting state

Introduction: The phenotypes of resting WT and MARCKS null cells were compared under conditions of adherence to fibronectin.

Methods: Images of the x-y plane of live adherent cells labeled with FM 4-64 FX fixable analog were captured, using an automatic stage, moving through the z-axis at designated increments from the bottom to the top of the cell. The image series was then imported into Volocity v4.4 and assimilated into a 3-D image, which was used to quantitatively measure specific cell characteristics.

(A) The frequency distribution for the heights of individual cells was compared between WT and MARCKS-deficient cells. MARCKS null cells demonstrated a left-shifted distribution, hence shorter cells compared to WT.

(B) The frequency distribution for the cross-sectional area was quantitated for WT and MARCKS-deficient cells. MARCKS null cells had a left-shifted distribution compared to their WT counterparts. Results are derived from three independent experiments per genotype. Each experiment consisted of analyzing approximately 50 cells per genotype.

Conclusions: Adherent MARCKS null cells have decreased cell heights and cross-sectional areas compared to adherent WT eHMCs.

A

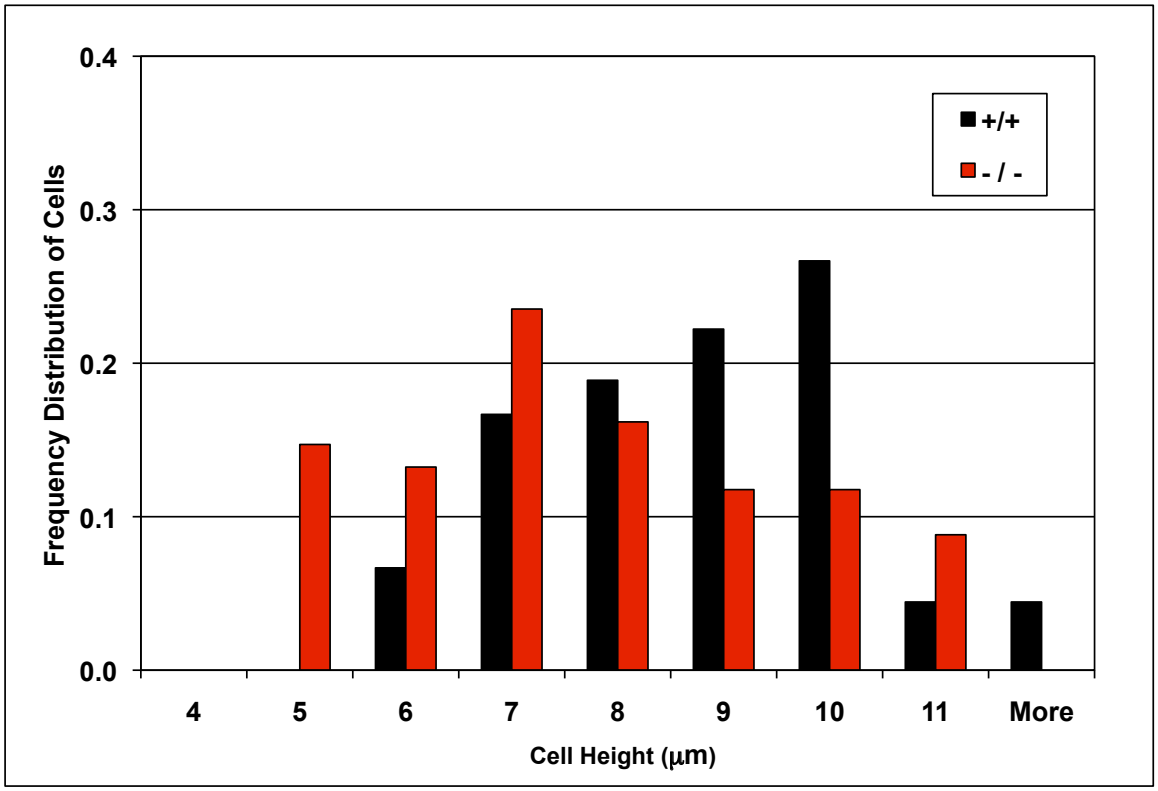
0.4
0.3
0.2
0.1
0.0
Frequency Distribution of Cells
+/+
- / -
4
5
6
7
8
9
10
11
More
Cell Height (μm)

B

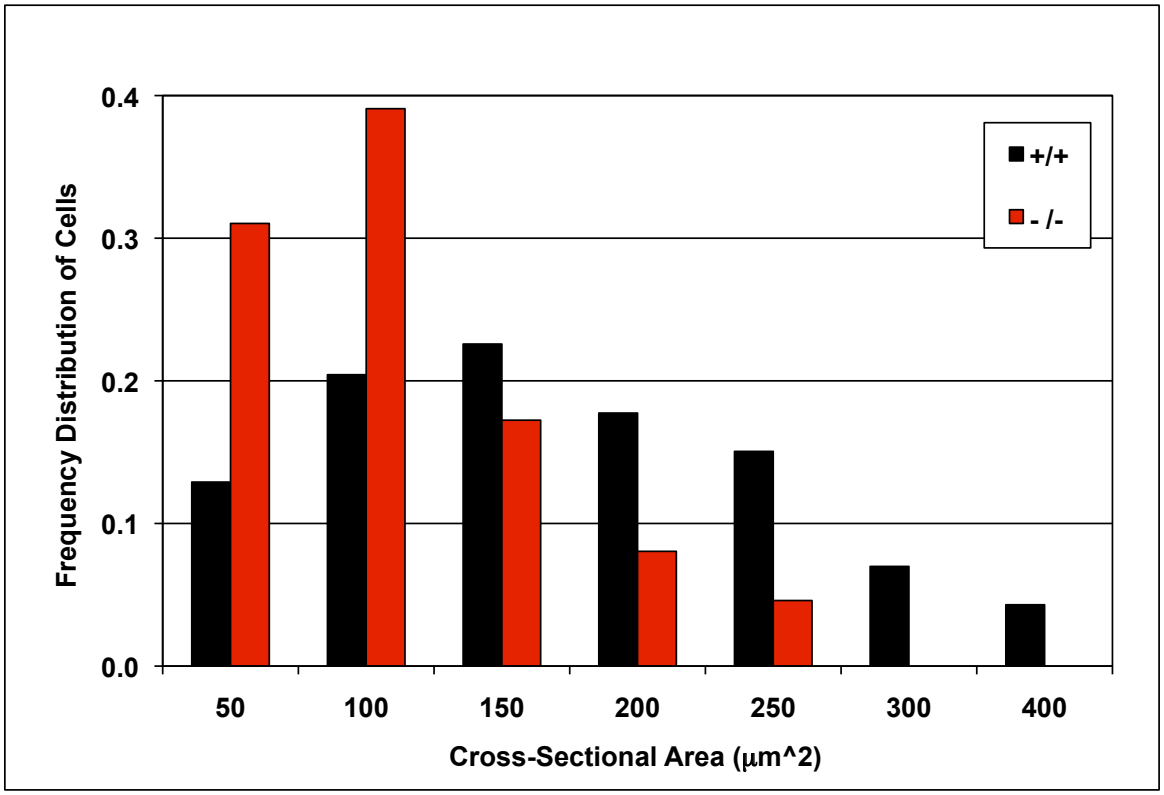
0.4
0.3
0.2
0.1
0.0
Frequency Distribution of Cells
+/+
- /-
50
100
150
200
250
300
400
Cross-Sectional Area (μm^2)

Supplemental Figure S8: Further comparison of phenotypes in resting, adherent cells.

Methods: The average cell volume of adherent mast cells was estimated by staining them with Alexa Fluor-594 phalloidin, which labels F-actin. Individual cell volumes were quantitated using Velocity (v.4.4 Perkin Elmer) after 3-D renders of z-stacks were generated using the Leica SP2 confocal microscope. Thresholding parameters were set to exclude 5% of the lowest intensity voxels, to avoid measuring background fluorescence, then a confluent mask filling in areas of lower intensity surrounded on all sides by areas of high intensity was generated. A confluent mask had to be generated, since fishnet-like gaps in the F-actin staining of the cortex was present in all cells. Results were derived from three independent experiments per genotype, with each experiment consisting of approximately 25 cells per genotype.

(A) The average cell volume for WT and MARCKS-deficient adherent cells, as quantitated by the above method of phalloidin staining. On average, MARCKS-deficient adherent cells demonstrated a significantly decreased cell volume compared to WT cells.

(B) The table shows the average means for WT and MARCKS-deficient adherent cells, including the total cellular β-hexosaminidase content of the two genotypes.

Standard error is representative of the number of cells analyzed. The p-value represents the significance of the difference between the genotypes; *** $p<0.001$.

Conclusions: While both WT and MARCKS null cells exhibited similar hexosaminidase content, a decrease in cell volume for MARCKS-deficient cells was observed compared to their WT counterparts.

A

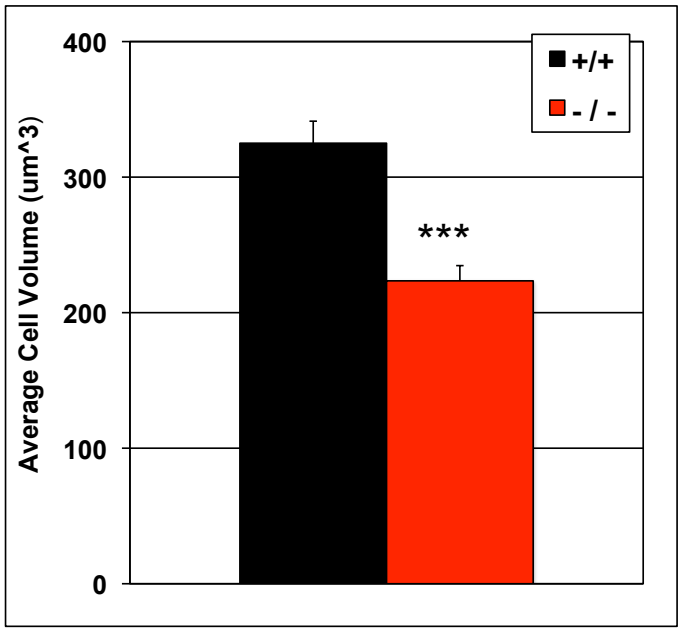

B

	+ / +	– / –	p-values
Cell Height (μm)	9.6 +/- 0.2	7.1 +/- 0.2	***
Cross-Sectional Area (μm²)	182 +/- 8	133 +/- 6	***
Total Hexosaminidase (A.U.)	609 +/- 85	615 +/- 70	

Supplemental Figure S9: DNP-stimulated regulated exocytosis in eHMCs adherent for 96 hours.

Introduction: To determine if the effects of MARCKS-deficiency on adherent mast cells were present even under long term incubation with fibronection, the responsivity of WT and MARCKS-deficient eHMCS incubated in fibronectin-coated wells for 96 hours was compared.

Methods: The secretion assay was performed in the same way, with one variation. Cells were left in the fibronectin-coated wells of a 96-well plate for 96 hours, which included one media change, prior to stimulation with 3 ng/mL DNP.

Conclusions: The extended exposure to fibronectin enhanced DNP-stimulated secretion in both cell types, but at 3 ng/mL regulated exocytosis from MARCKS null cells was still significantly increased compared to WT cells. Mean values represent three independent experiments. *= $p<0.05$

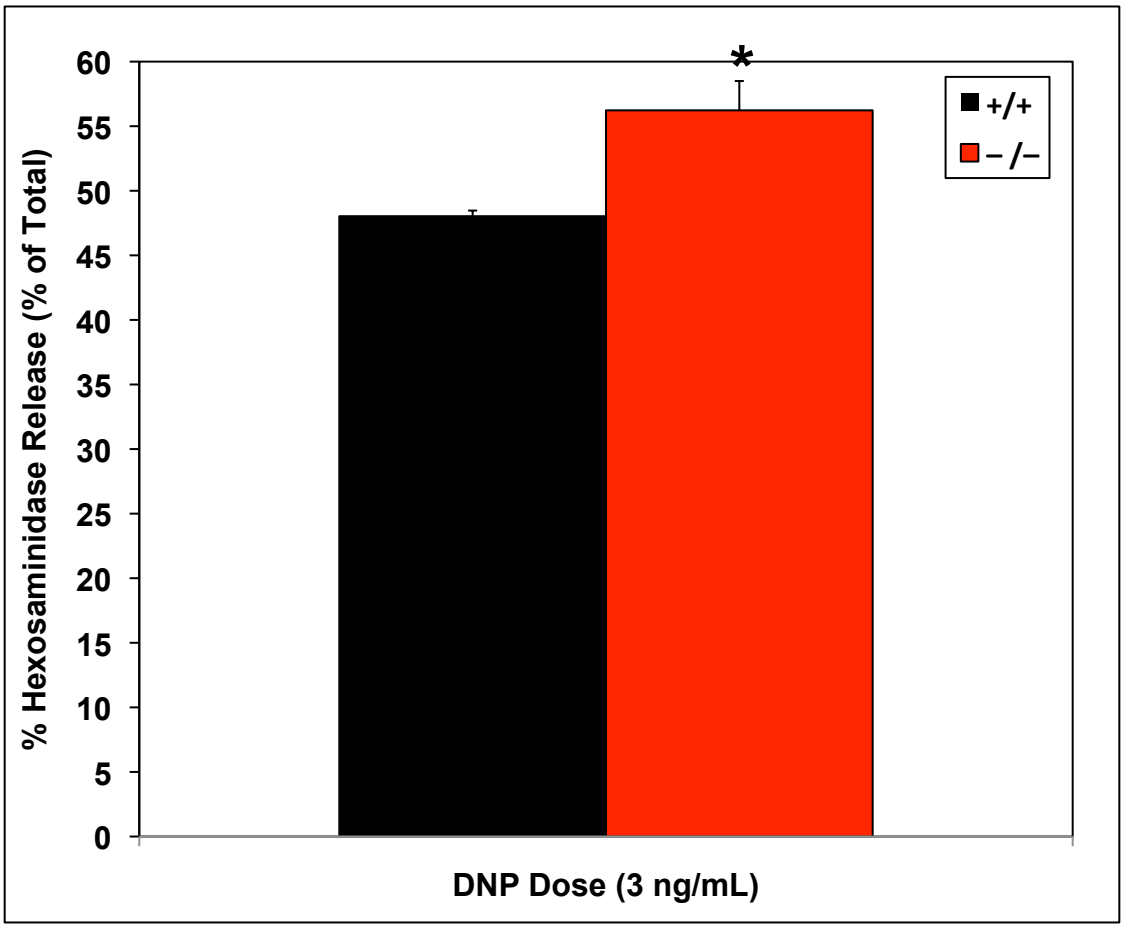
60
55
50
45
40
35
30
25
20
15
10
5
0
% Hexosaminidase Release (% of Total)
*
+/+
– /–
DNP Dose (3 ng/mL)

Chapter 3

MARCKS Translocation and the Necessary Conserved Sequences

INTRODUCTION

Understanding the subcellular behavior of MARCKS following cell activation is essential for understanding how or where MARCKS may be participating in regulated exocytosis. It is established that phosphorylation of MARCKS by PKC induces its movement to the cytosol (Ohmori, *et al*., 2000). What is not yet fully elucidated is which components of MARCKS structure regulate this characteristic change. Three evolutionarily conserved regions of sequence present in both members of the MARCKS gene family may be involved in MARCKS subcellular targeting upon PKC phosphorylation: a myristoyl moiety consensus sequence site, a MARCKS homology-2 (MH2) domain, and the phosphorylation site domain (PSD) (Aderem, 1992). Additionally, between the myristoyl consensus sequence site and the MH2 domain lies a conservatively substituted region, evolutionarily conserved in MARCKS across species, but not formally described as a domain. This region was targeted because a peptide of this sequence has been used to significantly inhibit regulated exocytosis, a function believed to require proper MARCKS targeting (Seykora, *et al.*, 1996; Singer, *et al.*, 2004) (Fig. 1.2).

To determine whether these domains affect subcellular targeting, we transiently transfected mutant MARCKS cDNA constructs, fused at the C-terminus to enhanced yellow fluo-

rescent protein (eYFP), into human embryonic kidney cells (HEK293) for live cell fluorescent imaging. Each construct was mutated in a specific region implicated for MARCKS's sub-cellular targeting, and transfected cells were stimulated with PKC activators ATP or phorbol 12-myristate 13-acetate (PMA).

MATERIALS AND METHODS

Culturing of Human Embryonic Kidney (HEK293) Cells

Human embryonic kidney cells of low passage (<P12) number were thawed from -80º C stock and seeded into 60 mm plates (Corning) Cells were cultured in Dulbecco's Modified Essential Medium (Gibco) supplemented with 10% FBS (Gibco). Media was changed every other day and passaged when approximately 60% confluence was reached.

Site-directed Mutation and Cloning of the G2A, ΔMH2, PsPi MARCKS cDNA Mutants

Mutant constructs of MARCKS were generated with the Advantage GC-2 PCR kit (Clontech), using human MARCKS cDNA. WT human MARCKS in the pcDNA3.1 plasmid, a gift from the laboratory of Wanda O'Neal (UNC-Chapel Hill), was used as a template for the non-myristoylatable (G2A), scrambled MARCKS (SM), MH2 deletion (ΔMH2), and pseudo-phosphorylated MARCKS (PsPi) mutants. The G2A, ΔMH2, PsPi MARCKS mutants were generated by PCR using the QuikChange™ Site-Directed Mutagenesis Kit (Stratagene) and transformed into XL-10 Gold Supercompetent cells. The PCR primers used to generate the MARCKS mutant constructs were as follows: 5'–CAGAATTC-CACCATGGCTGCCCAGTTC–3' forward for G2A; 5'–AGAACTGGGCAGCCATG-GTGGAATTCTG–3' reverse for G2A; 5'–ATTATCCGGACACAGCCGCCTCCCCA–3' forward for ΔMH2; 5'–GTAATCCGGAGCGGCCGCCGAGTC–3' reverse for ΔMH2; 5'–GAAGCGCTTTGACTTCAAGAAGGATTTCAAGCTG–3' forward (1) for PsPi; 5'–CAGCTTGAAATCCTTCTTGAAGTCAAAGCGCTT–3' reverse (1) PsPi; 5'–CAAGCT-GAGCGGCTTCGACTTCAAGAAGAAC–3' forward (2) for PsPi; and 5'–GTTCTTCTT-GAAGTCGAAGCCGCTCAGCTT–3' reverse (2) for PsPi. The MH2 deletion mutant was

transformed into INV110 Competent cells (Invitrogen). The plasmids were grown up in ampicillin LB and DNA isolated using the Qiaprep Miniprep Kit (Qiagen) for sequence analysis by the UNC Sequencing Core at UNC-Chapel Hill, NC. For each MARCKS mutant construct, at least ten clones were analyzed for the presence of the proper mutation(s) and reading frame. From the successful transformers, MARCKS was extracted with a double digest by the enzymes EcoRI and HindIII (New England Biolabs). The DNA band was isolated using a Qiaprep Gel Extraction kit (Qiagen) and maxipreps of the isolated DNA were prepared using the Qiaprep Endo–Free Maxiprep Kit (Qiagen). The purified DNA (50 ug) was ligated into the pML2 retroviral vector (Clontech), and maxipreps of the full-length mutated DNA were isolated for transfection experiments.

Synthesis and Cloning of the Scrambled MARCKS cDNA Mutant

The desired scrambled sequence was synthesized using Sequenase, a modified T7 DNA Polymerase (USB Corporation) and long oligonucleotides that serve as both primers and template (Moore, 2001). Primers (1 ug/uL), Sequenase (10 U), buffer and dNTP (10 mM) were incubated for 30 minutes at 37º C. The long oligonucleotides were 5'–TAGAATTCCACCATGGGTGCCCAGTTCTCCACCCCTGCGGAAGGAGCCGGGGCGGAGGTGAAGAGGGCG–3' as forward primer and 5'–TTCACGTGGCCATTCTCCTGTCCGTTCGCTTTGGAAGGCGACGAGGCCTTAGCCTCTGCCGCCCTCTTCACCTCC–3' as the reverse primer. The polymerase was then heat inactivated and the product subcloned into the TOPO vector using the TOPO TA cloning kit (Invitrogen) and transformed into XL–10 Gold Supercompetent Cells. Once sequencing and proper reading frame were confirmed, the scrambled region was double digested and ligated into the pML2 retroviral vector, containing the

remaining MARCKS sequence. Qiaprep Endo–Free Maxiprep (Qiagen) was used to isolate the mutated DNA for transfection.

Live Cell Imaging of HEK293 Cells

MARCKS cDNA constructs were transfected using Fugene 6 (Roche). After 48 hours, cells were imaged using a Nikon TE 2000-U microscope equipped with a Yokogawa Spinning Disc Confocal scanhead (CSU10) and live images were acquired with a 60X 1.4 NA oil objective. The Hamamatsu Orca ER camera was controlled by Simple PCI software version 6.0 (Hamamatsu). Filter settings for FITC (excitation at 488 and emission at 525/50) were used to capture the eYFP fluorescence. Live cells were stimulated with various concentrations of ATP or phorbol 12-myristate 13-acetate (PMA), a DAG mimic (Sigma).

Statistical Analysis

Statistical differences between the means of two groups were determined by the unpaired two-tail student's t-test. *P* values below 0.05 are regarded as statistically significant and are indicated by asterisks.

Figure 3.1: Generated MARCKS cDNA Mutants

MARCKS cDNA mutants were generated for each potential targeting region.

(A) Full–length and unmutated human MARCKS cDNA (WT) was fused to enhanced yellow fluorescent protein (eYFP) at the C-terminus.

(B) A single point nucleotide mutation translates the glycine residue to an alanine generating the non-myristoylatable (G2A) mutant.

(C) The novel MH2 deletion mutant (ΔMH2) lacks the MH2 domain of unknown function and was substituted for a BspE1 restriction site.

(D) The scrambled MARCKS mutant (SM) contains the scrambled sequence of the random NH_2-terminal sequence (RNS) peptide from Li, *et al.*, 2001.

(E) The final mutant is the pseudo-phosphorylated mutant (PsPi) with the serine residues of the PSD mutated to aspartate, mimicking a partial phosphorylation state.

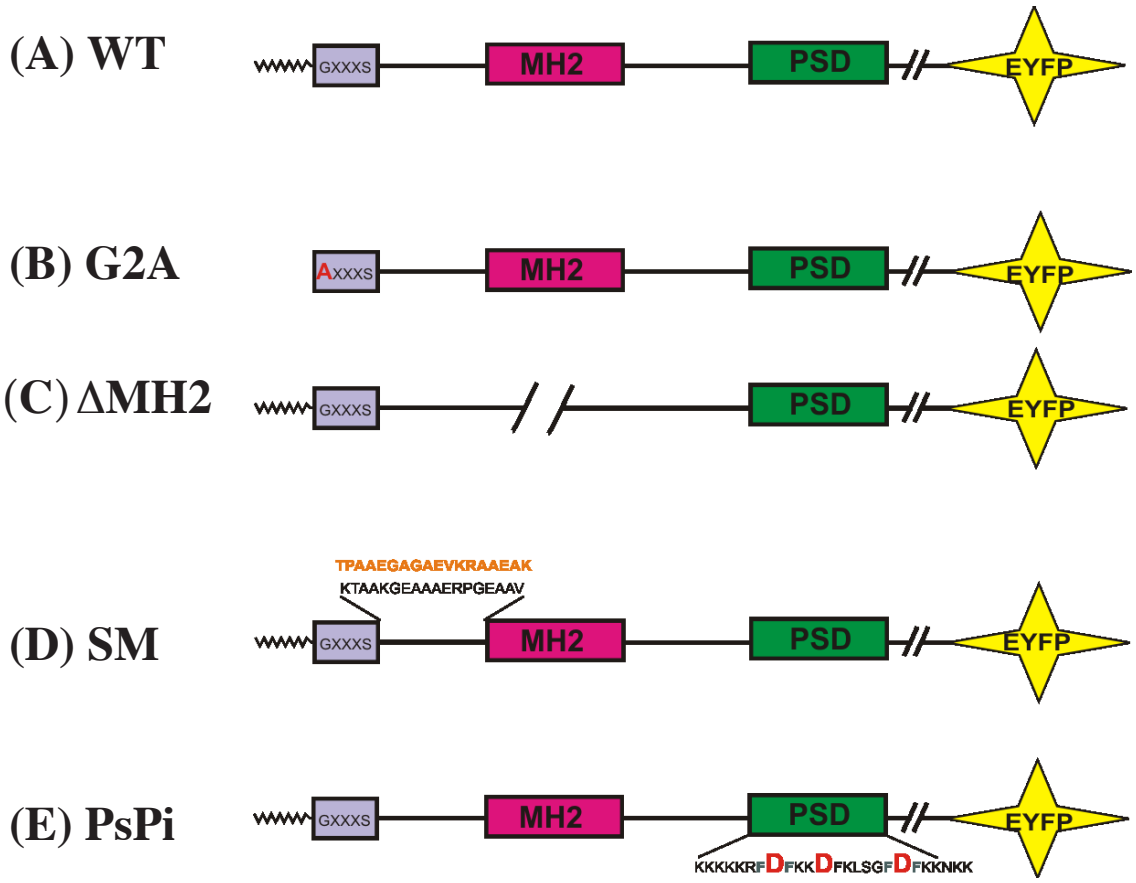
(A) WT
GXXXS
MH2
PSD
EYFP
(B) G2A
AXXXS
MH2
PSD
EYFP
(C) ΔMH2
GXXXS
PSD
EYFP
(D) SM
TPAAEGAGAEVKRAAEAK
KTAAKGEAAAERPGEAAV
GXXXS
MH2
PSD
EYFP
(E) PsPi
GXXXS
MH2
PSD
EYFP
KKKKKRFDFKKDFKLSGFDFKKNKK

RESULTS

Live visualization of WT MARCKS Translocation

First, the translocation of WT MARCKS upon PKC phosphorylation was experimentally confirmed in human embryonic kidney (HEK293) cells. After HEK293 cells were transfected with the full-length WT MARCKS cDNA fused to eYFP (Fig. 3.1A), the translocation process was recorded in real time after addition of PKC activators (Fig. 3.2). As previously shown (Ohmori, *et al.*, 2000), WT MARCKS was found primarily associated with the PM in resting cells. Upon stimulation with the DAG mimic, PMA, which phosphosphorylates and activates PKC, WT MARCKS moved to the cytosol where it associated with vesicular membranes. The identity of these cytosolic vesicles remains unclear since HEK293 cells are a non-secretory cell line. Since PMA was never removed from the solution, MARCKS remained in the cytosol until the completion of a 20-minute time period. However, when the cells were stimulated with adenosine trisphosphate (ATP), an activator of a receptor-mediated signaling pathway which includes PKC activation, a transient translocation of MARCKS was induced. Three minutes after stimulation, a peak in the intensity changes of the PM and the cytosol occurred (Fig. 3.3), reflective of the movement of MARCKS-eYFP to the cytosol. By ten minutes, a small amount of recovery was observed, indicating a return of MARCKS-eYFP to the PM.

Non-myristoylatable MARCKS does not associate with membranes

The non-myristoylatable (G2A) MARCKS mutant (Fig. 3.1B) was generated by a single point nucleotide mutation in the sequence recognized for MARCKS to be co-translationally myristoylated. In resting cells, G2A was primarily localized in the cytosol in a dif-

Figure 3.2: Translocation of WT MARCKS After PMA stimulation

HEK293 cells were transfected with WT MARCKS labelled with eYFP. PMA mimics DAG, the activator of PKC, and induces the translocation of PKC to the PM, where it phosphorylates MARCKS. As long as PMA is present in the bath, MARCKS will continually be phosphorylated and translocated to the cytosol.

(A) In unstimulated cells, MARCKS flourescence is clearly PM-associated. After addition of PMA, MARCKS fluorescence was found in the cytosol, not just in a diffuse pattern, but also associated with vesicular membranes (arrow).

(B) The fluorescent intensity of the PM and cytosol of PMA-treated cells was compared to the fluorescent intensity of the PM and cytosol of the same cells prior to stimulation (control). The intensity values were normalized to the control cells and the normalized values (absolute values) show the smaller amount of decrease in PM intensity compared to the large increase in cytosolic intensity.

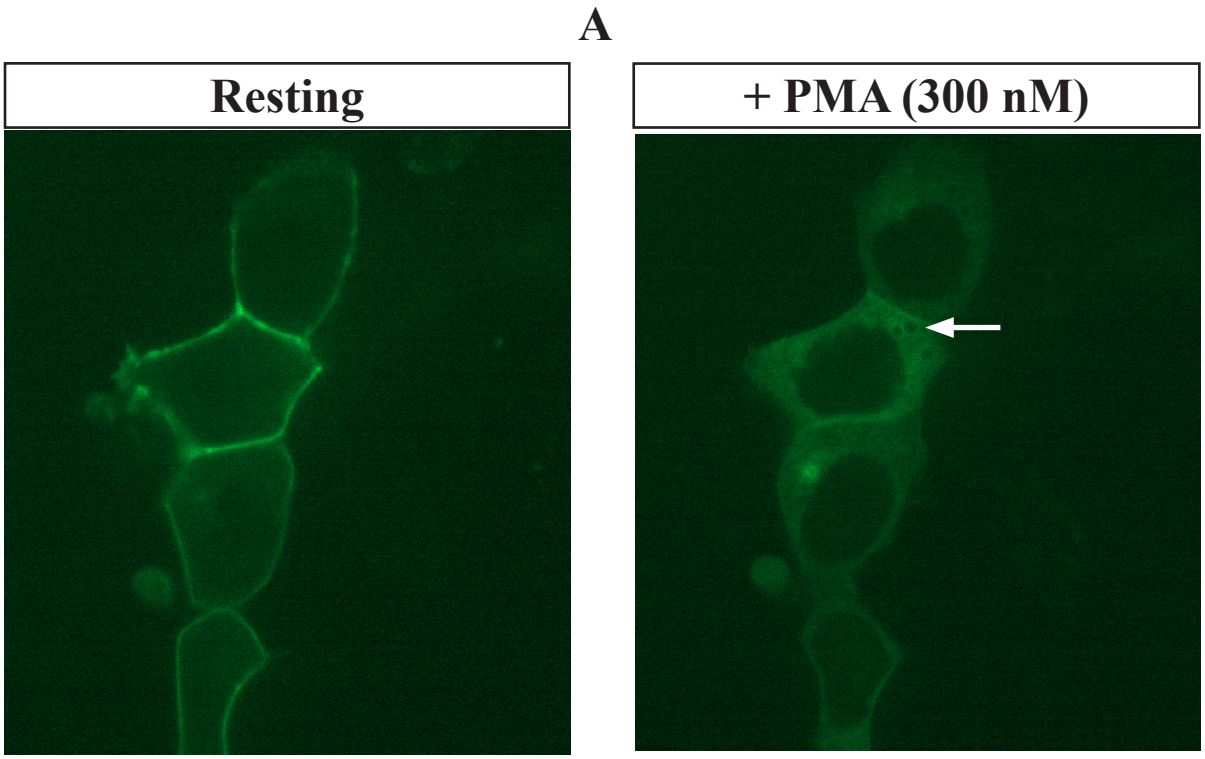
A
Resting
+ PMA (300 nM)

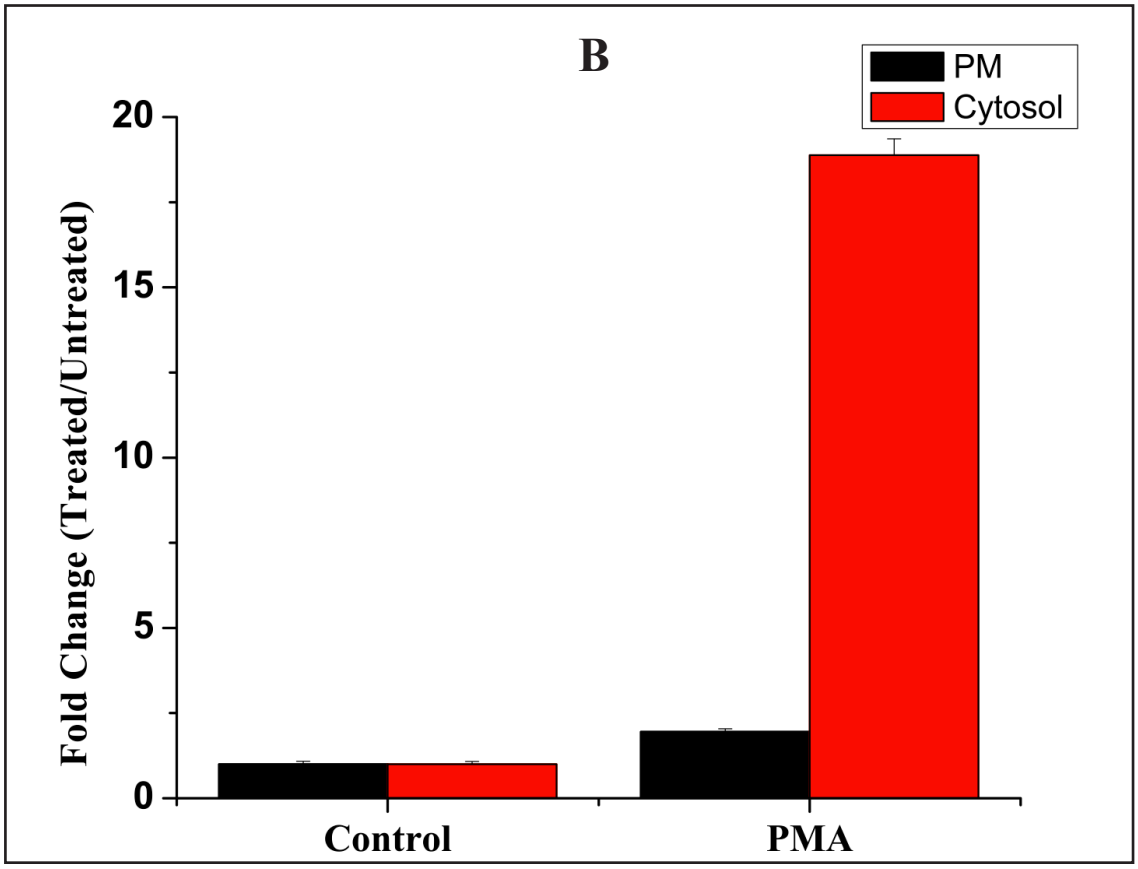
B
PM
Cytosol
Fold Change (Treated/Untreated)
20
15
10
5
0
Control
PMA

Figure 3.3: Translocation of WT MARCKS After ATP stimulation

ATP, an agonist for a G protein-coupled purinergic receptor, was added to HEK293 cells transfected with WT MARCKS-eYFP. Unlike phorbol ester stimulation, ATP only activates a transient translocation of MARCKS. In unstimulated cells, the amount of MARCKS flourescence associated with the PM and the cytosol were quantified before ATP addition. These intensity values were normalized to be the control values (black). ATP stimulation induced a significant decrease in PM intensity, approximately 0.60 fold, and a corresponding significant increase in cytosolic intensity, by more than two-fold. Recovery of the process was marked by return to previous PM intensity levels, and a significant decrease in cytosolic intensity. Interestingly, the cytosolic intensity was further decreased compared to the control values, perhaps due to photobleaching.

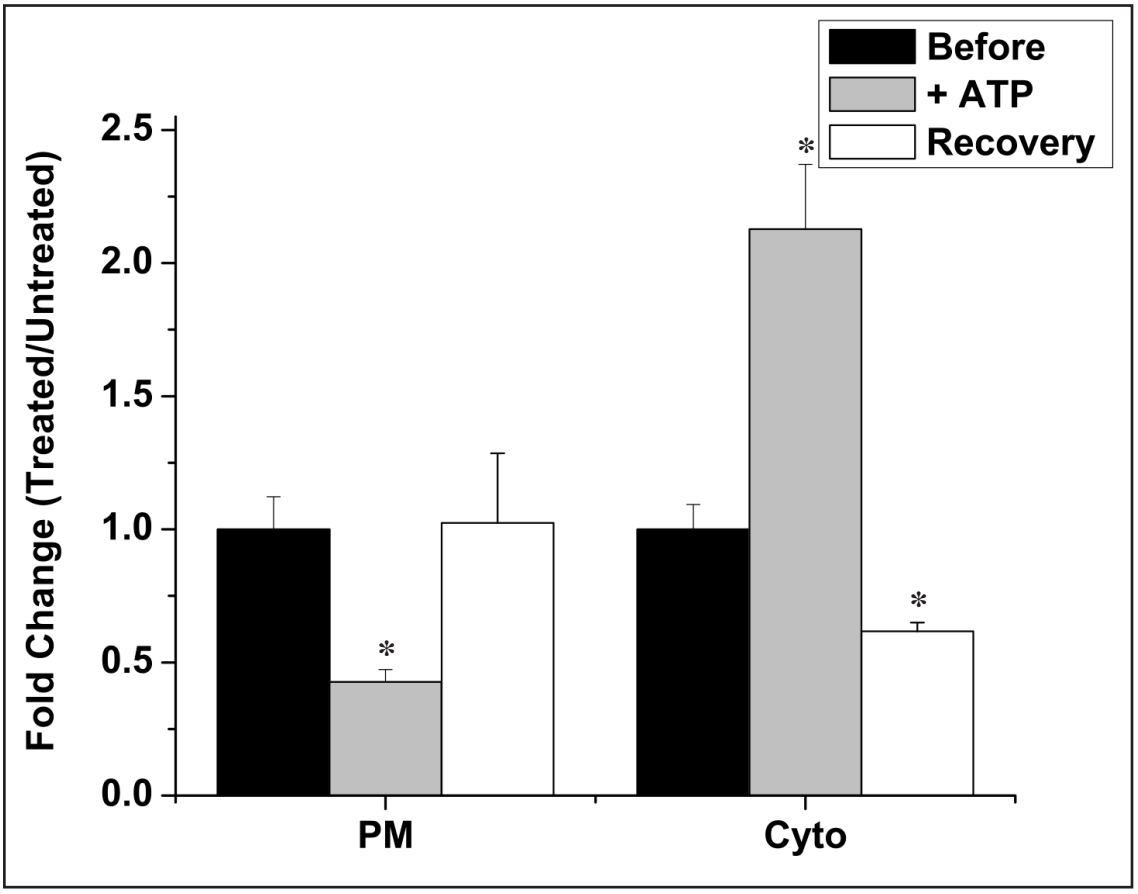
Before
+ ATP
Recovery
Fold Change (Treated/Untreated)
2.5
2.0
1.5
1.0
0.5
0.0
*
*
*
PM
Cyto

fuse pattern (Fig. 3.4). Additionally, the diffuse pattern did not appear to be associating with vesicular membranes in the cytosol, either under resting conditions or in response to PKC.

Pseudo-phosphorylated MARCKS shows increased cytosolic localization.

The pseudo-phosphorylated (PsPi) MARCKS mutant (Fig. 3.1E) was generated by mutating the three serine residues, normally phosphorylated by PKC, to aspartate residues. Consequently, this mutant is insensitive to PKC phosphorylation and carries a partial negative charge. (Arbuzova *et al.*, 2002). This results in a mutant which mimicks PKC phosphorylation effects, even in resting cells. In resting cells, PsPi MARCKS was found to be both PM and significantly more cytosol-associated (Fig. 3.5, 3.8), in contrast to WT MARCKS (Fig. 3.2). After stimulation, the mutant localization remained unchanged, as expected, due to its insensitivity to PKC.

Translocation of the novel Scrambled MARCKS mutant quantitatively mimics WT behavior

The two novel mutants, the scrambled MARCKS and MH2 deletion mutants (Fig. 3.2 C–D), are based on observations from Seykora, *et al*., 1996. They demonstrated *in vitro* that deletion of residues 6-140, lying between the myristoyl moiety and the PSD, showed impairment of PKC-dependent MARCKS translocation. Another group identified six novel phosphorylation sites in this portion of sequence, suggesting the presence of post-translational regulation, a sign of significance (Taniguchi, *et al.*, 1994). What remains to be clarified is by what mechanism this post-translationally regulated region is significant to the PKC-dependent targeting process. This question is particularly intriguing since the original deletion encompassed the intermediate region of conservatively substituted sequence and the conserved

Figure 3.4: Translocation of G2A MARCKS After PMA stimulation

HEK293 cells were transfected with G2A MARCKS-eYFP and stimulated with PMA (300 nM). In resting cells, MARCKS is localized in a diffuse cyosolic pattern. A small portion of MARCKS was localized to the PM (arrowheads). Addition of PMA did not result in any significant change in localization, despite obvious intracellular movement and the only change observed was translocation of the small amount of PM-associated G2A MARCKS to the cytsol.

Resting

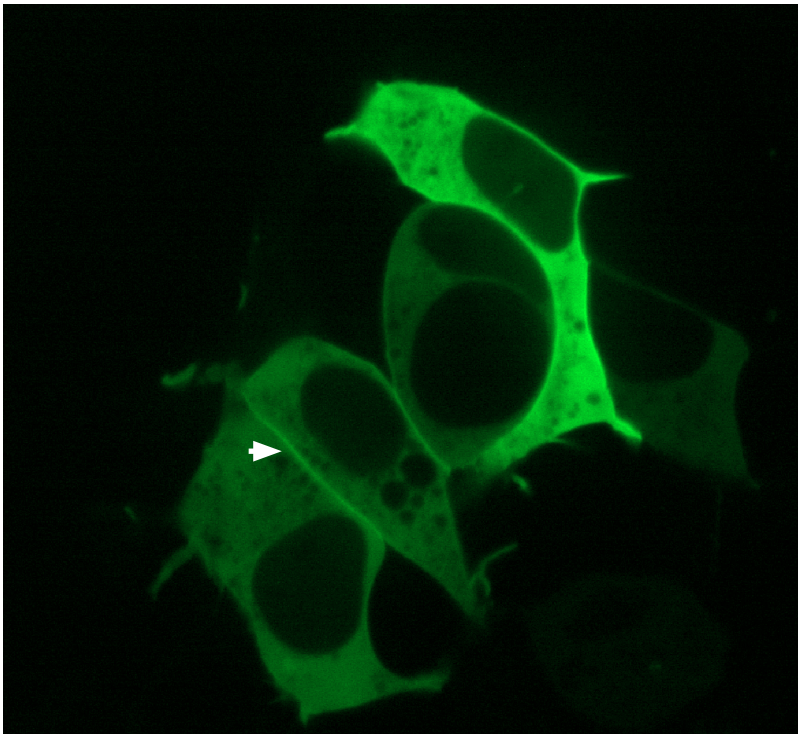

+ PMA (300 nM)

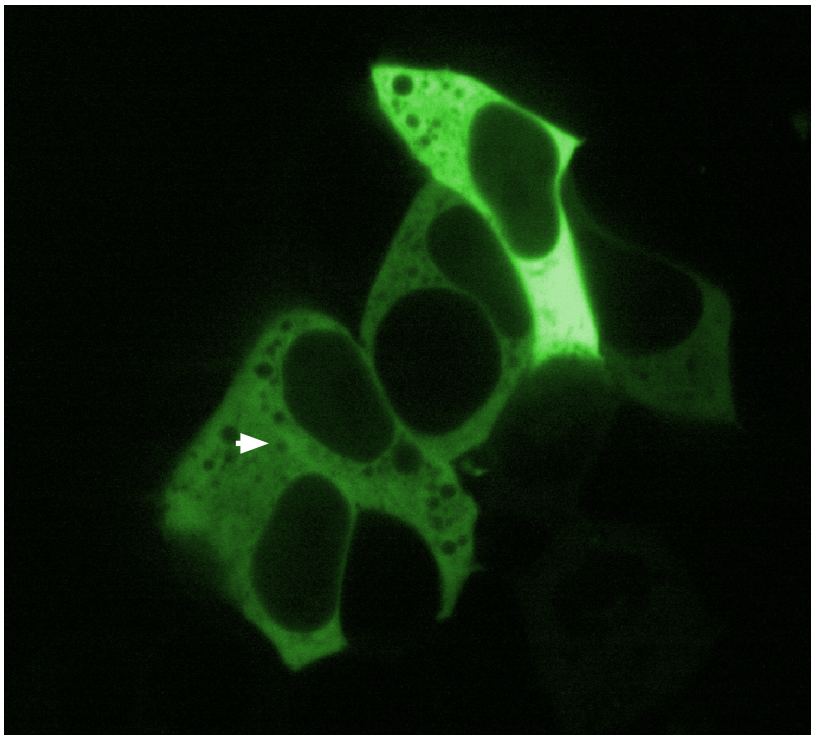

MH2 domain. Potential targeting defects were tested by creating two separate cDNA mutants for the two components of the region.

The Scrambled MARCKS (SM) mutant targets the intermediate region of conservatively substituted sequence by utilizing a scrambled sequence derived from an existing peptide (Li, *et al.*, 2001). This technique allowed any non-specific electrostatic contributions to be preserved. The idea was derived from experiments showing that a peptide corresponding to this intermediate region of the MARCKS sequence reduced mucin secretion in NHBE cells, suggesting significance of this region in regulation of MARCKS function in exocytic secretion (Li, *et al.*, 2001; Singer, *et al.*, 2004).

Live cell imaging experiments in HEK293 cells showed no quantitative difference between SM (Fig. 3.6) and WT MARCKS targeting. However, while the majority of cells resembled WT behavior, some SM-transfected cells, as shown in Fig. 3.6, exhibited pronounced vesicular membrane association prior to activation, compared to similar levels of overexpression in WT control cells.

Translocation of the novel MH2 deletion mutant mimics WT behavior

The MH2 domain, the second portion of the deleted region, has been suggested to play a role in targeting or regulation, but the effect of the MH2 domain alone has not been experimentally tested. HEK293 cells transfected with a ΔMH2 MARCKS mutant, where only the conserved 72 bp MH2 domain was deleted, showed no qualitative difference in targeting compared to WT MARCKS (Fig. 3.8). While in resting cells, ΔMH2 MARCKS was localized to the PM. Upon PMA-induced PKC activation, ΔMH2 translocated to the cytosol and associated with vesicular membranes, mimicking WT behavior.

Figure 3.5: Translocation of PsPi MARCKS After PMA stimulation.

HEK293 cells were transfected with PsPi MARCKS-eYFP and stimulated with PMA (300 nM). In resting cells, MARCKS is localized to both the PM (arrowheads) and the cytosol with vesicular membrane association (arrows). PMA stimulation did not result in any significant change in the PM-associated localization of the PsPi mutant or a significant change in vesicular membrane association.

Resting

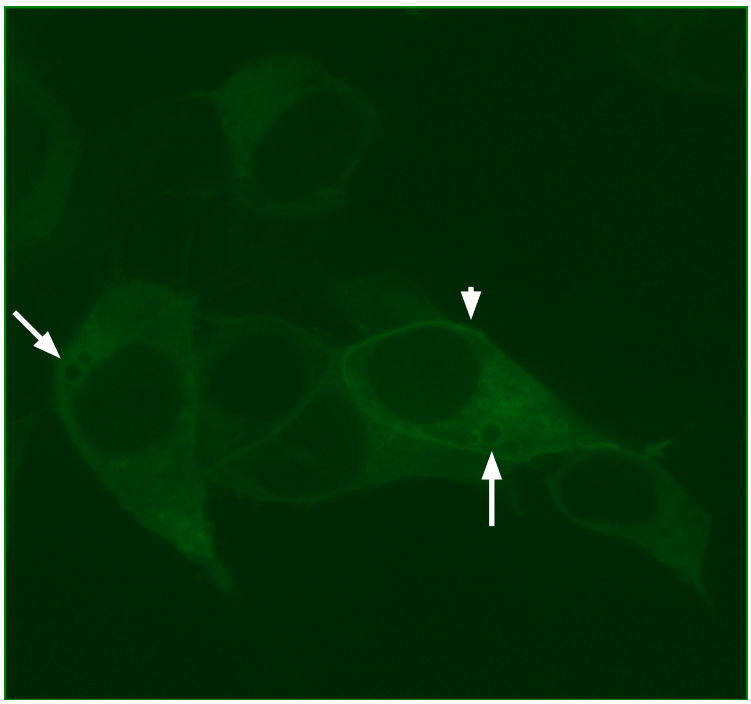

+ PMA (300 nM)

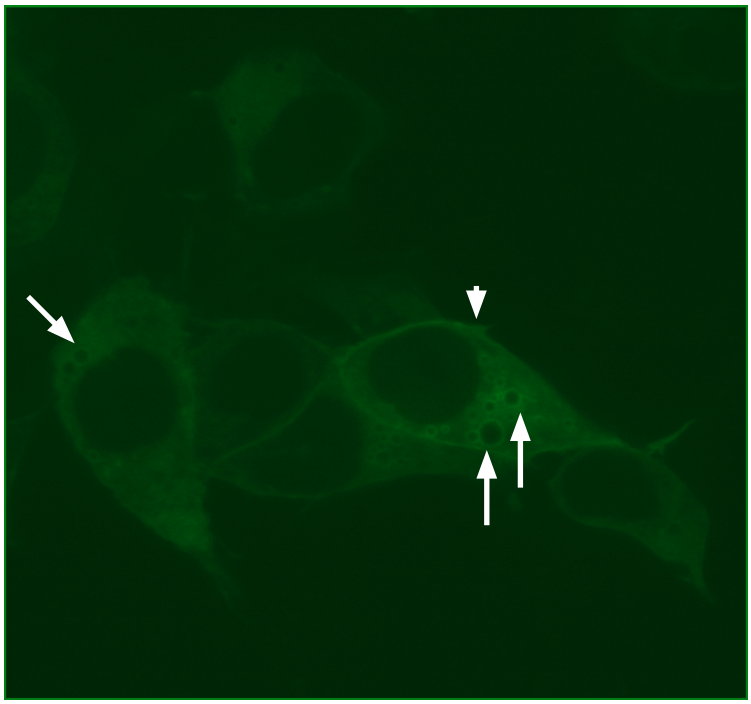

DISCUSSION

First, observations from previous studies were confirmed by showing the translocation of MARCKS in a live cell system using the HEK293 cell line. Cells transfected with WTMARCKS clearly associated with the PM in the resting state. After being stimulated with either PMA, a DAG mimic (Fig. 3.2), or ATP, activating a receptor-mediated response (Fig. 3.3), MARCKS translocated to the cytosol. Interestingly, though, cytosolic MARCKS associated with the vesicular membranes in the cytosol. This is not unexpected since previous studies have demonstrated association of MARCKS with lysosomes and possibly SGs in airway epithelial cells (Singer, *et al.*, 2004; Ohmori, *et al*., 2000; Allen & Aderem, 1995). However, because HEK293 cells are not a secretory cell type, it remains unclear to what intracellular membranes MARCKS associates with in the cytosol. The reversible translocation upon ATP activation clearly demonstrated the disparity between the physiological response and pharmacological treatment of cell culture studies. In ATP stimulated cells, the maximal translocation was observed approximately three minutes after stimulation, and reversal of the process was found to occur by approximately ten minutes after stimulation. This translocation timing correlates well with the rate of release observed in mast cells upon agonist stimulation, as quantitated previously in Chapter 2 (Fig. 2.5). Despite the differences of non-secretory cells versus secretory cells, timing for complete translocation of MARCKS to the cytosol at approximately three minutes correlates well with the 2.5 (+/– 0.5) minutes required for 50% of the cells total secretory cargo to be released from WT mast cells (see Chapter 2).

Previous observations were also confirmed in real-time for the G2A MARCKS mutant. Our live cell imaging confirmed previous observations from both mice and *in vitro* studies that the myristoyl moiety is necessary for membrane association (Swierczynski, *et al.*, 1996;

Ohmori, *et al.*, 2000). Membrane association both in the PM and the cytosol was lacking in G2A-transfected cells (Fig. 3.4). It has been demonstrated that without the myristoyl moiety, mice lack normal postnatal viability, suggesting a physiological importance for the membrane association (Swierczynski, *et al.*, 1996) mutated in the above studies. However, the functional consequences on regulated exocytosis remain undetermined.

Observations of the pseudo-phosphorylated MARCKS mutant, despite having been utilized by other groups, revealed surprising results. Attenuation of PM association in the PsPi mutant has already been eloquently demonstrated and was quantitatively shown in these studies (Fig. 3.8) (Ohmori, *et al.*, 2000). However, in HEK293 cells the PsPi mutant still associated with vesicular membranes before and after PMA addition (arrows in Fig. 3.5). In the myristoyl-electrostatic switch model proposed by Stuart McLaughlin, translocation of MARCKS to the cytosol is induced by addition of phosphorylation charges to the PSD, thereby inhibiting the electrostatic interaction between the polybasic PSD and the PM (Seykora, *et al*., 1996, Tzlil, *et al*., 2008). The localization pattern observed in the PsPi-transfected cells revealed another aspect of membrane association. Despite the obviously diminished PM association found in mutant cells, the principally cytosolic mutant still associated with vesicular membranes (Fig. 3.5). These results could be unique to HEK293 cells, but they raise the possibility that association with vesicular membranes is not mediated through the same mechanism as PM association. Another group has proposed that MARCKS positively regulates secretion by binding to the membranes of SGs in mucin-secreting goblet cells. This mechanism has been proposed as a model by which MARCKS regulates granule trafficking (Singer, *et al.*, 2004). PsPi MARCKS associating with vesicular membranes supports the concept of phosphorylated MARCKS localizing to SG membranes. Further studies, however, would be required to link observations

Figure 3.6: Overall, Scrambled MARCKS demonstrates WT behavior

In resting cells, Scrambled MARCKS localizes to the PM (arrowheads) and cytosolic vesicular membranes (arrows). Addition of PMA resulted in a significant shift from PM to labeling with cytosolic vesicular membranes. The distribution in most cells before and after stimulation were comparable to cells infected with WT MARCKS. However, some cells overexpressing the mutant showed vesicular membrane localization even prior to stimulation.

Resting

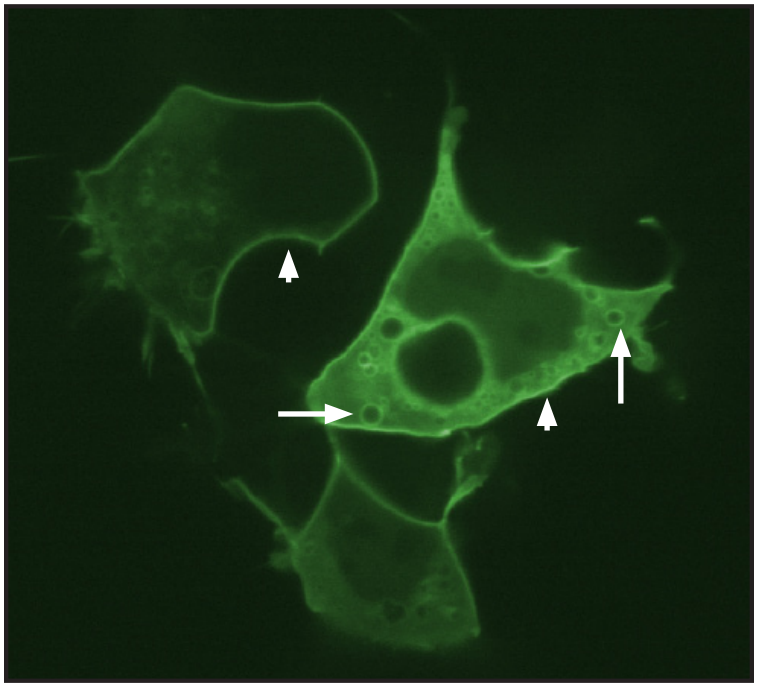

+ PMA (300 nM)

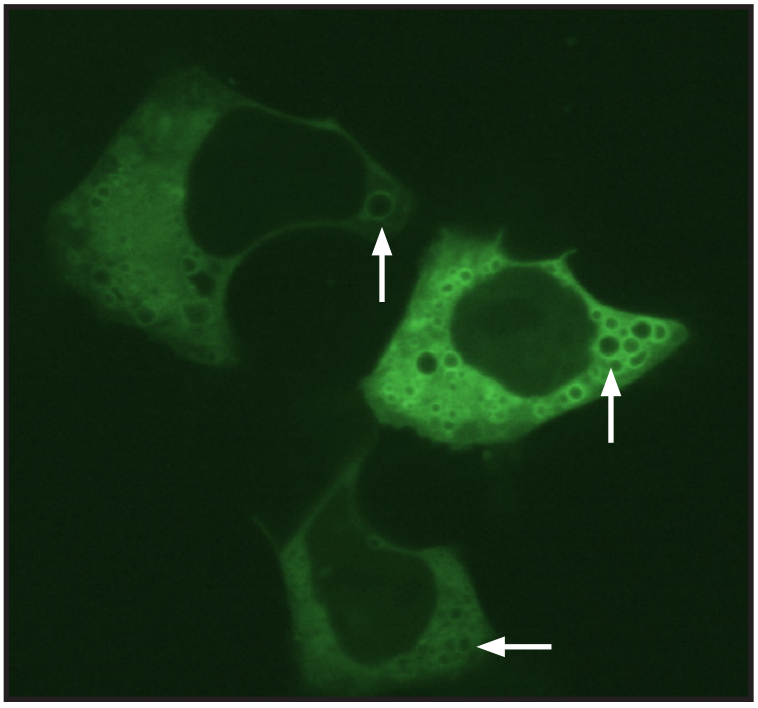

Figure 3.7: Deletion of the MH2 domain does not affect translocation

In both resting and stimulated cells, deletion of the MH2 domain mimicked WT behavior. PMA activation induced MARCKS to translocate from the PM (arrowheads) to the cytosol and cytosolic vesicular membranes (arrows).

Resting

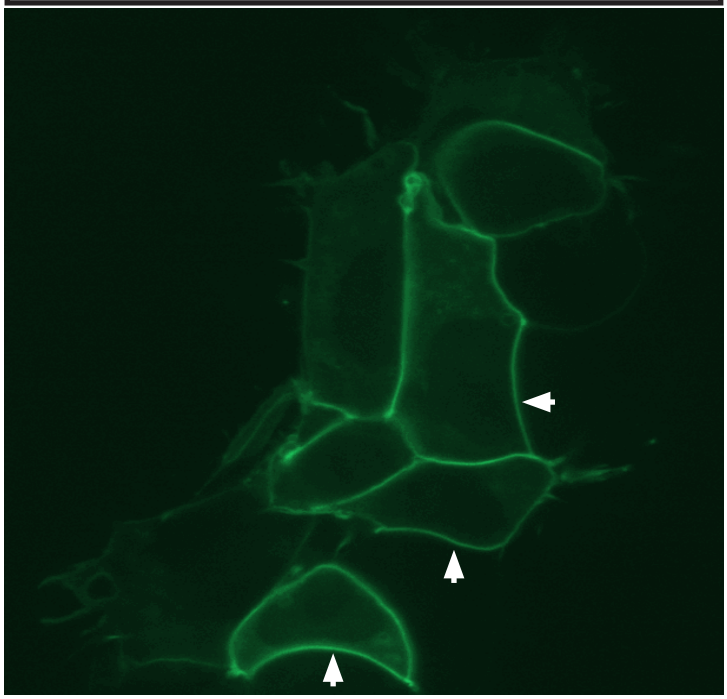

+ PMA (300 nM)

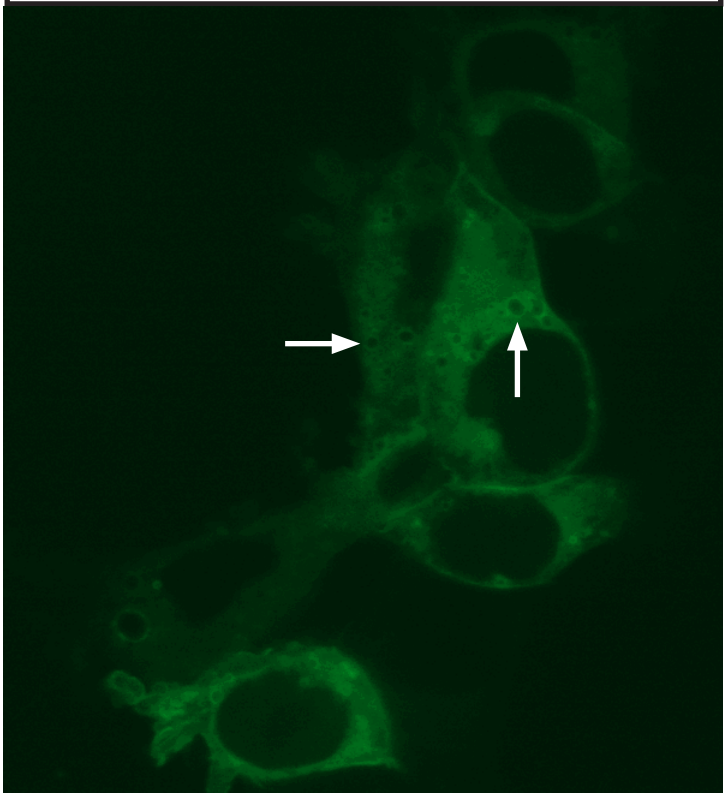

made in non-secretory cells to secretory cells

While the remaining localization studies of the SM and ΔMH2 mutant constructs did not implicate these regions for subcellular targeting, the generation of the constructs and live imaging experiments were the first to clearly isolate and test the importance of the amino terminus for translocation. SM-transfected cells lacked any quantitative differences in PKC-induced movement to the cytosol, but did qualitatively appear disparate from WT in cells expressing similar levels of overexpression. The difference seen in several different experiments was the presence of cytosolic localization found in the SM mutant cells even prior to activation. As is demonstrated in the representative image (Fig. 3.6), while most cells had a slight, insignificant increase in cytosolic association, other cells appeared to have a much more obvious non-PM association before PKC activation. While the significance of this occassional change in subcellular behavior was intriguing, it was a question beyond the focus of this study. Cells transfected with the ΔMH2 mutant, alternatively, mirrored WT behavior before and after PKC activation, with strikingly similar PM localization between the MH2 mutant and WT in the resting state (Fig. 3.3, Fig. 3.7).

Consequently, these studies demonstrated that the only mutations affecting the ability of MARCKS to associate with the PM were the lack of myristoylation and the addition of phosphorylation groups (Fig. 3.8). Association with vesicular membranes, alternatively, was inhibited only by myristoylation. In testing the novel mutations of deleting the conserved MH2 domain of unknown function, or the sequence mimicked by the MANS peptide, which significantly inhibits secretion (Singer, *et al.*, 2004), we surprisingly found no quantifiable effect on MARCKS translocation behavior. Future studies could be greatly enhanced by utilizing full-length mutants, such as these, in determining the effect of the conserved regions of

Figure 3.8: Association of MARCKS Mutants with the PM in resting cells

All of the MARCKS mutants were quantitated for their ability to bind to the PM prior to PKC activation. The measurements were derived from at least three independently transfected imaging experiments, where the mean fluorescent PM and non-nuclear cytosolic intensity were measured using Simple PCI software (Hamamatsu). The PM:cytosol ratio for each individual cell in every experiment was calculated. Compared to WT MARCKS, only the G2A and PsPi MARCKS mutants demonstrated a significant difference in the PM: cytosol ratio, where the values below 1.0 represent a greater cytosolic intensity compared to PM intensity. (Error bars represent S.E.; *** $p<0.001$)

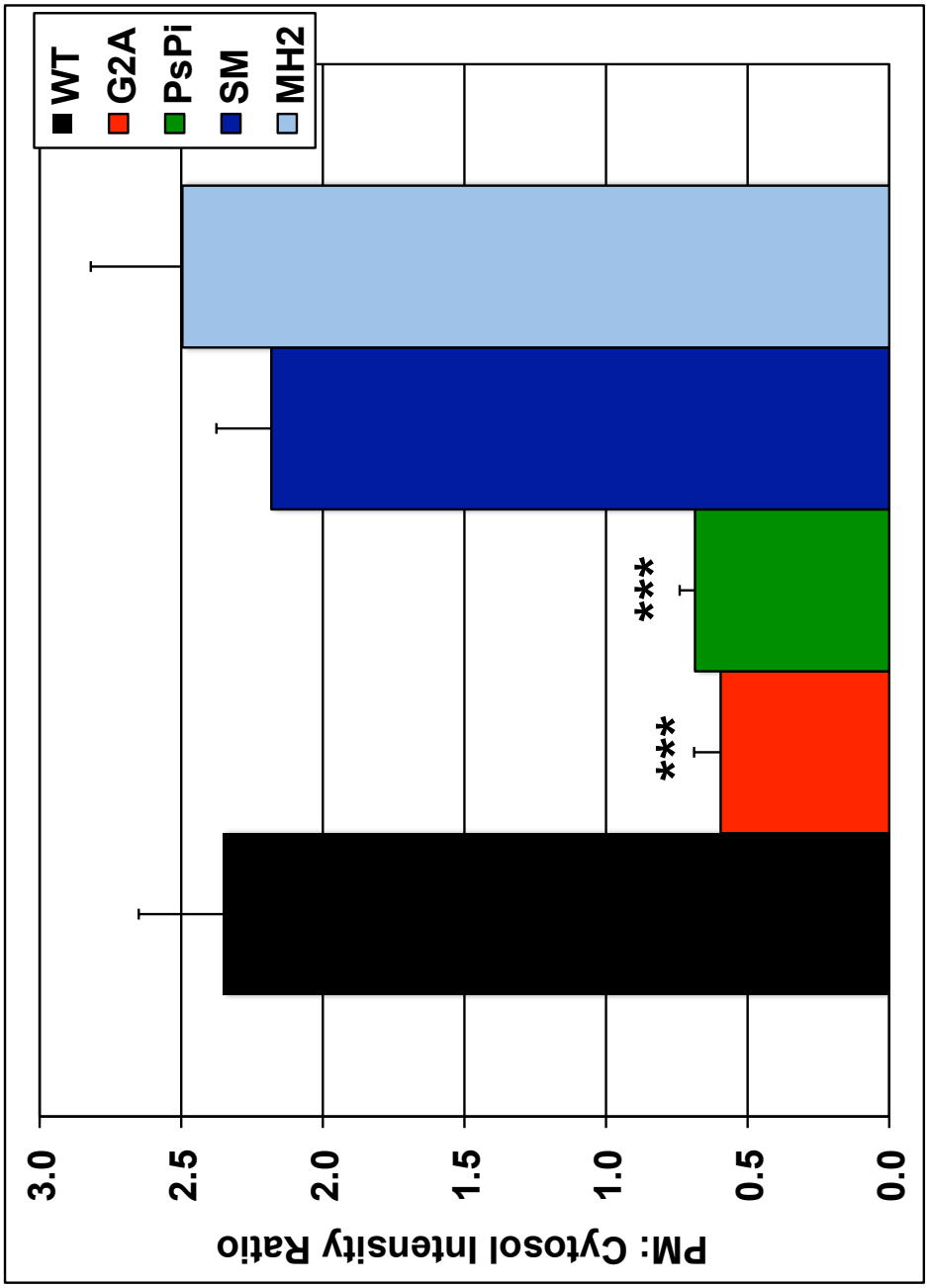
WT
G2A
PsPi
SM
MH2
PM: Cytosol Intensity Ratio
3.0
2.5
2.0
1.5
1.0
0.5
0.0
***
***

MARCKS on some of the proteins' subcellular functions, such as regulated exocytosis and cell motility. For example, the ability of MARCKS to be phosphorylated and de-phosphorylated in myoblasts was correlated with the ability of the cells to adhere using full-length MARCKS mutants (Disatnik, *et al*., 2004). Consequences for mutations of these conserved regions in multiple cellular functions involving MARCKS, beyond translocation behavior, could easily be studied utilizing these constructs.

Chapter 4

Conclusions and Future Directions

Regulated exocytosis is an important physiological process in multiple organ systems, including the nervous system (Li, *et al.,* 2005; Jacques & Abdel-Samad, 2007), circulatory system (Sanchez-Mejorada & Rosales, 1998; Watanabe, *et al.,* 1999; Shiota, *et al.*, 2003; Burley, *et al.,* 2007) and respiratory system (Baumann, *et al.,* 2001; Singer, *et al.*, 2004; Davis & Dickey, 2008). In the respiratory system, excessive regulated exocytosis of mucin results in mucus-clogged airways (Singer, *et al.*, 2004; Davis & Dickey, 2008) and eventually death by asphyxiation. Elucidation of how the regulatory mechanisms controlling the exocytic pathway could provide important insight into future therapeutic techniques for preventing patient morbidity in multiple lung pathologies. One protein that has been purported to be a critical, positive regulator of regulated exocytosis is Myristoylated alanine-rich C kinase substrate (MARCKS) (Elzagallaai, *et al.*, 2000; Rose, *et al.*, 2001; Jerdeva, *et al.*, 2005; Li, *et al.*, 2005; Eliyahu, *et al.*, 2006; Park, *et al.*, 2006; Doreian, *et al.*, 2009). MARCKS is a ubiquitously expressed PKC substrate and one of the two MARCKS gene family members which share multiple conserved regions of sequence. While both MARCKS family proteins, MARCKS and MRP, have been implicated in multiple cell functions, little direct testing of their involvement has occurred because the MARCKS and MRP null mice are perinatally lethal (Stumpo, *et al.*, 1995; Chen, *et al.*, 1996) due to severe neurological defects. We avoided this obstacle by isolating mast cells

from the livers of E14-E18 embryos, which were either MARCKS-deficient, MRP-deficient or WT, and focused on directly testing the role of MARCKS in regulated exocytosis.

Mast cells, however, were not just a convenient secretory cell model in which to test MARCKS function. Mast cells are key mediators of the physiological inflammation response to immune challenge or tissue damage, including pulmonary physiology. Often, mast cells are the initial immune cells activated, upon which they release numerous pro-inflammatory mediators, including chemotactic signals that promote PMN immune cell infiltration to the site of challenge. This role for mast cells is served through secretion of the necessary pro-inflammatory mediators, a process mediated by regulated exocytosis (Shiota, *et al.*, 2003; Bischoff & Kramer, 2007; Metz & Maurer, 2007). By testing MARCKS in mast cells, the function of MARCKS in both immune cell secretion and the regulated exocytic pathway in general could be analyzed.

Proceeding with these studies, the eHMC system was first confirmed as a valid secretory model. Immunohistochemical staining of BMMCs and eHMCs with two separate antibodies to the high-affinity IgE tyrosine kinase receptor, FcεRI, confirmed that both culturing techniques yielded pure and mature mast cell populations (Suppl. Fig. S1). By comparing the responsivity of WT BMMCs and eHMCs to various agonists, similar secretory responses demonstrated that eHMCs were a viable method for testing mast cell degranulation (Suppl. Fig. S2-S4).

With validation of eHMCs as effective mast cells, the secretory phenotypes of WT and MARCKS-deficient mast cells were compared after activating the FcεRI-mediated pathway by cross-linking the receptor with DNP (Suppl. Fig. S5). The first condition tested was secretion of the cells while in suspension, which is the common mast cell secretion assay. When tested, MARCKS-deficient cells mimicked the regulated exocytic levels of WT cells. It should

be noted, though, that MARCKS was not necessary for secretion, since antigen-mediated secretion was still present in MARCKS null cells. This result was surprising due to previous implications for MARCKS function in the pathway.

The next set of experiments, though, tested mast cells under the more physiological condition of adherence to a substrate, conditions that revealed different results. Most major organs contain populations of resident mature mast cells, adherent to the extracellular matrix and primed to activate the inflammation response upon challenge (Columbo, *et al.*, 1995; Kruger-Krasagakes, *et al.*, 1996; Kruger-Krasagakes, *et al.*, 1999) . To simulate these circumstances, WT and MARCKS-deficient mast cells were allowed to adhere to fibronectin for 24 hours prior to DNP activation of FceRI. A dose response curve showed the maximal secretory response occurred at 3 ng/mL of DNP (Fig. 2.3A), the DNP dose used for the remaining experiments. At the optimal dose, MARCKS null cells released significantly more hexosaminidase in response to DNP than WT cells (Fig. 2.3 A), while the total amount of secretory cargo content remained the same between WT and MARCKS-deficient cells (Fig. 2.3B). This secretory enhancement in the magnitude of release was even present when cells were allowed to adhere to fibronectin for an extended time period of 96 hours (Suppl. Fig. S9). Another phenotypic difference between the two populations was in the shape of the cells prior to activation (Suppl. Fig. S7, S8). MARCKS null cells in the resting state exhibited decreased cross-sectional areas, cell heights (Suppl. Fig. S7) and an approximately 30% decrease in cell volume (Suppl. Fig. S8) compared to their WT counterparts. Further experiments could extend these studies to determine if the change in cell shape persisted even after the cells were activated. For example, the morphological change in individual WT cells from the resting state to thirty minutes after activation was also an approximately 30% decrease in cross-sectional area (Fig. 4.1). It would be of in-

terest to learn if the smaller MARCKS-deficient mast cells lost the same ratio of cell volume after stimulation.

After the magnitude of the secretory response was examined, the time course of secretory cargo release was compared between WT and MARCKS null cells. MARCKS null cells released 50% of their total secretory cargo 2.4 times faster than WT cells (Fig. 2.5). The accelerated rate of release of cargo for the MARCKS-deficient eHMCs was restricted to the early time points, from 30 seconds up to 2 minutes after activation, upon which the disparity disappeared. Preliminary experiments testing if the cortical actin in WT and MARCKS null cells showed any significant disparity 30 seconds after pathway activation, did not demonstrate any noticable differences (Fig. 4.2). Further studies at other time points could lead to different results.

Hence, MARCKS-deficiency affects both the magnitude and time course of mast cell regulated exocytosis, findings which suggest that MARCKS is not essential for exocytosis, but acts as a negative modulator. Significantly, this function indicates an anti-inflammatory role for MARCKS, an important therapeutic implication by itself, even if these observations do not translate from mast cells into other secretory cell types. These secretion studies could be significantly furthered by determining the *in vivo* effect of MARCKS-deficiency on mast cell regulated exocytosis. The experiment would involve mast cell reconstitution studies using mast cell-deficient W^{sh}/W^{sh} mice reconstituted with either MARCKS-sufficient or MARCKS-deficient mast cells, as done for other regulators of mast cell secretion (Melicoff, *et al.*, 2009). The obstacle is that MARCKS null mice are perinatally lethal, so first hematopoietic mast cells would have to be differentiated from embryonic stem cells. Simpler experiments would be to determine if MARCKS-

deficiency affects any other receptor-mediated mast cell degranulation pathways, particularly G-protein coupled receptors which also involve PKC activation (Dugina, *et al.*, 2003; Vines & Prossnitz, 2004; Rivera & Gilfillan, 2006; Hua, *et al.*, 2007; Lattin, *et al.*, 2007). Live cell imaging of both WT and MARCKS-deficient mast cells activated through the FcεRI would allow visual confirmation of whether or not a difference in the amount of release could be observed at earlier time points in individual cells. These imaging experiments could be labor intensive due to the fact that mast cells are known for their heterologous nature at the level of individual cell behavior and microenvironment (Baumann, *et al.*, 2001; Jamur, *et al.*, 2005).

Since the finding of MARCKS as a negative regulator was novel and indicated a possible cell-specific function for MARCKS in mast cells, previous experimental methods for establishing a critical, positive regulatory role for MARCKS in airway epithelia cells were applied to eHMCS (Li, *et al.*, 2001; Singer, *et al.*, 2004). The MANS peptide, acting by an unknown mechanism, has been clearly shown to inhibit regulated exocytosis of several secretory cells. In eHMCS, the MANS peptide was still inhibitory, but in a non-specific manner. Both WT and MARCKS-deficient cells demonstrated equal inhibition of mast cell degranulation when the peptide was applied. The random NH2-sequence (RNS) peptide also inhibited mast cell secretion at the highest dose, suggesting involvement of a non-specific electrostatic interaction. Application of a novel non-myristoylated MANS peptide (NONG) almost obliterated secretion due to even higher levels of inhibition than the MANS peptide. Taken together, these results demonstrate the clear lack of a MARCKS-specific mechanism of action that does not require myristoyl-mediated cell entrance for inhibition of mast cell degranulation. However, a comparison between our observations and previous studies does not eliminate the possibility of a role for the peptide in inhibiting both members of the MARCKS gene family. MRP,

the second MARCKS family member is present in both the WT and MARCKS-deficient cells (Fig. 2.1). The only obstacle to this observation is the significant inhibition observed with the NONG peptide. If the peptide is not able to enter the cell, no effect on MARCKS or MRP would be observed, yet an almost complete inhibition of regulated exocytosis occurred. Future experiments applying the non-myristoylated MANS peptide to airway epithelial cells, would adequately address this conundrum.

In summary, the direct effect of MARCKS-deficiency on mast cell regulated exocytosis was a significant increase in the amount of regulated exocytosis and an accelerated rate of release following mast cell activation. These results demonstrate a negative, modulatory role for MARCKS. However, since these were not mechanistic studies, multiple hypotheses can be derived from these observations. One possible explanation is that lack of MARCKS decreases cell volume, which in turn increases SG density and cell priming for regulated exocytosis. Cell morphology studies demonstrated a MARCKS-dependent attenuation in cell volume of adherent cells compared to WT cells. Since the amount of total secretory content, measured as total hexosaminidase activity, was similar between WT and MARCKS null cells, the cells are likely to be more densely packed with the same number of pre-formed SGs. This increased density could lead to a closer proximity of SGs to exocytic fusion sites on the PM, decreasing the amount of time required for SG trafficking and accelerating the rate of release in MARCKS null cells compared to their WT counterparts.

A separate possibility is that MARCKS-deficient effects in mast cells can be attributed to a change in the cortical actin filaments underlying the the PM. It is impossible, without further experimentation, to determine if altered cell volume or cortical actin volume are the cause or the effect of one another. Either way, the change observed in the decreased cortical actin

Figure 4.1: Cell shape changes in WT cells after antigen-stimulated mast cell regulated exocytosis.

Images of WT eHMCS adherent to fibronectin and labeled with FM 4-64 were captured in the x-y plane as an automatic stage stepped through the z-plane at designated increments. Thirty minutes after antigen stimulation with 3 ng/mL of DNP z-stacks were again captured and imported into Volocity v 4.4. Once 3-D images were assimilated, cell height and cross-sectional area were measured for individual cells.

Mean values of cell height, cross-sectional area, and cell volume are shown in the table. The p-value demonstrates the significance difference between cell morphology features before and after antigen stimulation. Values were derived from at least two independent experiments where measurements of at least 50 cells were analyzed. ***= $p<0.001$

	0 min	30 min	p-value
Cell Height (μm)	9.6 +/- 0.2	7.6 +/- 0.2	***
Cross-Sectional Area (μm²)	182 +/- 8	161 +/- 6	***

volume of MARCKS-deficient cells, could support the hypothesis that MARCKS regulates the cortical actin barrier. Disruption of the cortical actin barrier is one of the initial events SGs must overcome to reach their docking sites on the PM. If lack of MARCKS results in disruption of the actin filaments of the barrier, cells would be more primed for regulated exocytosis once the receptor pathway is stimulated. This situation would similar to the process that occurs in neuronal secretion, where a pool of vesicles already lies near the PM and vesicles are partially docked with the PM even prior to activation of regulated exocytosis. Consequently, when the high affinity IgE receptor is activated, the result is the accelerated kinetics found in MARCKS-deficient mast cells.

To follow up these studies, the focus moved from direct testing of MARCKS-deficiency effects on regulated exocytosis to determining which regions of MARCKS sequence were necessary for MARCKS to properly translocate from the PM to the cytosol. Understanding the translocation of MARCKS is crucial since all hypotheses of MARCKS function revolve around the timing and coordination of this movement. In resting secretory cells, MARCKS is localized to the PM. However, MARCKS moves to the cytosol following phosphorylation by PKC, which is activated when the regulated exocytic pathway is initiated. The regions of MARCKS that were mutated were conserved sequences previously implicated as important to the subcellular behavior of MARCKS. While the non-myristoyalatable MARCKS and pseudo-phosphorylated MARCKS had been generated in previous studies as full-length MARCKS or peptides, the MH2 deletion and scrambled MARCKS mutants were novel constructs. HEK293 cells were transfected with these various constructs and imaged in real-time following application of PKC activators. Either PMA, a DAG mimic, or ATP, a ligand for a receptor-mediated pathway were used as the PKC activators. The translocation of WT-transfected cells was cap-

Figure 4.2: Actin staining of WT and MARCKS-deficient mast cells before and after regulated exocytosis.

The x-z planes through the center of adherent eHMCS labeled with Alexa Fluor-488-phalloidin were captured for individual cells. Cells were incubated overnight with IgE, then either fixed immediately with 4% PFA or stimulated with DNP-IgE (3 ng/mL) and fixed thirty seconds after stimulation. Displayed images are representative of two independent experiments with at least 25 cells per experiment captured.

(A) Three representative images are shown for both WT and MARCKS-deficient cells stained with phalloidin prior to activation. The phalloidin labeling of cells prior to activation did not reveal any obvious differences between the staining of WT and null cells.

(B) Three representative images are shown for WT and MARCKS-deficient cells stained with phalloidin thirty seconds after mast cell activation with antigen (3 ng/mL). In this brief period, no change in the fluidity of the phalloidin-labeling pattern was detectable in MARCKS null cells (n=10 cells, 2 samples), similar to WT cells (n=10 cells, 2 samples) remained unchanged. Further expansion of these experiments would be required to support the rate of release differences observed in Fig. 2.6.

(A) Before Stimulation

WT eHMCs

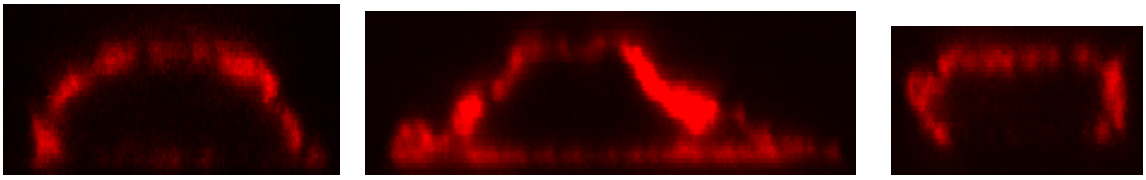

MARCKS-deficient eHMCs

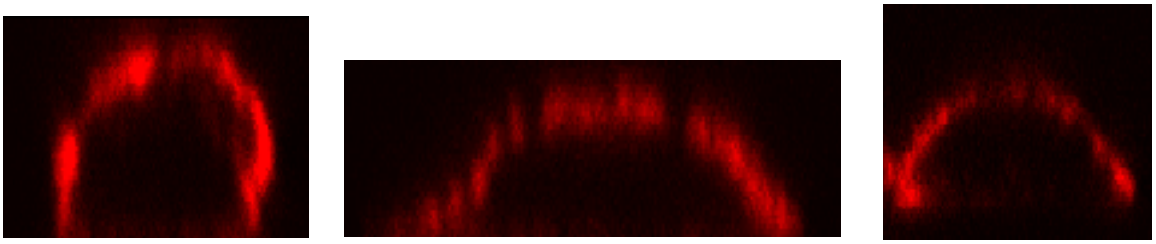

(B) 30 seconds after Stimulation

WT eHMCs

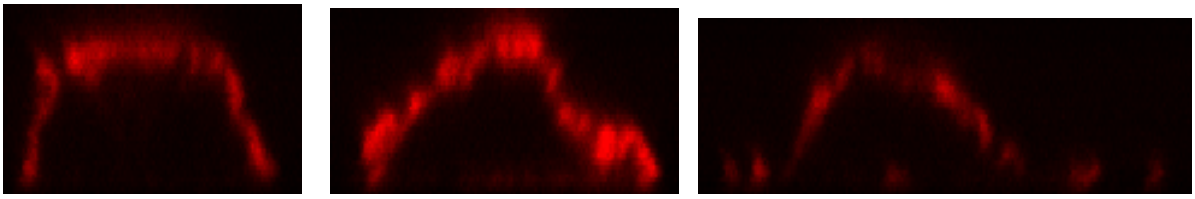

MARCKS-deficient eHMCs

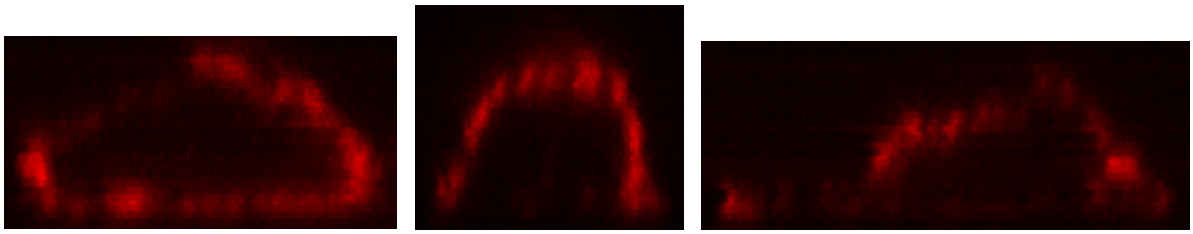

tured live and demonstrated the anticipated movement from the PM to the cytosol after activation. Surprisingly, though, cytosolic MARCKS associated with vesicular membranes. Only a few other studies have suggested MARCKS association with membranes in the cytosol, but this association had not been captured in live cells . The obstacle with this finding is that HEK293 cells are non-secretory cells and the previous findings observed association with SGs in secretory cells or lysosomes. However, it remains unclear with which vesicular membranes MARCKS associates in HEK293 cells.

The significance of vesicular membrane association is a much more important question if addressed in secretory cells where MARCKS is postulated to play an important role in regulated exocytosis. If association to cytosolic membranes, such as SG membranes, is a critical aspect of MARCKS function in regulated exocytosis, as has been suggested by other researchers (Li, *et al.*, 2001; Singer, *et al.*, 2004), capturing the timing and localization of MARCKS in real time would strongly clarify any cytosolic function for MARCKS. The hypothesis for MARCKS currently embraced by much of the field is that MARCKS functions in regulated exocytosis by disrupting, through controversial mechanisms, the cortical actin filaments underlying the PM, so that SGs can reach their exocytic fusion sites. This hypothesis implicates that the role for MARCKS is complete once phosphoMARCKS moves to the cytosol. Another group has suggested that MARCKS function in regulated exocytosis only begins once phosphoMARCKS moves to the cytosol. By this mechanism, MARCKS associates with and promotes SG trafficking to the PM, by enabling *de novo* actin synthesis around the SGs. While neither MARCKS function is exclusive of the other, determining the timing and localization of MARCKS following PKC phosphorylation could clarify if a cytosolic role for MARCKS exist in regulated exocytosis.

Important progress in understanding this observation could be made by live cell imaging of secretory cells infected with a fluorescent-tagged WT MARCKS. An alternative method our lab begun to pursue led to the generation of genomic MARCKS-eYFP transgenic mice on a C57Bl/6J background driven by the endogenous MARCKS promoter. These mice have been backcrossed and are viable into adulthood with no obvious phenotype. Isolation of eHMCs from MARCKS transgenic embryos, WT for endogenous MARCKS showed a high autofluorescent background with a detectable MARCKS-eYFP fluorescence. Transgenic mice heterozygous for MARCKS and carriers of the MARCKS-eYFP transgene have now been bred in an attempt to reduce the background autofluorescence. If the breeding remains successful, mast cells from these mice could be utilized for parallel live cell imaging studies done on the HEK293 cells. Continuation of these studies could yield a way to directly address the significance of MARCKS association with cytosolic membranes using cells containing near endogenous levels of MARCKS.

In this initial study, though, once the initial observations were made in WT MARCKS-transfected cells, HEK293 cells were then transfected with the previously tested or novel full-length MARCKS cDNA mutant constructs and activated by PMA to yield more surprising results. The non-myristoylatable MARCKS mutant, as expected, demonstrated severe impairment of membrane association, both PM and cytosolic vesicular membranes. Observations of the pseudo-phosphorylated MARCKS, a mutant partially mimicking phosphoMARCKS and insensitive to PKC, were not completely as predicted though. Impaired PM association, as expected was observed in resting cells, but cytosolic vesicular membrane association was not inhibited. Additionally, while the small amount of PM-associated PsPi did not translocate when PKC activators were added, as expected, application of PKC activators resulted in

increased cytosolic vesicular membrane association. The unexpected aspect of these results is that MARCKS translocation is believed to occur because addition of the phosphorylation groups added by PKC causes loss of membrane association. Observations of PsPi MARCKS effectively associating with vesicular membranes in the cytosol while having impaired PM association, suggests two different mechanisms for MARCKS association with the PM and cytosolic membranes, respectively. Studies of other cell types infected with this mutant construct and stimulated for PKC activation could clarify if these observations are a consistent trend.

In the next set of studies, HEK293 cells transfected with the novel MH2 deletion and scrambled MARCKS mutant constructs, which were surprisingly similar to WT cells. MH2 deletion cells were clearly associated with the PM in the resting state and translocated to vesicular membranes following PKC activation. All of the cells imaged mimicked WT behavior. Observations of SM cells could not be so easily categorized. Most SM cells mimicked WT behavior in every aspect of the translocation process, but some of the cells were different from WT cells in the resting state. As shown in Fig. 3.6, some SM cells, even with the same levels of overexpression as WT-transfected cells, showed an increased cytosolic localization even prior to PKC activation. The behavior of the mutant cells following activation, though, mimicked WT behavior with no aberrant characteristics. When the membrane to cytosol ratio was measured in SM cells, the average ratio was not significantly different from the WT intensity ratios. Therefore, no quantitative difference was detected in either mutant.

Depite these results, the observation of MH2 domain deletion and the SM region were the first ever recorded. Absence of any effect on MARCKS translocation still does not eliminate the possibility that these mutations could affect MARCKS function in regulated exocytosis or any other cellular process. Further studies could utilize cells transfected with these

mutants to determine if these regions, particularly the MH2 domain of unknown function, are necesary for any of MARCKS functions.

Overall, the MARCKS mutation studies detailed in Chapter 3 resulted in generation of a set of MARCKS mutant constructs with possibilities for furthering multiple types of MARCKS studies. They demonstrated that only the myristoyl moiety was necessary for membrane association and that all other mutations, except for PsPi MARCKS, mimicked WT translocation behavior. The PsPi MARCKS study suggested some novel concepts for cytosolic membrane association, but further studies in other cell types would be necessary to validate these findings. The observation of MARCKS associating with a population of intracellular vesicular membranes, while surprising, will also remain a mystery until further studies can be conducted in other cell types.

Appendix A

Factorial Combination Statistics

In the experiments determining if there was a difference in the total magnitude of secretory response, MARCKS null cells significantly enhanced the maximal secretory response by approximately one-third compared to the secretory responses of WT cells (n=16) (Fig. 2.3). However, where the time course data of Fig. 2.5 (n=6), at the thirty minute incubation period, is the same as used for the experiments of Fig. 2.3 the data does not show a significant increase in the magnitude of secretion between MARCKS null and WT cells. To verify statistically that this outcome is largely attributable to a smaller number of experiments, we determined the number of significant p-values for all combinations of 6 that could be derived from the 16 data sets in Fig. 2.3. An algorithm was written for us by Abijhit Gurhardaphye at Virginia Tech, which automatically created the 8,008 possible combinations of six data sets and the corresponding p-value for each combination. The p-values were manually verified for approximately 100 of the combinations, while all 8,008 combinatiaons were sorted using Excel to determine how many p-values were below 0.05. From all of the possible combinations, 50.2% of the time an n of 6 would generate a p-value of <0.05 and 49.8% of the time it would be >0.05. Consequently, it is not surprising that the total amount of secretion in the time course experiment was insignificant, while the experiments of Fig. 2.3 were statistically significant. In fact, this analysis supports the use of a larger number of embryos to account for mast cell variability, and implies the subtle, inessential nature of the MARCKS-deficient effects on the magnitude of secretion. Included are ten out of the 174 pages of random combinations and their corresponding p-values. The analysis also emphasizes that the effect of MARCKS-deficiency is on the rate of cargo release in mast cells (Fig. 2.5) is more likely to be the primary defect, rather than the magnitude of mast cell secretion.

SET 1							SET 2							p-values
28.23	15.42	29.73	38.43	24.75	28.26		40.84	56.15	39.81	41.50	47.51	49.23		0.001
28.23	15.42	29.73	38.43	24.75	37.38		40.84	56.15	39.81	41.50	47.51	46.95		0.003
28.23	15.42	29.73	38.43	24.75	38.13		40.84	56.15	39.81	41.50	47.51	51.50		0.003
28.23	15.42	29.73	38.43	24.75	52.11		40.84	56.15	39.81	41.50	47.51	55.94		0.027
28.23	15.42	29.73	38.43	24.75	57.78		40.84	56.15	39.81	41.50	47.51	53.22		0.057
28.23	15.42	29.73	38.43	24.75	45.09		40.84	56.15	39.81	41.50	47.51	58.30		0.010
28.23	15.42	29.73	38.43	24.75	49.14		40.84	56.15	39.81	41.50	47.51	55.76		0.018
28.23	15.42	29.73	38.43	24.75	35.92		40.84	56.15	39.81	41.50	47.51	63.06		0.004
28.23	15.42	29.73	38.43	24.75	43.81		40.84	56.15	39.81	41.50	47.51	59.78		0.009
28.23	15.42	29.73	38.43	24.75	50.19		40.84	56.15	39.81	41.50	47.51	40.71		0.037
28.23	15.42	29.73	38.43	24.75	42.51		40.84	56.15	39.81	41.50	47.51	54.23		0.007
28.23	15.42	29.73	38.43	28.26	37.38		40.84	56.15	39.81	41.50	49.23	46.95		0.003
28.23	15.42	29.73	38.43	28.26	38.13		40.84	56.15	39.81	41.50	49.23	51.50		0.003
28.23	15.42	29.73	38.43	28.26	52.11		40.84	56.15	39.81	41.50	49.23	55.94		0.027
28.23	15.42	29.73	38.43	28.26	57.78		40.84	56.15	39.81	41.50	49.23	53.22		0.058
28.23	15.42	29.73	38.43	28.26	45.09		40.84	56.15	39.81	41.50	49.23	58.30		0.010
28.23	15.42	29.73	38.43	28.26	49.14		40.84	56.15	39.81	41.50	49.23	55.76		0.018
28.23	15.42	29.73	38.43	28.26	35.92		40.84	56.15	39.81	41.50	49.23	63.06		0.004
28.23	15.42	29.73	38.43	28.26	43.81		40.84	56.15	39.81	41.50	49.23	59.78		0.009
28.23	15.42	29.73	38.43	28.26	50.19		40.84	56.15	39.81	41.50	49.23	40.71		0.039
28.23	15.42	29.73	38.43	28.26	42.51		40.84	56.15	39.81	41.50	49.23	54.23		0.007
28.23	15.42	29.73	38.43	37.38	38.13		40.84	56.15	39.81	41.50	46.95	51.50		0.008
28.23	15.42	29.73	38.43	37.38	52.11		40.84	56.15	39.81	41.50	46.95	55.94		0.047
28.23	15.42	29.73	38.43	37.38	57.78		40.84	56.15	39.81	41.50	46.95	53.22		0.093
28.23	15.42	29.73	38.43	37.38	45.09		40.84	56.15	39.81	41.50	46.95	58.30		0.020
28.23	15.42	29.73	38.43	37.38	49.14		40.84	56.15	39.81	41.50	46.95	55.76		0.033
28.23	15.42	29.73	38.43	37.38	35.92		40.84	56.15	39.81	41.50	46.95	63.06		0.008
28.23	15.42	29.73	38.43	37.38	43.81		40.84	56.15	39.81	41.50	46.95	59.78		0.017
28.23	15.42	29.73	38.43	37.38	50.19		40.84	56.15	39.81	41.50	46.95	40.71		0.069
28.23	15.42	29.73	38.43	37.38	42.51		40.84	56.15	39.81	41.50	46.95	54.23		0.014
28.23	15.42	29.73	38.43	38.13	52.11		40.84	56.15	39.81	41.50	51.50	55.94		0.041
28.23	15.42	29.73	38.43	38.13	57.78		40.84	56.15	39.81	41.50	51.50	53.22		0.081
28.23	15.42	29.73	38.43	38.13	45.09		40.84	56.15	39.81	41.50	51.50	58.30		0.017
28.23	15.42	29.73	38.43	38.13	49.14		40.84	56.15	39.81	41.50	51.50	55.76		0.029
28.23	15.42	29.73	38.43	38.13	35.92		40.84	56.15	39.81	41.50	51.50	63.06		0.007
28.23	15.42	29.73	38.43	38.13	43.81		40.84	56.15	39.81	41.50	51.50	59.78		0.015
28.23	15.42	29.73	38.43	38.13	50.19		40.84	56.15	39.81	41.50	51.50	40.71		0.062
28.23	15.42	29.73	38.43	38.13	42.51		40.84	56.15	39.81	41.50	51.50	54.23		0.013
28.23	15.42	29.73	38.43	52.11	57.78		40.84	56.15	39.81	41.50	55.94	53.22		0.161
28.23	15.42	29.73	38.43	52.11	45.09		40.84	56.15	39.81	41.50	55.94	58.30		0.057
28.23	15.42	29.73	38.43	52.11	49.14		40.84	56.15	39.81	41.50	55.94	55.76		0.081
28.23	15.42	29.73	38.43	52.11	35.92		40.84	56.15	39.81	41.50	55.94	63.06		0.030
28.23	15.42	29.73	38.43	52.11	43.81		40.84	56.15	39.81	41.50	55.94	59.78		0.051
28.23	15.42	29.73	38.43	52.11	50.19		40.84	56.15	39.81	41.50	55.94	40.71		0.155
28.23	15.42	29.73	38.43	52.11	42.51		40.84	56.15	39.81	41.50	55.94	54.23		0.051

SET 1							SET 2							p-values
28.23	15.42	29.73	38.43	57.78	45.09		40.84	56.15	39.81	41.50	53.22	58.30		0.101
28.23	15.42	29.73	38.43	57.78	49.14		40.84	56.15	39.81	41.50	53.22	55.76		0.136
28.23	15.42	29.73	38.43	57.78	35.92		40.84	56.15	39.81	41.50	53.22	63.06		0.059
28.23	15.42	29.73	38.43	57.78	43.81		40.84	56.15	39.81	41.50	53.22	59.78		0.092
28.23	15.42	29.73	38.43	57.78	50.19		40.84	56.15	39.81	41.50	53.22	40.71		0.240
28.23	15.42	29.73	38.43	57.78	42.51		40.84	56.15	39.81	41.50	53.22	54.23		0.096
28.23	15.42	29.73	38.43	45.09	49.14		40.84	56.15	39.81	41.50	58.30	55.76		0.043
28.23	15.42	29.73	38.43	45.09	35.92		40.84	56.15	39.81	41.50	58.30	63.06		0.013
28.23	15.42	29.73	38.43	45.09	43.81		40.84	56.15	39.81	41.50	58.30	59.78		0.025
28.23	15.42	29.73	38.43	45.09	50.19		40.84	56.15	39.81	41.50	58.30	40.71		0.090
28.23	15.42	29.73	38.43	45.09	42.51		40.84	56.15	39.81	41.50	58.30	54.23		0.024
28.23	15.42	29.73	38.43	49.14	35.92		40.84	56.15	39.81	41.50	55.76	63.06		0.022
28.23	15.42	29.73	38.43	49.14	43.81		40.84	56.15	39.81	41.50	55.76	59.78		0.038
28.23	15.42	29.73	38.43	49.14	50.19		40.84	56.15	39.81	41.50	55.76	40.71		0.126
28.23	15.42	29.73	38.43	49.14	42.51		40.84	56.15	39.81	41.50	55.76	54.23		0.038
28.23	15.42	29.73	38.43	35.92	43.81		40.84	56.15	39.81	41.50	63.06	59.78		0.012
28.23	15.42	29.73	38.43	35.92	50.19		40.84	56.15	39.81	41.50	63.06	40.71		0.049
28.23	15.42	29.73	38.43	35.92	42.51		40.84	56.15	39.81	41.50	63.06	54.23		0.011
28.23	15.42	29.73	38.43	43.81	50.19		40.84	56.15	39.81	41.50	59.78	40.71		0.081
28.23	15.42	29.73	38.43	43.81	42.51		40.84	56.15	39.81	41.50	59.78	54.23		0.021
28.23	15.42	29.73	38.43	50.19	42.51		40.84	56.15	39.81	41.50	40.71	54.23		0.080
28.23	15.42	29.73	24.75	28.26	37.38		40.84	56.15	39.81	47.51	49.23	46.95		0.000
28.23	15.42	29.73	24.75	28.26	38.13		40.84	56.15	39.81	47.51	49.23	51.50		0.000
28.23	15.42	29.73	24.75	28.26	52.11		40.84	56.15	39.81	47.51	49.23	55.94		0.009
28.23	15.42	29.73	24.75	28.26	57.78		40.84	56.15	39.81	47.51	49.23	53.22		0.023
28.23	15.42	29.73	24.75	28.26	45.09		40.84	56.15	39.81	47.51	49.23	58.30		0.002
28.23	15.42	29.73	24.75	28.26	49.14		40.84	56.15	39.81	47.51	49.23	55.76		0.005
28.23	15.42	29.73	24.75	28.26	35.92		40.84	56.15	39.81	47.51	49.23	63.06		0.001
28.23	15.42	29.73	24.75	28.26	43.81		40.84	56.15	39.81	47.51	49.23	59.78		0.002
28.23	15.42	29.73	24.75	28.26	50.19		40.84	56.15	39.81	47.51	49.23	40.71		0.012
28.23	15.42	29.73	24.75	28.26	42.51		40.84	56.15	39.81	47.51	49.23	54.23		0.001
28.23	15.42	29.73	24.75	37.38	38.13		40.84	56.15	39.81	47.51	46.95	51.50		0.002
28.23	15.42	29.73	24.75	37.38	52.11		40.84	56.15	39.81	47.51	46.95	55.94		0.018
28.23	15.42	29.73	24.75	37.38	57.78		40.84	56.15	39.81	47.51	46.95	53.22		0.040
28.23	15.42	29.73	24.75	37.38	45.09		40.84	56.15	39.81	47.51	46.95	58.30		0.006
28.23	15.42	29.73	24.75	37.38	49.14		40.84	56.15	39.81	47.51	46.95	55.76		0.011
28.23	15.42	29.73	24.75	37.38	35.92		40.84	56.15	39.81	47.51	46.95	63.06		0.002
28.23	15.42	29.73	24.75	37.38	43.81		40.84	56.15	39.81	47.51	46.95	59.78		0.005
28.23	15.42	29.73	24.75	37.38	50.19		40.84	56.15	39.81	47.51	46.95	40.71		0.025
28.23	15.42	29.73	24.75	37.38	42.51		40.84	56.15	39.81	47.51	46.95	54.23		0.004
28.23	15.42	29.73	24.75	38.13	52.11		40.84	56.15	39.81	47.51	51.50	55.94		0.015
28.23	15.42	29.73	24.75	38.13	57.78		40.84	56.15	39.81	47.51	51.50	53.22		0.035
28.23	15.42	29.73	24.75	38.13	45.09		40.84	56.15	39.81	47.51	51.50	58.30		0.005
28.23	15.42	29.73	24.75	38.13	49.14		40.84	56.15	39.81	47.51	51.50	55.76		0.010
28.23	15.42	29.73	24.75	38.13	35.92		40.84	56.15	39.81	47.51	51.50	63.06		0.002

SET 1							SET 2							p-values
28.23	15.42	29.73	24.75	38.13	43.81		40.84	56.15	39.81	47.51	51.50	59.78		0.004
28.23	15.42	29.73	24.75	38.13	50.19		40.84	56.15	39.81	47.51	51.50	40.71		0.023
28.23	15.42	29.73	24.75	38.13	42.51		40.84	56.15	39.81	47.51	51.50	54.23		0.003
28.23	15.42	29.73	24.75	52.11	57.78		40.84	56.15	39.81	47.51	55.94	53.22		0.083
28.23	15.42	29.73	24.75	52.11	45.09		40.84	56.15	39.81	47.51	55.94	58.30		0.024
28.23	15.42	29.73	24.75	52.11	49.14		40.84	56.15	39.81	47.51	55.94	55.76		0.036
28.23	15.42	29.73	24.75	52.11	35.92		40.84	56.15	39.81	47.51	55.94	63.06		0.011
28.23	15.42	29.73	24.75	52.11	43.81		40.84	56.15	39.81	47.51	55.94	59.78		0.021
28.23	15.42	29.73	24.75	52.11	50.19		40.84	56.15	39.81	47.51	55.94	40.71		0.074
28.23	15.42	29.73	24.75	52.11	42.51		40.84	56.15	39.81	47.51	55.94	54.23		0.021
28.23	15.42	29.73	24.75	57.78	45.09		40.84	56.15	39.81	47.51	53.22	58.30		0.048
28.23	15.42	29.73	24.75	57.78	49.14		40.84	56.15	39.81	47.51	53.22	55.76		0.068
28.23	15.42	29.73	24.75	57.78	35.92		40.84	56.15	39.81	47.51	53.22	63.06		0.026
28.23	15.42	29.73	24.75	57.78	43.81		40.84	56.15	39.81	47.51	53.22	59.78		0.043
28.23	15.42	29.73	24.75	57.78	50.19		40.84	56.15	39.81	47.51	53.22	40.71		0.126
28.23	15.42	29.73	24.75	57.78	42.51		40.84	56.15	39.81	47.51	53.22	54.23		0.044
28.23	15.42	29.73	24.75	45.09	49.14		40.84	56.15	39.81	47.51	58.30	55.76		0.017
28.23	15.42	29.73	24.75	45.09	35.92		40.84	56.15	39.81	47.51	58.30	63.06		0.004
28.23	15.42	29.73	24.75	45.09	43.81		40.84	56.15	39.81	47.51	58.30	59.78		0.009
28.23	15.42	29.73	24.75	45.09	50.19		40.84	56.15	39.81	47.51	58.30	40.71		0.039
28.23	15.42	29.73	24.75	45.09	42.51		40.84	56.15	39.81	47.51	58.30	54.23		0.008
28.23	15.42	29.73	24.75	49.14	35.92		40.84	56.15	39.81	47.51	55.76	63.06		0.008
28.23	15.42	29.73	24.75	49.14	43.81		40.84	56.15	39.81	47.51	55.76	59.78		0.015
28.23	15.42	29.73	24.75	49.14	50.19		40.84	56.15	39.81	47.51	55.76	40.71		0.057
28.23	15.42	29.73	24.75	49.14	42.51		40.84	56.15	39.81	47.51	55.76	54.23		0.014
28.23	15.42	29.73	24.75	35.92	43.81		40.84	56.15	39.81	47.51	63.06	59.78		0.003
28.23	15.42	29.73	24.75	35.92	50.19		40.84	56.15	39.81	47.51	63.06	40.71		0.019
28.23	15.42	29.73	24.75	35.92	42.51		40.84	56.15	39.81	47.51	63.06	54.23		0.003
28.23	15.42	29.73	24.75	43.81	50.19		40.84	56.15	39.81	47.51	59.78	40.71		0.034
28.23	15.42	29.73	24.75	43.81	42.51		40.84	56.15	39.81	47.51	59.78	54.23		0.007
28.23	15.42	29.73	24.75	50.19	42.51		40.84	56.15	39.81	47.51	40.71	54.23		0.032
28.23	15.42	29.73	28.26	37.38	38.13		40.84	56.15	39.81	49.23	46.95	51.50		0.002
28.23	15.42	29.73	28.26	37.38	52.11		40.84	56.15	39.81	49.23	46.95	55.94		0.018
28.23	15.42	29.73	28.26	37.38	57.78		40.84	56.15	39.81	49.23	46.95	53.22		0.041
28.23	15.42	29.73	28.26	37.38	45.09		40.84	56.15	39.81	49.23	46.95	58.30		0.006
28.23	15.42	29.73	28.26	37.38	49.14		40.84	56.15	39.81	49.23	46.95	55.76		0.011
28.23	15.42	29.73	28.26	37.38	35.92		40.84	56.15	39.81	49.23	46.95	63.06		0.002
28.23	15.42	29.73	28.26	37.38	43.81		40.84	56.15	39.81	49.23	46.95	59.78		0.005
28.23	15.42	29.73	28.26	37.38	50.19		40.84	56.15	39.81	49.23	46.95	40.71		0.026
28.23	15.42	29.73	28.26	37.38	42.51		40.84	56.15	39.81	49.23	46.95	54.23		0.004
28.23	15.42	29.73	28.26	38.13	52.11		40.84	56.15	39.81	49.23	51.50	55.94		0.015
28.23	15.42	29.73	28.26	38.13	57.78		40.84	56.15	39.81	49.23	51.50	53.22		0.036
28.23	15.42	29.73	28.26	38.13	45.09		40.84	56.15	39.81	49.23	51.50	58.30		0.005
28.23	15.42	29.73	28.26	38.13	49.14		40.84	56.15	39.81	49.23	51.50	55.76		0.010
28.23	15.42	29.73	28.26	38.13	35.92		40.84	56.15	39.81	49.23	51.50	63.06		0.002

SET 1							SET 2							p-values
28.23	15.42	29.73	28.26	38.13	43.81		40.84	56.15	39.81	49.23	51.50	59.78		0.004
28.23	15.42	29.73	28.26	38.13	50.19		40.84	56.15	39.81	49.23	51.50	40.71		0.024
28.23	15.42	29.73	28.26	38.13	42.51		40.84	56.15	39.81	49.23	51.50	54.23		0.003
28.23	15.42	29.73	28.26	52.11	57.78		40.84	56.15	39.81	49.23	55.94	53.22		0.084
28.23	15.42	29.73	28.26	52.11	45.09		40.84	56.15	39.81	49.23	55.94	58.30		0.024
28.23	15.42	29.73	28.26	52.11	49.14		40.84	56.15	39.81	49.23	55.94	55.76		0.036
28.23	15.42	29.73	28.26	52.11	35.92		40.84	56.15	39.81	49.23	55.94	63.06		0.011
28.23	15.42	29.73	28.26	52.11	43.81		40.84	56.15	39.81	49.23	55.94	59.78		0.021
28.23	15.42	29.73	28.26	52.11	50.19		40.84	56.15	39.81	49.23	55.94	40.71		0.076
28.23	15.42	29.73	28.26	52.11	42.51		40.84	56.15	39.81	49.23	55.94	54.23		0.020
28.23	15.42	29.73	28.26	57.78	45.09		40.84	56.15	39.81	49.23	53.22	58.30		0.048
28.23	15.42	29.73	28.26	57.78	49.14		40.84	56.15	39.81	49.23	53.22	55.76		0.068
28.23	15.42	29.73	28.26	57.78	35.92		40.84	56.15	39.81	49.23	53.22	63.06		0.026
28.23	15.42	29.73	28.26	57.78	43.81		40.84	56.15	39.81	49.23	53.22	59.78		0.043
28.23	15.42	29.73	28.26	57.78	50.19		40.84	56.15	39.81	49.23	53.22	40.71		0.129
28.23	15.42	29.73	28.26	57.78	42.51		40.84	56.15	39.81	49.23	53.22	54.23		0.044
28.23	15.42	29.73	28.26	45.09	49.14		40.84	56.15	39.81	49.23	58.30	55.76		0.017
28.23	15.42	29.73	28.26	45.09	35.92		40.84	56.15	39.81	49.23	58.30	63.06		0.004
28.23	15.42	29.73	28.26	45.09	43.81		40.84	56.15	39.81	49.23	58.30	59.78		0.008
28.23	15.42	29.73	28.26	45.09	50.19		40.84	56.15	39.81	49.23	58.30	40.71		0.039
28.23	15.42	29.73	28.26	45.09	42.51		40.84	56.15	39.81	49.23	58.30	54.23		0.008
28.23	15.42	29.73	28.26	49.14	35.92		40.84	56.15	39.81	49.23	55.76	63.06		0.007
28.23	15.42	29.73	28.26	49.14	43.81		40.84	56.15	39.81	49.23	55.76	59.78		0.015
28.23	15.42	29.73	28.26	49.14	50.19		40.84	56.15	39.81	49.23	55.76	40.71		0.058
28.23	15.42	29.73	28.26	49.14	42.51		40.84	56.15	39.81	49.23	55.76	54.23		0.014
28.23	15.42	29.73	28.26	35.92	43.81		40.84	56.15	39.81	49.23	63.06	59.78		0.003
28.23	15.42	29.73	28.26	35.92	50.19		40.84	56.15	39.81	49.23	63.06	40.71		0.019
28.23	15.42	29.73	28.26	35.92	42.51		40.84	56.15	39.81	49.23	63.06	54.23		0.003
28.23	15.42	29.73	28.26	43.81	50.19		40.84	56.15	39.81	49.23	59.78	40.71		0.035
28.23	15.42	29.73	28.26	43.81	42.51		40.84	56.15	39.81	49.23	59.78	54.23		0.007
28.23	15.42	29.73	28.26	50.19	42.51		40.84	56.15	39.81	49.23	40.71	54.23		0.033
28.23	15.42	29.73	37.38	38.13	52.11		40.84	56.15	39.81	46.95	51.50	55.94		0.027
28.23	15.42	29.73	37.38	38.13	57.78		40.84	56.15	39.81	46.95	51.50	53.22		0.058
28.23	15.42	29.73	37.38	38.13	45.09		40.84	56.15	39.81	46.95	51.50	58.30		0.010
28.23	15.42	29.73	37.38	38.13	49.14		40.84	56.15	39.81	46.95	51.50	55.76		0.018
28.23	15.42	29.73	37.38	38.13	35.92		40.84	56.15	39.81	46.95	51.50	63.06		0.004
28.23	15.42	29.73	37.38	38.13	43.81		40.84	56.15	39.81	46.95	51.50	59.78		0.009
28.23	15.42	29.73	37.38	38.13	50.19		40.84	56.15	39.81	46.95	51.50	40.71		0.042
28.23	15.42	29.73	37.38	38.13	42.51		40.84	56.15	39.81	46.95	51.50	54.23		0.007
28.23	15.42	29.73	37.38	52.11	57.78		40.84	56.15	39.81	46.95	55.94	53.22		0.122
28.23	15.42	29.73	37.38	52.11	45.09		40.84	56.15	39.81	46.95	55.94	58.30		0.039
28.23	15.42	29.73	37.38	52.11	49.14		40.84	56.15	39.81	46.95	55.94	55.76		0.057
28.23	15.42	29.73	37.38	52.11	35.92		40.84	56.15	39.81	46.95	55.94	63.06		0.020
28.23	15.42	29.73	37.38	52.11	43.81		40.84	56.15	39.81	46.95	55.94	59.78		0.034
28.23	15.42	29.73	37.38	52.11	50.19		40.84	56.15	39.81	46.95	55.94	40.71		0.116

SET 1							SET 2							p-values
28.23	15.42	29.73	37.38	52.11	42.51		40.84	56.15	39.81	46.95	55.94	54.23		0.034
28.23	15.42	29.73	37.38	57.78	45.09		40.84	56.15	39.81	46.95	53.22	58.30		0.074
28.23	15.42	29.73	37.38	57.78	49.14		40.84	56.15	39.81	46.95	53.22	55.76		0.101
28.23	15.42	29.73	37.38	57.78	35.92		40.84	56.15	39.81	46.95	53.22	63.06		0.042
28.23	15.42	29.73	37.38	57.78	43.81		40.84	56.15	39.81	46.95	53.22	59.78		0.066
28.23	15.42	29.73	37.38	57.78	50.19		40.84	56.15	39.81	46.95	53.22	40.71		0.188
28.23	15.42	29.73	37.38	57.78	42.51		40.84	56.15	39.81	46.95	53.22	54.23		0.069
28.23	15.42	29.73	37.38	45.09	49.14		40.84	56.15	39.81	46.95	58.30	55.76		0.028
28.23	15.42	29.73	37.38	45.09	35.92		40.84	56.15	39.81	46.95	58.30	63.06		0.008
28.23	15.42	29.73	37.38	45.09	43.81		40.84	56.15	39.81	46.95	58.30	59.78		0.015
28.23	15.42	29.73	37.38	45.09	50.19		40.84	56.15	39.81	46.95	58.30	40.71		0.064
28.23	15.42	29.73	37.38	45.09	42.51		40.84	56.15	39.81	46.95	58.30	54.23		0.015
28.23	15.42	29.73	37.38	49.14	35.92		40.84	56.15	39.81	46.95	55.76	63.06		0.014
28.23	15.42	29.73	37.38	49.14	43.81		40.84	56.15	39.81	46.95	55.76	59.78		0.025
28.23	15.42	29.73	37.38	49.14	50.19		40.84	56.15	39.81	46.95	55.76	40.71		0.092
28.23	15.42	29.73	37.38	49.14	42.51		40.84	56.15	39.81	46.95	55.76	54.23		0.024
28.23	15.42	29.73	37.38	35.92	43.81		40.84	56.15	39.81	46.95	63.06	59.78		0.007
28.23	15.42	29.73	37.38	35.92	50.19		40.84	56.15	39.81	46.95	63.06	40.71		0.034
28.23	15.42	29.73	37.38	35.92	42.51		40.84	56.15	39.81	46.95	63.06	54.23		0.006
28.23	15.42	29.73	37.38	43.81	50.19		40.84	56.15	39.81	46.95	59.78	40.71		0.057
28.23	15.42	29.73	37.38	43.81	42.51		40.84	56.15	39.81	46.95	59.78	54.23		0.013
28.23	15.42	29.73	37.38	50.19	42.51		40.84	56.15	39.81	46.95	40.71	54.23		0.056
28.23	15.42	29.73	38.13	52.11	57.78		40.84	56.15	39.81	51.50	55.94	53.22		0.106
28.23	15.42	29.73	38.13	52.11	45.09		40.84	56.15	39.81	51.50	55.94	58.30		0.032
28.23	15.42	29.73	38.13	52.11	49.14		40.84	56.15	39.81	51.50	55.94	55.76		0.048
28.23	15.42	29.73	38.13	52.11	35.92		40.84	56.15	39.81	51.50	55.94	63.06		0.016
28.23	15.42	29.73	38.13	52.11	43.81		40.84	56.15	39.81	51.50	55.94	59.78		0.029
28.23	15.42	29.73	38.13	52.11	50.19		40.84	56.15	39.81	51.50	55.94	40.71		0.102
28.23	15.42	29.73	38.13	52.11	42.51		40.84	56.15	39.81	51.50	55.94	54.23		0.029
28.23	15.42	29.73	38.13	57.78	45.09		40.84	56.15	39.81	51.50	53.22	58.30		0.063
28.23	15.42	29.73	38.13	57.78	49.14		40.84	56.15	39.81	51.50	53.22	55.76		0.087
28.23	15.42	29.73	38.13	57.78	35.92		40.84	56.15	39.81	51.50	53.22	63.06		0.035
28.23	15.42	29.73	38.13	57.78	43.81		40.84	56.15	39.81	51.50	53.22	59.78		0.057
28.23	15.42	29.73	38.13	57.78	50.19		40.84	56.15	39.81	51.50	53.22	40.71		0.166
28.23	15.42	29.73	38.13	57.78	42.51		40.84	56.15	39.81	51.50	53.22	54.23		0.059
28.23	15.42	29.73	38.13	45.09	49.14		40.84	56.15	39.81	51.50	58.30	55.76		0.024
28.23	15.42	29.73	38.13	45.09	35.92		40.84	56.15	39.81	51.50	58.30	63.06		0.006
28.23	15.42	29.73	38.13	45.09	43.81		40.84	56.15	39.81	51.50	58.30	59.78		0.013
28.23	15.42	29.73	38.13	45.09	50.19		40.84	56.15	39.81	51.50	58.30	40.71		0.056
28.23	15.42	29.73	38.13	45.09	42.51		40.84	56.15	39.81	51.50	58.30	54.23		0.012
28.23	15.42	29.73	38.13	49.14	35.92		40.84	56.15	39.81	51.50	55.76	63.06		0.011
28.23	15.42	29.73	38.13	49.14	43.81		40.84	56.15	39.81	51.50	55.76	59.78		0.021
28.23	15.42	29.73	38.13	49.14	50.19		40.84	56.15	39.81	51.50	55.76	40.71		0.081
28.23	15.42	29.73	38.13	49.14	42.51		40.84	56.15	39.81	51.50	55.76	54.23		0.020
28.23	15.42	29.73	38.13	35.92	43.81		40.84	56.15	39.81	51.50	63.06	59.78		0.005

SET 1							SET 2							p-values
28.23	15.42	29.73	38.13	35.92	50.19		40.84	56.15	39.81	51.50	63.06	40.71		0.029
28.23	15.42	29.73	38.13	35.92	42.51		40.84	56.15	39.81	51.50	63.06	54.23		0.005
28.23	15.42	29.73	38.13	43.81	50.19		40.84	56.15	39.81	51.50	59.78	40.71		0.050
28.23	15.42	29.73	38.13	43.81	42.51		40.84	56.15	39.81	51.50	59.78	54.23		0.010
28.23	15.42	29.73	38.13	50.19	42.51		40.84	56.15	39.81	51.50	40.71	54.23		0.049
28.23	15.42	29.73	52.11	57.78	45.09		40.84	56.15	39.81	55.94	53.22	58.30		0.119
28.23	15.42	29.73	52.11	57.78	49.14		40.84	56.15	39.81	55.94	53.22	55.76		0.155
28.23	15.42	29.73	52.11	57.78	35.92		40.84	56.15	39.81	55.94	53.22	63.06		0.074
28.23	15.42	29.73	52.11	57.78	43.81		40.84	56.15	39.81	55.94	53.22	59.78		0.108
28.23	15.42	29.73	52.11	57.78	50.19		40.84	56.15	39.81	55.94	53.22	40.71		0.271
28.23	15.42	29.73	52.11	57.78	42.51		40.84	56.15	39.81	55.94	53.22	54.23		0.118
28.23	15.42	29.73	52.11	45.09	49.14		40.84	56.15	39.81	55.94	58.30	55.76		0.059
28.23	15.42	29.73	52.11	45.09	35.92		40.84	56.15	39.81	55.94	58.30	63.06		0.022
28.23	15.42	29.73	52.11	45.09	43.81		40.84	56.15	39.81	55.94	58.30	59.78		0.037
28.23	15.42	29.73	52.11	45.09	50.19		40.84	56.15	39.81	55.94	58.30	40.71		0.122
28.23	15.42	29.73	52.11	45.09	42.51		40.84	56.15	39.81	55.94	58.30	54.23		0.039
28.23	15.42	29.73	52.11	49.14	35.92		40.84	56.15	39.81	55.94	55.76	63.06		0.033
28.23	15.42	29.73	52.11	49.14	43.81		40.84	56.15	39.81	55.94	55.76	59.78		0.053
28.23	15.42	29.73	52.11	49.14	50.19		40.84	56.15	39.81	55.94	55.76	40.71		0.161
28.23	15.42	29.73	52.11	49.14	42.51		40.84	56.15	39.81	55.94	55.76	54.23		0.056
28.23	15.42	29.73	52.11	35.92	43.81		40.84	56.15	39.81	55.94	63.06	59.78		0.019
28.23	15.42	29.73	52.11	35.92	50.19		40.84	56.15	39.81	55.94	63.06	40.71		0.073
28.23	15.42	29.73	52.11	35.92	42.51		40.84	56.15	39.81	55.94	63.06	54.23		0.020
28.23	15.42	29.73	52.11	43.81	50.19		40.84	56.15	39.81	55.94	59.78	40.71		0.111
28.23	15.42	29.73	52.11	43.81	42.51		40.84	56.15	39.81	55.94	59.78	54.23		0.034
28.23	15.42	29.73	52.11	50.19	42.51		40.84	56.15	39.81	55.94	40.71	54.23		0.117
28.23	15.42	29.73	57.78	45.09	49.14		40.84	56.15	39.81	53.22	58.30	55.76		0.100
28.23	15.42	29.73	57.78	45.09	35.92		40.84	56.15	39.81	53.22	58.30	63.06		0.043
28.23	15.42	29.73	57.78	45.09	43.81		40.84	56.15	39.81	53.22	58.30	59.78		0.067
28.23	15.42	29.73	57.78	45.09	50.19		40.84	56.15	39.81	53.22	58.30	40.71		0.188
28.23	15.42	29.73	57.78	45.09	42.51		40.84	56.15	39.81	53.22	58.30	54.23		0.072
28.23	15.42	29.73	57.78	49.14	35.92		40.84	56.15	39.81	53.22	55.76	63.06		0.060
28.23	15.42	29.73	57.78	49.14	43.81		40.84	56.15	39.81	53.22	55.76	59.78		0.091
28.23	15.42	29.73	57.78	49.14	50.19		40.84	56.15	39.81	53.22	55.76	40.71		0.238
28.23	15.42	29.73	57.78	49.14	42.51		40.84	56.15	39.81	53.22	55.76	54.23		0.098
28.23	15.42	29.73	57.78	35.92	43.81		40.84	56.15	39.81	53.22	63.06	59.78		0.039
28.23	15.42	29.73	57.78	35.92	50.19		40.84	56.15	39.81	53.22	63.06	40.71		0.120
28.23	15.42	29.73	57.78	35.92	42.51		40.84	56.15	39.81	53.22	63.06	54.23		0.041
28.23	15.42	29.73	57.78	43.81	50.19		40.84	56.15	39.81	53.22	59.78	40.71		0.173
28.23	15.42	29.73	57.78	43.81	42.51		40.84	56.15	39.81	53.22	59.78	54.23		0.065
28.23	15.42	29.73	57.78	50.19	42.51		40.84	56.15	39.81	53.22	40.71	54.23		0.185
28.23	15.42	29.73	45.09	49.14	35.92		40.84	56.15	39.81	58.30	55.76	63.06		0.016
28.23	15.42	29.73	45.09	49.14	43.81		40.84	56.15	39.81	58.30	55.76	59.78		0.028
28.23	15.42	29.73	45.09	49.14	50.19		40.84	56.15	39.81	58.30	55.76	40.71		0.100
28.23	15.42	29.73	45.09	49.14	42.51		40.84	56.15	39.81	58.30	55.76	54.23		0.029

SET 1							SET 2							p-values
28.23	15.42	29.73	45.09	35.92	43.81		40.84	56.15	39.81	58.30	63.06	59.78		0.009
28.23	15.42	29.73	45.09	35.92	50.19		40.84	56.15	39.81	58.30	63.06	40.71		0.040
28.23	15.42	29.73	45.09	35.92	42.51		40.84	56.15	39.81	58.30	63.06	54.23		0.009
28.23	15.42	29.73	45.09	43.81	50.19		40.84	56.15	39.81	58.30	59.78	40.71		0.065
28.23	15.42	29.73	45.09	43.81	42.51		40.84	56.15	39.81	58.30	59.78	54.23		0.016
28.23	15.42	29.73	45.09	50.19	42.51		40.84	56.15	39.81	58.30	40.71	54.23		0.067
28.23	15.42	29.73	49.14	35.92	43.81		40.84	56.15	39.81	55.76	63.06	59.78		0.014
28.23	15.42	29.73	49.14	35.92	50.19		40.84	56.15	39.81	55.76	63.06	40.71		0.058
28.23	15.42	29.73	49.14	35.92	42.51		40.84	56.15	39.81	55.76	63.06	54.23		0.014
28.23	15.42	29.73	49.14	43.81	50.19		40.84	56.15	39.81	55.76	59.78	40.71		0.091
28.23	15.42	29.73	49.14	43.81	42.51		40.84	56.15	39.81	55.76	59.78	54.23		0.025
28.23	15.42	29.73	49.14	50.19	42.51		40.84	56.15	39.81	55.76	40.71	54.23		0.095
28.23	15.42	29.73	35.92	43.81	50.19		40.84	56.15	39.81	63.06	59.78	40.71		0.036
28.23	15.42	29.73	35.92	43.81	42.51		40.84	56.15	39.81	63.06	59.78	54.23		0.007
28.23	15.42	29.73	35.92	50.19	42.51		40.84	56.15	39.81	63.06	40.71	54.23		0.036
28.23	15.42	29.73	43.81	50.19	42.51		40.84	56.15	39.81	59.78	40.71	54.23		0.060
28.23	15.42	38.43	24.75	28.26	37.38		40.84	56.15	41.50	47.51	49.23	46.95		0.001
28.23	15.42	38.43	24.75	28.26	38.13		40.84	56.15	41.50	47.51	49.23	51.50		0.001
28.23	15.42	38.43	24.75	28.26	52.11		40.84	56.15	41.50	47.51	49.23	55.94		0.014
28.23	15.42	38.43	24.75	28.26	57.78		40.84	56.15	41.50	47.51	49.23	53.22		0.033
28.23	15.42	38.43	24.75	28.26	45.09		40.84	56.15	41.50	47.51	49.23	58.30		0.005
28.23	15.42	38.43	24.75	28.26	49.14		40.84	56.15	41.50	47.51	49.23	55.76		0.009
28.23	15.42	38.43	24.75	28.26	35.92		40.84	56.15	41.50	47.51	49.23	63.06		0.001
28.23	15.42	38.43	24.75	28.26	43.81		40.84	56.15	41.50	47.51	49.23	59.78		0.004
28.23	15.42	38.43	24.75	28.26	50.19		40.84	56.15	41.50	47.51	49.23	40.71		0.021
28.23	15.42	38.43	24.75	28.26	42.51		40.84	56.15	41.50	47.51	49.23	54.23		0.003
28.23	15.42	38.43	24.75	37.38	38.13		40.84	56.15	41.50	47.51	46.95	51.50		0.004
28.23	15.42	38.43	24.75	37.38	52.11		40.84	56.15	41.50	47.51	46.95	55.94		0.025
28.23	15.42	38.43	24.75	37.38	57.78		40.84	56.15	41.50	47.51	46.95	53.22		0.055
28.23	15.42	38.43	24.75	37.38	45.09		40.84	56.15	41.50	47.51	46.95	58.30		0.010
28.23	15.42	38.43	24.75	37.38	49.14		40.84	56.15	41.50	47.51	46.95	55.76		0.017
28.23	15.42	38.43	24.75	37.38	35.92		40.84	56.15	41.50	47.51	46.95	63.06		0.004
28.23	15.42	38.43	24.75	37.38	43.81		40.84	56.15	41.50	47.51	46.95	59.78		0.008
28.23	15.42	38.43	24.75	37.38	50.19		40.84	56.15	41.50	47.51	46.95	40.71		0.038
28.23	15.42	38.43	24.75	37.38	42.51		40.84	56.15	41.50	47.51	46.95	54.23		0.007
28.23	15.42	38.43	24.75	38.13	52.11		40.84	56.15	41.50	47.51	51.50	55.94		0.022
28.23	15.42	38.43	24.75	38.13	57.78		40.84	56.15	41.50	47.51	51.50	53.22		0.047
28.23	15.42	38.43	24.75	38.13	45.09		40.84	56.15	41.50	47.51	51.50	58.30		0.008
28.23	15.42	38.43	24.75	38.13	49.14		40.84	56.15	41.50	47.51	51.50	55.76		0.015
28.23	15.42	38.43	24.75	38.13	35.92		40.84	56.15	41.50	47.51	51.50	63.06		0.003
28.23	15.42	38.43	24.75	38.13	43.81		40.84	56.15	41.50	47.51	51.50	59.78		0.007
28.23	15.42	38.43	24.75	38.13	50.19		40.84	56.15	41.50	47.51	51.50	40.71		0.034
28.23	15.42	38.43	24.75	38.13	42.51		40.84	56.15	41.50	47.51	51.50	54.23		0.006
28.23	15.42	38.43	24.75	52.11	57.78		40.84	56.15	41.50	47.51	55.94	53.22		0.103
28.23	15.42	38.43	24.75	52.11	45.09		40.84	56.15	41.50	47.51	55.94	58.30		0.032

SET 1							SET 2							p-values
28.23	15.42	38.43	24.75	52.11	49.14		40.84	56.15	41.50	47.51	55.94	55.76		0.047
28.23	15.42	38.43	24.75	52.11	35.92		40.84	56.15	41.50	47.51	55.94	63.06		0.016
28.23	15.42	38.43	24.75	52.11	43.81		40.84	56.15	41.50	47.51	55.94	59.78		0.028
28.23	15.42	38.43	24.75	52.11	50.19		40.84	56.15	41.50	47.51	55.94	40.71		0.097
28.23	15.42	38.43	24.75	52.11	42.51		40.84	56.15	41.50	47.51	55.94	54.23		0.028
28.23	15.42	38.43	24.75	57.78	45.09		40.84	56.15	41.50	47.51	53.22	58.30		0.061
28.23	15.42	38.43	24.75	57.78	49.14		40.84	56.15	41.50	47.51	53.22	55.76		0.085
28.23	15.42	38.43	24.75	57.78	35.92		40.84	56.15	41.50	47.51	53.22	63.06		0.034
28.23	15.42	38.43	24.75	57.78	43.81		40.84	56.15	41.50	47.51	53.22	59.78		0.055
28.23	15.42	38.43	24.75	57.78	50.19		40.84	56.15	41.50	47.51	53.22	40.71		0.158
28.23	15.42	38.43	24.75	57.78	42.51		40.84	56.15	41.50	47.51	53.22	54.23		0.057
28.23	15.42	38.43	24.75	45.09	49.14		40.84	56.15	41.50	47.51	58.30	55.76		0.023
28.23	15.42	38.43	24.75	45.09	35.92		40.84	56.15	41.50	47.51	58.30	63.06		0.006
28.23	15.42	38.43	24.75	45.09	43.81		40.84	56.15	41.50	47.51	58.30	59.78		0.012
28.23	15.42	38.43	24.75	45.09	50.19		40.84	56.15	41.50	47.51	58.30	40.71		0.053
28.23	15.42	38.43	24.75	45.09	42.51		40.84	56.15	41.50	47.51	58.30	54.23		0.012
28.23	15.42	38.43	24.75	49.14	35.92		40.84	56.15	41.50	47.51	55.76	63.06		0.011
28.23	15.42	38.43	24.75	49.14	43.81		40.84	56.15	41.50	47.51	55.76	59.78		0.020
28.23	15.42	38.43	24.75	49.14	50.19		40.84	56.15	41.50	47.51	55.76	40.71		0.076
28.23	15.42	38.43	24.75	49.14	42.51		40.84	56.15	41.50	47.51	55.76	54.23		0.020
28.23	15.42	38.43	24.75	35.92	43.81		40.84	56.15	41.50	47.51	63.06	59.78		0.005
28.23	15.42	38.43	24.75	35.92	50.19		40.84	56.15	41.50	47.51	63.06	40.71		0.027
28.23	15.42	38.43	24.75	35.92	42.51		40.84	56.15	41.50	47.51	63.06	54.23		0.005
28.23	15.42	38.43	24.75	43.81	50.19		40.84	56.15	41.50	47.51	59.78	40.71		0.047
28.23	15.42	38.43	24.75	43.81	42.51		40.84	56.15	41.50	47.51	59.78	54.23		0.010
28.23	15.42	38.43	24.75	50.19	42.51		40.84	56.15	41.50	47.51	40.71	54.23		0.045
28.23	15.42	38.43	28.26	37.38	38.13		40.84	56.15	41.50	49.23	46.95	51.50		0.003
28.23	15.42	38.43	28.26	37.38	52.11		40.84	56.15	41.50	49.23	46.95	55.94		0.025
28.23	15.42	38.43	28.26	37.38	57.78		40.84	56.15	41.50	49.23	46.95	53.22		0.055
28.23	15.42	38.43	28.26	37.38	45.09		40.84	56.15	41.50	49.23	46.95	58.30		0.009
28.23	15.42	38.43	28.26	37.38	49.14		40.84	56.15	41.50	49.23	46.95	55.76		0.017
28.23	15.42	38.43	28.26	37.38	35.92		40.84	56.15	41.50	49.23	46.95	63.06		0.003
28.23	15.42	38.43	28.26	37.38	43.81		40.84	56.15	41.50	49.23	46.95	59.78		0.008
28.23	15.42	38.43	28.26	37.38	50.19		40.84	56.15	41.50	49.23	46.95	40.71		0.039
28.23	15.42	38.43	28.26	37.38	42.51		40.84	56.15	41.50	49.23	46.95	54.23		0.006
28.23	15.42	38.43	28.26	38.13	52.11		40.84	56.15	41.50	49.23	51.50	55.94		0.021
28.23	15.42	38.43	28.26	38.13	57.78		40.84	56.15	41.50	49.23	51.50	53.22		0.047
28.23	15.42	38.43	28.26	38.13	45.09		40.84	56.15	41.50	49.23	51.50	58.30		0.008
28.23	15.42	38.43	28.26	38.13	49.14		40.84	56.15	41.50	49.23	51.50	55.76		0.014
28.23	15.42	38.43	28.26	38.13	35.92		40.84	56.15	41.50	49.23	51.50	63.06		0.003
28.23	15.42	38.43	28.26	38.13	43.81		40.84	56.15	41.50	49.23	51.50	59.78		0.007
28.23	15.42	38.43	28.26	38.13	50.19		40.84	56.15	41.50	49.23	51.50	40.71		0.035
28.23	15.42	38.43	28.26	38.13	42.51		40.84	56.15	41.50	49.23	51.50	54.23		0.005
28.23	15.42	38.43	28.26	52.11	57.78		40.84	56.15	41.50	49.23	55.94	53.22		0.103
28.23	15.42	38.43	28.26	52.11	45.09		40.84	56.15	41.50	49.23	55.94	58.30		0.031

SET 1							SET 2							p-values
28.23	15.42	38.43	28.26	52.11	49.14		40.84	56.15	41.50	49.23	55.94	55.76		0.046
28.23	15.42	38.43	28.26	52.11	35.92		40.84	56.15	41.50	49.23	55.94	63.06		0.015
28.23	15.42	38.43	28.26	52.11	43.81		40.84	56.15	41.50	49.23	55.94	59.78		0.027
28.23	15.42	38.43	28.26	52.11	50.19		40.84	56.15	41.50	49.23	55.94	40.71		0.098
28.23	15.42	38.43	28.26	52.11	42.51		40.84	56.15	41.50	49.23	55.94	54.23		0.027
28.23	15.42	38.43	28.26	57.78	45.09		40.84	56.15	41.50	49.23	53.22	58.30		0.061
28.23	15.42	38.43	28.26	57.78	49.14		40.84	56.15	41.50	49.23	53.22	55.76		0.084
28.23	15.42	38.43	28.26	57.78	35.92		40.84	56.15	41.50	49.23	53.22	63.06		0.034
28.23	15.42	38.43	28.26	57.78	43.81		40.84	56.15	41.50	49.23	53.22	59.78		0.054
28.23	15.42	38.43	28.26	57.78	50.19		40.84	56.15	41.50	49.23	53.22	40.71		0.161
28.23	15.42	38.43	28.26	57.78	42.51		40.84	56.15	41.50	49.23	53.22	54.23		0.056
28.23	15.42	38.43	28.26	45.09	49.14		40.84	56.15	41.50	49.23	58.30	55.76		0.022
28.23	15.42	38.43	28.26	45.09	35.92		40.84	56.15	41.50	49.23	58.30	63.06		0.006
28.23	15.42	38.43	28.26	45.09	43.81		40.84	56.15	41.50	49.23	58.30	59.78		0.012
28.23	15.42	38.43	28.26	45.09	50.19		40.84	56.15	41.50	49.23	58.30	40.71		0.053
28.23	15.42	38.43	28.26	45.09	42.51		40.84	56.15	41.50	49.23	58.30	54.23		0.011
28.23	15.42	38.43	28.26	49.14	35.92		40.84	56.15	41.50	49.23	55.76	63.06		0.010
28.23	15.42	38.43	28.26	49.14	43.81		40.84	56.15	41.50	49.23	55.76	59.78		0.019
28.23	15.42	38.43	28.26	49.14	50.19		40.84	56.15	41.50	49.23	55.76	40.71		0.077
28.23	15.42	38.43	28.26	49.14	42.51		40.84	56.15	41.50	49.23	55.76	54.23		0.019
28.23	15.42	38.43	28.26	35.92	43.81		40.84	56.15	41.50	49.23	63.06	59.78		0.005
28.23	15.42	38.43	28.26	35.92	50.19		40.84	56.15	41.50	49.23	63.06	40.71		0.027
28.23	15.42	38.43	28.26	35.92	42.51		40.84	56.15	41.50	49.23	63.06	54.23		0.004
28.23	15.42	38.43	28.26	43.81	50.19		40.84	56.15	41.50	49.23	59.78	40.71		0.047
28.23	15.42	38.43	28.26	43.81	42.51		40.84	56.15	41.50	49.23	59.78	54.23		0.009
28.23	15.42	38.43	28.26	50.19	42.51		40.84	56.15	41.50	49.23	40.71	54.23		0.046
28.23	15.42	38.43	37.38	38.13	52.11		40.84	56.15	41.50	46.95	51.50	55.94		0.036
28.23	15.42	38.43	37.38	38.13	57.78		40.84	56.15	41.50	46.95	51.50	53.22		0.074
28.23	15.42	38.43	37.38	38.13	45.09		40.84	56.15	41.50	46.95	51.50	58.30		0.015
28.23	15.42	38.43	37.38	38.13	49.14		40.84	56.15	41.50	46.95	51.50	55.76		0.025
28.23	15.42	38.43	37.38	38.13	35.92		40.84	56.15	41.50	46.95	51.50	63.06		0.006
28.23	15.42	38.43	37.38	38.13	43.81		40.84	56.15	41.50	46.95	51.50	59.78		0.013
28.23	15.42	38.43	37.38	38.13	50.19		40.84	56.15	41.50	46.95	51.50	40.71		0.059
28.23	15.42	38.43	37.38	38.13	42.51		40.84	56.15	41.50	46.95	51.50	54.23		0.011
28.23	15.42	38.43	37.38	52.11	57.78		40.84	56.15	41.50	46.95	55.94	53.22		0.148
28.23	15.42	38.43	37.38	52.11	45.09		40.84	56.15	41.50	46.95	55.94	58.30		0.049
28.23	15.42	38.43	37.38	52.11	49.14		40.84	56.15	41.50	46.95	55.94	55.76		0.071
28.23	15.42	38.43	37.38	52.11	35.92		40.84	56.15	41.50	46.95	55.94	63.06		0.026
28.23	15.42	38.43	37.38	52.11	43.81		40.84	56.15	41.50	46.95	55.94	59.78		0.043
28.23	15.42	38.43	37.38	52.11	50.19		40.84	56.15	41.50	46.95	55.94	40.71		0.146
28.23	15.42	38.43	37.38	52.11	42.51		40.84	56.15	41.50	46.95	55.94	54.23		0.044
28.23	15.42	38.43	37.38	57.78	45.09		40.84	56.15	41.50	46.95	53.22	58.30		0.091
28.23	15.42	38.43	37.38	57.78	49.14		40.84	56.15	41.50	46.95	53.22	55.76		0.123
28.23	15.42	38.43	37.38	57.78	35.92		40.84	56.15	41.50	46.95	53.22	63.06		0.052
28.23	15.42	38.43	37.38	57.78	43.81		40.84	56.15	41.50	46.95	53.22	59.78		0.082

SET 1							SET 2							p-values
28.23	15.42	38.43	37.38	57.78	50.19		40.84	56.15	41.50	46.95	53.22	40.71		0.230
28.23	15.42	38.43	37.38	57.78	42.51		40.84	56.15	41.50	46.95	53.22	54.23		0.086
28.23	15.42	38.43	37.38	45.09	49.14		40.84	56.15	41.50	46.95	58.30	55.76		0.036
28.23	15.42	38.43	37.38	45.09	35.92		40.84	56.15	41.50	46.95	58.30	63.06		0.011
28.23	15.42	38.43	37.38	45.09	43.81		40.84	56.15	41.50	46.95	58.30	59.78		0.020
28.23	15.42	38.43	37.38	45.09	50.19		40.84	56.15	41.50	46.95	58.30	40.71		0.083
28.23	15.42	38.43	37.38	45.09	42.51		40.84	56.15	41.50	46.95	58.30	54.23		0.020
28.23	15.42	38.43	37.38	49.14	35.92		40.84	56.15	41.50	46.95	55.76	63.06		0.018
28.23	15.42	38.43	37.38	49.14	43.81		40.84	56.15	41.50	46.95	55.76	59.78		0.032
28.23	15.42	38.43	37.38	49.14	50.19		40.84	56.15	41.50	46.95	55.76	40.71		0.118
28.23	15.42	38.43	37.38	49.14	42.51		40.84	56.15	41.50	46.95	55.76	54.23		0.032
28.23	15.42	38.43	37.38	35.92	43.81		40.84	56.15	41.50	46.95	63.06	59.78		0.009
28.23	15.42	38.43	37.38	35.92	50.19		40.84	56.15	41.50	46.95	63.06	40.71		0.045
28.23	15.42	38.43	37.38	35.92	42.51		40.84	56.15	41.50	46.95	63.06	54.23		0.009
28.23	15.42	38.43	37.38	43.81	50.19		40.84	56.15	41.50	46.95	59.78	40.71		0.075
28.23	15.42	38.43	37.38	43.81	42.51		40.84	56.15	41.50	46.95	59.78	54.23		0.017
28.23	15.42	38.43	37.38	50.19	42.51		40.84	56.15	41.50	46.95	40.71	54.23		0.074
28.23	15.42	38.43	38.13	52.11	57.78		40.84	56.15	41.50	51.50	55.94	53.22		0.127
28.23	15.42	38.43	38.13	52.11	45.09		40.84	56.15	41.50	51.50	55.94	58.30		0.040
28.23	15.42	38.43	38.13	52.11	49.14		40.84	56.15	41.50	51.50	55.94	55.76		0.059
28.23	15.42	38.43	38.13	52.11	35.92		40.84	56.15	41.50	51.50	55.94	63.06		0.021
28.23	15.42	38.43	38.13	52.11	43.81		40.84	56.15	41.50	51.50	55.94	59.78		0.036
28.23	15.42	38.43	38.13	52.11	50.19		40.84	56.15	41.50	51.50	55.94	40.71		0.127
28.23	15.42	38.43	38.13	52.11	42.51		40.84	56.15	41.50	51.50	55.94	54.23		0.037
28.23	15.42	38.43	38.13	57.78	45.09		40.84	56.15	41.50	51.50	53.22	58.30		0.077
28.23	15.42	38.43	38.13	57.78	49.14		40.84	56.15	41.50	51.50	53.22	55.76		0.106
28.23	15.42	38.43	38.13	57.78	35.92		40.84	56.15	41.50	51.50	53.22	63.06		0.044
28.23	15.42	38.43	38.13	57.78	43.81		40.84	56.15	41.50	51.50	53.22	59.78		0.069
28.23	15.42	38.43	38.13	57.78	50.19		40.84	56.15	41.50	51.50	53.22	40.71		0.203
28.23	15.42	38.43	38.13	57.78	42.51		40.84	56.15	41.50	51.50	53.22	54.23		0.073
28.23	15.42	38.43	38.13	45.09	49.14		40.84	56.15	41.50	51.50	58.30	55.76		0.030
28.23	15.42	38.43	38.13	45.09	35.92		40.84	56.15	41.50	51.50	58.30	63.06		0.009
28.23	15.42	38.43	38.13	45.09	43.81		40.84	56.15	41.50	51.50	58.30	59.78		0.016
28.23	15.42	38.43	38.13	45.09	50.19		40.84	56.15	41.50	51.50	58.30	40.71		0.072
28.23	15.42	38.43	38.13	45.09	42.51		40.84	56.15	41.50	51.50	58.30	54.23		0.016
28.23	15.42	38.43	38.13	49.14	35.92		40.84	56.15	41.50	51.50	55.76	63.06		0.015
28.23	15.42	38.43	38.13	49.14	43.81		40.84	56.15	41.50	51.50	55.76	59.78		0.026
28.23	15.42	38.43	38.13	49.14	50.19		40.84	56.15	41.50	51.50	55.76	40.71		0.102
28.23	15.42	38.43	38.13	49.14	42.51		40.84	56.15	41.50	51.50	55.76	54.23		0.026
28.23	15.42	38.43	38.13	35.92	43.81		40.84	56.15	41.50	51.50	63.06	59.78		0.007
28.23	15.42	38.43	38.13	35.92	50.19		40.84	56.15	41.50	51.50	63.06	40.71		0.039
28.23	15.42	38.43	38.13	35.92	42.51		40.84	56.15	41.50	51.50	63.06	54.23		0.007
28.23	15.42	38.43	38.13	43.81	50.19		40.84	56.15	41.50	51.50	59.78	40.71		0.064
28.23	15.42	38.43	38.13	43.81	42.51		40.84	56.15	41.50	51.50	59.78	54.23		0.014
28.23	15.42	38.43	38.13	50.19	42.51		40.84	56.15	41.50	51.50	40.71	54.23		0.064

References

Aderem A. 1992. The MARCKS brothers: a family of protein kinase C substrates. Cell. 71: 713-716.

Aderem A. 1995. The MARCKS family of protein kinase C substrates. Biochem. Soc. Trans. 23: 587-591.

Allen LH and Aderem A. 1995. Protein kinase C regulates MARCKS cycling between the plasma membrane and lysosomes in fibroblasts. EMBO. 14: 1109-1121.

Andreas K, Haupl T, Lubke C, Ringe J, Morawietz L, Wachtel A, Sittinger M, and Kaps C. 2009. Antirheumatic drug response signatures in human chondrocytes: potential molecular targets to stimulate cartilage regeneration. Arthritis Research & Therapy. 11: R15.

Arbuzova A, Schmitz AA, Vergeres G. 2002. Cross-talk unfolded: MARCKS proteins. Biochem. J. 362: 1-12.

Bader MF, Doussau F, Chasserot-Golaz S, Vitale N and Gasman, S. 2004. Coupling actin and membrane dynamics during calcium-regulated exocytosis: a role for Rho and ARF GTPases. Biochim. Biophysic. Acta. 1742: 37-49.

Balakumar P, Singh AP, Ganti SS, Krishan P, Ramasamy, Singh M. 2007. Resident cardiac mast cells: are they the major culprit in the pathogenesis of cardiac hypertrophy? Basic Clin. Pharm. Toxicol. 102(1): 5-9.

Barker, JE. 1968. Development of the mouse hematopoietic system. I. Types of hemoglobin produced in embryonic yolk sac and liver. Dev. Biol. 18: 14-29.

Baumann U, Chouchakova N, Gewecke B, Kohl J, Carroll MC, Schmidt RE, Gessner JE. 2001. Distinct tissue site-specific requirements of mast cells and complement components C3/C5a receptor in IgG immune complex-induced injury of skin and lung. J. Imm. 167: 1022-1027.

Blackshear PJ. 1993. The MARCKS family of cellular PKC substrates. J. Biol. Chem. 268:1501-1504.

Blackshear PJ, Verghese GM, Johnson JD, Haupt DM, Stumpo DJ. 1992. Characteristics of the F52 protein, a MARCKS homologue. J. Biol. Chem. 267: 13540-13546.

Bischoff SC and Kramer S. 2007. Human mast cells, bacteria, and intestinal immunity. Imm. Revs. 217: 329-337.

Bradding P, Walls AF, Holgate ST. 2006. The role of the mast cell in the pathophysiology of asthma. J. Allergy. Clin. Immunol. 117(6): 1277-1284.

Bulanova E, Budagian V, Orinska Z, Hein M, Petersen F, Thon L, et al. 2005. Extracellular ATP induces cytokine expression and apoptosis through P2Xy receptor in murine mast cells. J. Imm. 174: 3880-3890.

Burley DS, Hamid SA and Baxter GF. 2007. Cardioprotective actions of peptide hormones in myocardial ischemia. Heart Fail Rev. 12: 279-291.

Carballo E, Pitterle DM, Stumpo DJ, Sperling RT, Blackshear PJ. 2009. Phagocytic and macropinocytic activity in MARCKS-deficient macrophages and fibroblasts. Am. J. Physiol. (Cell Physiol.) 277: C163-C173.

Caroni P. 2001. Actin cytoskeleton regulation through modulation of PI(4,5)P2 rafts. EMBO. 20: 4332-4336.

Carr CM and Munson M. (2007). Tag team action at the synapse. EMBO Rep. 8: 834-838.

Chang S, Stacey KJ, Chen J, Costelloe EO, Aderem A, Hume DA. 1999. Mechanisms of regulation of the MacMARCKS gene in macrophages by bacterial lipopolysaccharide. J. Leukoc. Biol. 66: 528-534.

Chen J, Chang S, Duncan SA, Okano HJ, Fishell G, Aderem A. 1996. Disruption of the MacMARCKS gene prevents cranial neural tube closure and results in anencephaly. PNAS. 93: 6275-6279.

Chu AJ, Lin SH, Piasentin E. 2002. Possible role of MARCKS in cellular modulation of monocytic tissue factor-initiated hypercoagulation. Br. J. Haem. 118: 569-576.

Chun KR, Bae EM, Kim JK, Suk K, Lee WH. 2009. Suppression of the lipopolysaccharide-induced expression of MARCKS-related protein (MRP) affects transmigration in activated RAW 264.7 cells. Cell Imm. 256: 92-98.

Columbo M, Bochner BS, and Marone G. 1995. Human skin mast cells express B1 integrins that mediate adhesion to extracellular matrix proteins. J. Imm. 154: 6058-6064.

Costello PS, Turner M, Walters AE, Cunningham CN, Bauer PH, Downward J. 1996. Critical role for the tyrosine kinase Syk in signaling through the high affinity IgE receptor of mast cells. Oncogene. 13: 2595-2605.

Davis CW and Dickey BF. 2008. Regulated airway goblet cell mucin secretion. Ann. Rev. Physiol. 70:16.1-16.26.

Disatnik MH, Boutet SC, Pacio W, Chan AY, Ross LB, Lee CH, Rando TA. 2004. The bi-directional translocation of MARCKS between membrane and cytosol regulates integrin-mediated muscle cell spreading. J. Cell Sci. 117: 4469-4479.

Doreian BW, Fulop TG, Meklemburg RL, Smith CB. 2009. Cortical F-actin, the exocytic mode, and neuropeptide release in mouse chromaffin cells is regulated by Myristoylated Alanine Rich C Kinase Substrate and myosin II. Mol. Biol. Cell. 20: 3142-3154.

Dugina TN, Kiseleva EV, Glusa E, Strukova SM. 2003. Activation of mast cells induced by agonists of proteinase-activated receptors under normal conditions and during acute inflammation in rats. Eur. J. Pharm. 471: 141-147.

Eckert RE, Neuder LE, Park J, Adler KB, Jones SL. Myristoylated alanine-rich C-kinase substrate (MARCKS) protein regulation of human neutrophil migration. Am J Respir Cell Mol Biol. 42(5): 586-594.

Eitzen G. 2003. Actin remodeling to facilitate membrane fusion. Biochim. Biophysic. Acta.; 1641: 175-81.

Eliyahu E, Tsaadon A, Shtraizent N, Shalgi R. 2005. The involvement of protein kinase C and actin filaments in cortical granule exocytosis in rats. Reproduction. 129: 161–170.

Eliyahu E, Shtraizent N, Tsaadon A, Shalgi R. 2006. Association between myristoylated Alanine-rich C kinase substrate (MARCKS) translocation and cortical granule exocytosis. Reproduction. 131: 221–31.

Elzagallaai A, Rose SD, and Trifaro JM. 2000. Platelet secretion induced by phorbol esters stimulation is mediated through phosphorylation of MARCKS: a MARCKS-derived peptide blocks MARCKS phosphorylation and serotonin release without affecting pleckstrin phosphorylation. Blood: 95(3): 894–902.

Finlayson AE and Freeman KW. 2009. A cell motility screen reveals role for MARCKS-related protein in adherens junction formation and tumorigenesis. PLos ONE: 4(11): e7833.

Gay EA, Klein RC, Melton MA, Blackshear PJ, Yakel JL. 2008. Inhibition of native and recombinant nicotinic acetylcholine receptors by the myristoylated Alanine-rich C kinase substrate peptide. J. Pharmacol. Exp. Ther. 327: 884–890.

Gonzalo JA, Qiu Y, Lora JM, Al-Garawi A, Villeval JL, Boyce JA, Martinez C, Marquez G, Goya I, Hamid Q, Fraser CC, Picarella D, Cote-Sierra J, Hodge MR, Gutierrez-Ramos JC, Kolbeck R, Coyle AJ. 2007. Coordinated involvement of mast cells and T cells in allergic mucosal inflammation: critical role of the CC chemokine ligand 1: CCR8 axis. J. Immunol. 179: 1740–1750.

Harlan DM, Graff JM, Stumpo DJ, Eddy RI, Shows TB, Boyle JM, Blackshear PJ. 1991. The human Myristoylated Alanine-rich C kinase substrate (MARCKS) gene (MACS). J. Biol. Chem. 266: 14399–14405.

Hata D, Kawakami Y, Inagaki N, Lantz CS, Kitamura T, Khan WN, Yamamoto MM. 1998. Involvement of Bruton's tyrosine kinase in FceRI-dependent mast cell degranulation and cytokine production. J. Exp. Med. 187: 1235–1247.

Hua X, Kovarova M, Chason KD, Nguyen MT, Koller BH, Tilley SL. 2007. Enhanced mast cell activation in mice deficient in the A2b adenosine receptor. J Exp. Med. 204: 117–128.

Jacques D and Abdel-Samad D. 2007. Neuropeptide Y and NPY receptors in the cardiovascular system: implication in the regulation of intracellular calcium. Can. J. Physiol. Pharmacol. 85(1): 43–53.

Jamur MC, Grodzki AC, Berenstein EH, Hamawy MM, Siraganian RP, Oliver C. 2005. Identification and characterization of undifferentiated mast cells in mouse bone marrow. Blood. 105: 4282–4289.

Janmey PA and Lindberg U. 2004. Cytoskeletal Regulation: Rich in Lipids. Nat. Rev. 5: 658–666.

Jerdeva GV, Yarber FA, Trousdale MD, Rhodes CJ, Okamoto CT. 2005. Dominant negative PKC-ε impairs apical actin remodeling in parallel with inhibition of carbachol-stimulated secretion in rabbit lacrimal acini. Am J. Physiol. Cell Physiol. 289: C1052–C1068.

Kalin TV, Meliton L, Zhu X, Whitsett JA, Kalinichenko VV. 2008. Pulmonary mastocytosis and enhanced lung inflammation in mice heterozygous null for the Foxf1 gene. Am J. Respir Cell Mol Biol. 39: 390–399.

Kim SH, Kim MK, Yu HS, Kim HS, Park IS, Park HG, Kang UG, Kim YS. 2010. Electroconvulsive seizure increases phosphorylation of PKC substrates, including GAP-43, MARCKS, and neurogranin, in rat brain. Prog. Neuro-Psychopharmacol. Biol. Psychiatry. 34: 115–121.

Kitamura Y, Shimada M, Go S. 1979. Presence of mast cells in fetal liver of mice. Dev. Biol. 70: 510–514.

Kruger-Krasagakes S, Grutzkau A, Krasagakis K, Hoffmann S & Henz BM. 1999. Adhesion of mast cells to extracellular matrix provides a co-stimulatory signal for cytokine production. Imm. 98: 253–257.

Kruger-Krasagakes S, Grutzkau A, Baghramian R & Henz BM. 1996. Interactions of immature human mast cells with extracellular matrix: expression of specific adhesion receptors and their role in cell binding to matrix proteins. J. Invest. Dermatol. 106: 538–543.

Lattin J, Zidar DA, Schroder K, Kellie S, Hume DA, Sweet MJ. 2007. G-protein-coupled receptor expression, function, and signaling in macrophages. J. Leuk. Biol. 82: 16–32.

Lee HS, Park CS, Lee YM, Suk HY, Clemons TC, Choi OH. 2005. Antigen-induced Ca2+ mobilization in RBL-2H3 cells: role of I(1,4,5)P3 and S1P and necessity of I(1,4,5)P3. Cell Calcium. 38: 581–592.

Li J, O'Connor KL, Greeley GH, Blackshear PJ, Townsend CM, Evers M. 2005. Myristoylated Alanine-rich C kinase substrate-mediated neurotensin release via protein kinase C-δ downstream of the Rho/ROK pathway. J. Biol. Chem. 280: 8351–8357.

Li T, Li D, Sha J, Sun P, Huang Y. 2009. MicroRNA-21 directly targets MARCKS and promotes apoptosis resistance and invasion in prostate cancer cells. Biochem. Biophys. Res. Comm.: 383(3): 280–285.

Li Y, Martin LD, Spizz G, Adler KB. 2001. MARCKS protein is a key molecule regulating mucin secretion by human airway epithelial cells in vitro. J. Biol. Chem. 276: 40982–40990.

Liu JP, Engler D, Funder JW, Robinson PJ. 1994. Arginine vasopressin (AVP) causes the reversible phosphorylation of the myristoylated alanine-rich C kinase substrate (MARCKS) protein in the ovine anterior pituitary: evidence that MARCKS phosphorylation is associated with adrenocorticotropin (ACTH) secretion. Mol. Cell Endocrinol. 105(2): 217–226.

Lobach DF, Rochelle JM, Watson ML, Seldin MF, Blacksher PJ. 1993. Nucleotide sequence, expression, and chromosomal mapping of Mrp and mapping of five related sequences. Genomics. 17: 194–204.

Malacombe M, Bader MF, Gasman S. 2006. Exocytosis in neuroendocrine cells: new tasks for actin. Biochim. Biophysic. Acta.; 1763: 1175–1183.

Matsuoka Y, Li X, Bennett V. 2000. Adducin: structure, function and regulation. Cell. Mol. Life Sci. 57: 884–895.

Melicoff E, Sansores-Garcia L, Gomez A, Moreira DC, Datta P, Thakur P, Petrova, Y, Siddiqi T, Murthy JN, Dickey BF, Heidelberger R. 2009. Synaptotagmin-2 controls regulated exocytosis but not other secretory responses of mast cells. J. Biol. Chem. 284 (29): 19445–19451.

Metcalfe, DD. 2008. Mast cells and mastocytosis. Blood. 112 (4): 946-956.

Metz M and Maurer M. 2007. Mast cells-key effector cells in immune responses. TRENDS Imm. 28: 234–240.

Micallef J, Taccone M, Mukherjee J, Croul S, Busby J, Moran MF, Guha A. 2009. Epidermal growth factor receptor variant III-induced glioma invasion is mediated through

myristoylated alanine-rich C kinase C substrate overexpression. Cancer Res. 69 (19): 7548–7556.

Moore, DD. 2001. Gene Synthesis: Assembly of target sequences using mutually priming oligonucleotides. In *Curr Protoc Mol Biol* (Chapter 8: Unit 8.2B).

Myat MM, Anderson S, Allen LA, Aderem A. 1997. MARCKS regulates membrane ruffling and cell spreading. Curr Biol. 7: 611–614.

Ohmori S, Sakai N, Shirai Y, Yamamoto H, Miyamoto E, Shimizu N, Saito N. 2000. Importance of protein kinase C targeting for the phosphorylation of its substrate, Myristoylated Alanine-rich C kinase substrate. J. Biol. Chem. 275: 26449–26457.

Olenchock BA, Guo R, Silverman MA, Wu JN, Carpenter JH, Koretzky GA, Zhong XP. 2006. Impaired degranulation but enhanced cytokine production after FcepsilonRI stimulation of diacylglycerol kinase zeta-deficient mast cells. J. Exp. Med. 203(6): 1471–1480.

Park YS, Hur EM, Choi BH, Kwak E, Jun DJ, Park SJ, Kim KT. 2006. Involvement of protein kinase C-ε in activity-dependent potentiation of large dense-core vesicle exocytosis in chromaffin cells. J. Neuro. 26: 8999–9005.

Peng Z & Beaven MA. 2005. An essential role for Phospholipase D in the activation of Protein kinase C and degranulation in mast cells. J. Imm. 174: 5201–5208.

Pene TD, Rose SD, Lejen T, Marcu MG, Trifaro MJ. 2005. Expression of various scinderin domains in chromaffin cells indicates that this protein acts as a molecular switch in the control of actin filament dynamics and exocytosis.

Prussin C and Metcalfe DD. 2003. IgE, mast cells, basophils, and eosinophils. J. All Clin Imm. 111: S486–S494.

Qin Z and Cafiso DS. 1996. Membrane structure of Protein Kinase C and calmodulin binding domain of myristoylated Alanine rich C Kinase substrate determined by site-directed spin labeling. Biochem. 35: 2917–2925.

Rivera J and Gilfillan AM. 2006. Molecular regulation of mast cell activation. J. All Clin. Imm. 117: 1214–1225.

Rizo J, Chen X, Arac D. 2006. Unraveling the mechanisms of synaptotagmin and SNARE function in neurotransmitter release. TRENDS Cell Biol. 16: 339–350.

Rose SD, Byers DM, Morash SC, Fedoroff MS, Cook HW. 1996. Lipopolysaccharide stimulates differential expression of Myristoylated protein kinase C substrates in murine microglia. J. Neuro. Res. 44: 235–242.

Rose SD, Lejen T, Zhang L, Trifaro JM. 2001. Chromaffin cell F-actin disassembly and potentiation of catecholamine release in response to protein kinase C activation by phorbol esters is mediated through myristoylated alanine-rich C kinase substrate phosphorylation. J. Biol. Chem. 276: 36757–36763.

Ryzhov S, Zaynagetdinov R, Goldstein AE, Novitskiy SV, Dikov MM, Blackburn MR, Biagionni I, Feotkistov I. 2008. Effect of A2B adenosine receptor gene ablation on proinflammatory adenosine signaling in mast cells. J. Immunol. 80(11): 7212–7220.

Salli U, Saito N, and Stormshak F. 2003. Spatiotemporal Interactions of Myristoylated Alanine-Rich C Kinase Substrate (MARCKS) Protein with the Actin Cytoskeleton and Exocytosis of Oxytocin upon Prostaglandin F2 Stimulation of Bovine Luteal Cells. Biol. Reprod. 69, 2053–2058.

Sanchez-Mejorada G and Rosales C. 1998. Signal transduction by immunoglobulin Fc receptors. J. Leuk. Biol. 63: 521–533.

Seykora JT, Myat MM, Allen LA, Ravetch JV, Aderem A. 1996. Molecular determinants of the myristoyl-electrostatic switch of MARCKS. J. Biol. Chem. 271: 18797–18802.

Sheetz MP, Sable JE, Dobereiner HG. 2006. Continuous membrane-cytoskeleton adhesion requires continuous accommodation to lipid and cytoskeleton dynamics. Annu. Rev. Biophys. Biomol. Struct. 35: 417–434.

Shiota N, Rysa J, Kovanen PT, Ruskoaho H, Kokkonen JO, Lindstedt KA. 2003. A role for cardiac mast cells in the pathogenesis of hypertensive heart disease. J. Hypertens. 21: 1935–1944.

Singer M, Martin LD, Vargaftig BB, Park J, Gruber AD. 2004. A MARCKS-related peptide blocks mucus hypersecretion in a mouse model of asthma. Nat. Med. 10: 193–196.

Stinchcombe J, Bossi G, Griffiths GM. 2004. Linking albinism and immunity: the secrets of secretory lysosomes. Science. 305: 55–59.

Streb JW and Miano JM. 2005. Cross-species sequence analysis reveals multiple charged residue-rich domains that regulate nuclear/cytoplasmic partitioning and membrane localization of AKAP 12 (SSeCKS/Gravin). J. Biol. Chem. 280: 28007–28014.

Stumpo DJ, Graff JM, Albert KA, Greengard P, Blackshear PJ. 1989. Molecular cloning, characterization, and expression of a cDNA encoding the “80- to 87-kDa” myristoylated alanine-rich C kinase substrate: a major cellular substrate for protein kinase C. Proc. Natl. Acad. Sci. 86: 4012–4016.

Stumpo DJ, Bock CB, Tuttle JS, Blackshear PJ. 1995. MARCKS deficiency in mice leads to abnormal brain development and perinatal death. Proc. Natl. Acad. Sci. 92: 944–948.

Sudo N, Tanaka K, Koga Y, Okumura Y, Kubo C, Nomoto K. 1996. Extracellular ATP activates mast cells via a mechanism that is different from activation induced by the cross-linking of Fc Receptors. J. Imm. 156: 3970–3979.

Sundaram M, Cook HW, Byers DM. 2004. The MARCKS family of phospholipid binding proteins: regulation of phospholipase D and other cellular components. Biochem. Cell. Biol. 82: 191–200.

Sur R, Cavender D, Malaviya R. 2007. Different approaches to study mast cell functions. Int. Immunoph. 7: 555–567.

Swierczynski SL and Blackshear PJ. 1995. Membrane association of the Myristoylated Alanine-Rich C Kinase Substrate (MARCKS) protein. J. Biol. Chem. 270: 13436–13445.

Swierczynski SL, Siddhanti SR, Tuttle JS, Blackshear PJ. 1996. Nonmyristoylated MARCKS complements some but not all of the developmental defects associated with MARCKS deficiency in mice. Dev. Biol. 179: 135–147.

Szabo S, Machado-Vieira R, Yuan P, Wang Y, Wei Y, Falke C, Cirelli C, Tononi G, Manji HK, Du J. 2009. Glutamate receptors as targets of protein kinase C in pathophysiology and treatment of animal models of mania. Neuropharm. 56(1): 47–55.

Takashi S, Park J, Fang S, Koyama S, Parikh I, Adler KB. 2006. A peptide against the N-terminus of Myristoylated alanine-rich C kinase substrate inhibits degranulation of human leukocytes *in vitro*. Am J Respir Cell Mol Biol. 34: 647–652.

Tam SY, Tsai M, Snouwaert JN, Kalesinoff J, Scherrer D, Nakae S, Chatterjea D, Bouley DM, Galli SJ. 2004. RabGEF1 is a negative regulator of mast cell activation and skin inflammation. N. Imm. 5(8): 844–852.

Taniguchi H, Manenti S, Suzuki M, Titani K. 1994. Myristoylated alanine-rich C kinase substrate (MARCKS), a major protein kinase C substrate, is an in vivo substrate of proline-directed protein kinase(s). A mass spectroscopic analysis of the post-translational modifications. J. Biol. Chem. 269:18299–18302.

Tapp H, Al-Naggar IM, Yarmola EG, Harrison A, Shaw G, Edison AS, Bubb MR. 2005. MARCKS is a natively unfolded protein with an inaccessible binding site: evidence for long-range intramolecular interactions. J. Biol. Chem. 280: 9946–9956.

Thelen M, Rosen A, Nairn AC, Aderem A. 1990. Tumor necrosis factor α modifies agonist-dependent responses in human neutrophils by inducing the synthesis and myristoylation of a specific protein kinase C substrate. Proc. Natl. Acad. Sci. 87: 5603–5607.

Timofeeva OA, Eddins D, Yakel JL, Blakshear PJ, Levin ED. 2009. Hippocampal infusions of MARCKS peptides impair memory of rats on the radial arm maze. Brain Res. 1308: 147–152.

Trifaro JM, Lejen T, Rose SD, Pene TD, Barkar ND, Seward EP. 2002. Pathways that control cortical F-actin dynamics during secretion. Neurochem Res. 27: 1371–1385.

Trifaro JM, Rose SD, Marcu MG. 2000. Scinderin, a Ca-dependent actin filament severing protein that controls cortical actin network dynamics during secretion. Neurochem. Res. 25: 133–144.

Tolmachova T, Anders R, Stinchcombe J, Bossi G, Griffiths GM, Huxley C, Seabra MC. 2004. A general role for Rab27a in secretory cells. Mol. Biol. Cell. 15: 332–344.

Tzlil S, Murray D, and Ben-Shaul A. 2008. The "Electrostatic Switch" Mechanism: Monte Carlo Study of MARCKS-Membrane Interactions. Biophys. J. 95: 1745–1757.

Umekage T and Kato K. 1991. A mouse brain cDNA encodes a novel protein with the protein kinase C phosphorylation site domain common to MARCKS. FEBS. 286: 147–151.

Underhill DM, Chen J, Allen LA, Aderem A. 1998. MacMARCKS is not essential for phagocytosis in macrophages. J. Biol. Chem. 273: 33619–33623.

Van den Bout I, van Rheenen J, van Angelen AA, de Rooij J, Wilhelmsen K, Jalink K, Divecha N, Sonnenberg A. 2008. Investigation into the mechanism regulating MRP localization. Exp. Cell Res. 314(2): 330–341.

Van der Kleij HP, Ma D, Redegeld FA, Kraneveld AD, Nijkamp FP, Bienenstock J. 2003. Functional expression of neurokinin 1 receptors on mast cells induced by IL-4 and stem cell factor. J. Imm. 171: 2074–2079.

Vines CM and Prossnitz ER. 2004. Mechanisms of G protein-coupled receptor-mediated degranulation. FEMS Microbiol. Letters. 236: 1–6.

Vitale ML, Rodrigues del Castillo A, TchakarovL, Trifaro JM. 1991. Cortical filamentous actin disassembly and scinderin redistribution during chromaffin cell stimulation precede exocytosis, a phenomenon not exhibited by gelsolin. J. Cell Biol. 113: 1057–1067.

Vuori K and Ruoslahti E. 1993. Activation of protein kinase C precedes a5B1 integrin-mediated cell spreading on fibronectin. J. Biol. Chem. 268: 21459–21462.

Wang J, Arbuzova A, Hangyas-Milhalyne, McLaughlin S. 2001. The effector domain of Myristoylated Alanine-rich C kinase substrate binds strongly to phosphatidylinositol 4,5-bisphosphate. J. Biol. Chem. 276: 5012–5019.

Wang J, Gambhir A, Hangyas-Mihalyne G, Murray D, Golebiewska U, McLaughlin S. 2002. Lateral sequestration of phosphatidylinositol 4,5-bisphosphate by the basic effector domain of myristoylated alanine-rich C kinase substrate is due to nonspecific electrostatic interactions. J. Biol. Chem. 277: 34401–34412.

Watanabe N, Akikusa B, Park SY, Ohno H, Fossati L, Vecchieti G. 1999. Mast cells induce autoantibody-mediated vasculitis syndrome through tumor necrosis factor production upon triggering Fcγ receptors. Blood. 11: 3855–3863.

Xia HZ, Du Z, Craig S, Klisch G, Noben-Trauth N, Kochan JP, Huff TH, Irani AM, Schwartz LB. 1997. Effect of recombinant human IL-4 on tryptase, chymase, and Fc epsilon receptor type I expression in recombinant human stem cell factor-dependent fetal liver-derived mast cells. J. Imm. 159: 2911–2921.

Yamaguchi M, Sayama K, Yano K, Lantz CS, Noben-Trauth N, Ra C, Costa JJ, Galli SJ. 1999. IgE enhances Fce receptor I expression and IgE-dependent release of histamine and lipid mediators from human umbilical cord blood-derived mast cells: synergistic effect of IL-4 and IgE on human mast cell Fce receptor I expression and mediator release. J. Imm. 162: 5455–5465.

Yarmola EG, Edison AS, Lenox RH, Bubb MR. 2001. Actin filament cross-linking by MARCKS: characterization of two actin-binding sites within the phosphorylation site domain. J. Biol. Chem. 276: 22351–22358.

Yokoyama Y, Ito T, Hanson V, Schwartz GK, Aderem AA, Holloway JF, Tamaya T, Ohnuma T. 1998. PMA-induced reduction in invasiveness is associated with hyperphosphorylation of MARCKS and Talin in invasive bladder cancer cells. Int. J. Cancer. 75: 774–779.

Zhou X, Li J. 2000. Macrophage-enriched myristoylated alanine-rich C kinase substrate and its phosphorylation is required for phorbol ester-stimulated diffusion of beta 2 integrin molecules. J. Biol. Chem. 275: 20217–20222.

Zhu Z, Bao Z, Li J. 1995. MacMARCKS mutation blocks macrophage phagocytosis of zymosan. J. Biol. Chem. 270: 17652–17655.